

UNIVERSITÉ DE GENÈVE
Section de chimie et biochimie
Department de biochimie

FACULTÉ DES SCIENCES
Professeur Marko Kaksonen

Regulation of membrane scission in yeast endocytosis

THÈSE
présentée à la Faculté des sciences de l'Université de Genève
pour obtenir le grade de Docteur ès sciences, mention biochimie

par
Deepikaa Menon
de
Chennai (India)

Thèse N° xxxx

GENÈVE / HEIDELBERG
photoshop EMBL
2018

Abstract

Endocytosis is an ancient pathway that regulates communication of the cell with its environment. During this process, the plasma membrane is reshaped in a controlled sequence: a flat membrane forms an invagination that undergoes scission to produce a cargo-filled vesicle. Breaking the membrane invagination to form a vesicle is perhaps the most dramatic shape transition in this development, exciting a large body of literature addressing the cause of membrane scission. Work on mammalian cells has converged on a scission mechanism based on membrane neck constriction by the GTPase dynamin. A clear understanding of what causes scission remains incomplete for the much simpler endocytic network in yeast cells.

In this thesis, I investigate the mechanism of membrane scission in *Saccharomyces cerevisiae* and the proteins involved by combining mutagenesis with live-cell imaging of fluorescently-tagged proteins.

Endocytic sites are very stereotypic in yeast, recruiting about 50 proteins- most with mammalian homologues- in a highly specific sequence. These proteins can be assigned to separable modules based on their role in endocytosis. Members of the coat module arrive when the membrane is still flat and form the template for invagination. Actin regulators arrive later and produce the forces required to pull up the membrane. Scission proteins arrive at the end of the timeline and regulate vesicle formation.

The yeast BAR domain complex Rvs is an important regulator of scission: in cells without Rvs, scission efficiency decreases by nearly 30%. The 70% of invaginations that undergo scission in the cells form smaller vesicles than in wild-type cells. Rvs thus appears to regulate both timing and likelihood of scission, but it has not been clear how it does so, or how it gets recruited to membrane tubes in the first place.

I find that Rvs localization is timed by its BAR domain. The BAR domain senses a particular membrane shape, and Rvs is only recruited to endocytic sites once this shape is acquired. Surprisingly, localization efficiency and localization itself is affected by a second domain of Rvs167, the SH3 domain. This domain helps recruitment of Rvs and could couple the actin network to vesicle scission, triggering disassembly of the actin network once scission occurs.

Several models have been proposed for what eventually causes scission. I test predictions of some of these models. I find that forces generated by dynamin and lipid hydrolysis do not drive vesicle formation. Scission timing is also independent of the number of BAR domains recruited to membrane tubes, so is not based on BAR concentration-dependent membrane rupture. Scission timing is instead determined by the amount of actin at endocytic sites, and hence by the magnitude of forces generated on the membrane. There appears to be a threshold force over which the membrane reliably ruptures. The function of Rvs is to scaffold the membrane, and prevent scission before this force is generated, allowing reliable formation of vesicles.

Résumé

L’endocytose est une voie ancienne qui régule la communication de la cellule avec son environnement. Au cours de ce processus, la membrane plasmique est déformée dans une séquence contrôlée: une membrane plate forme une invagination qui subit une scission pour produire une vésicule contenant une cargaison. La rupture de la membrane pour former une vésicule est peut-être le changement de forme le plus spectaculaire de ce processus. Cela a entraîné un grand nombre de publications sur la cause de la scission de la membrane. Les travaux sur les cellules de mammifères ont convergé vers un mécanisme de scission basé sur la constriction du col de la membrane par la GTPase dynamine. Une compréhension claire de ce qui cause la scission reste incomplète pour le réseau endocytaire beaucoup plus simple de la levure.

Dans cette thèse, j’étudie le mécanisme de la scission membranaire chez *Saccharomyces cerevisiae* et les protéines impliquées en combinant la mutagenèse avec l’imagerie de protéines marquées par fluorescence dans des cellules vivantes.

Les sites d’endocytose sont très stéréotypés chez la levure, recrutant environ 50 protéines, la plupart avec des homologues mammifères, selon une séquence très spécifique. Ces protéines peuvent être affectées à des modules séparables en fonction de leur rôle dans l’endocytose. Les membres du module « manteau » arrivent lorsque la membrane est encore plate et définissent le site de la future invagination. Les régulateurs de l’actine arrivent plus tard et produisent les forces nécessaires pour étirer la membrane. Les protéines de scission arrivent à la fin de la chronologie et régulent la formation des vésicules.

Chez la levure, le complexe à domaines BAR Rvs est un régulateur important de la scission: dans les cellules sans Rvs, l’efficacité de la scission diminue de près de 30%. Les 70% d’invaginations qui parviennent à la scission forment des vésicules plus petites que d’habitude.

Rvs semble donc réguler à la fois le moment et la probabilité de scission, mais l'on ne connaît ni le mécanisme sous-jacent, ni comment le complexe est recruté dans les tubes de membrane en premier lieu.

Je montre que la localisation de Rvs est déterminée par son domaine BAR. Le domaine BAR détecte une forme de membrane particulière et Rvs est recruté uniquement sur les sites endocytaires une fois cette forme acquise. De manière surprenante, l'efficacité de la localisation et la localisation elle-même sont affectées par un second domaine de Rvs167, le domaine SH3. Ce domaine facilite le recrutement de Rvs et couple probablement le réseau d'actine à la scission des vésicules, ce qui déclenche le désassemblage du réseau d'actine une fois que la scission se produit.

Plusieurs modèles ont été proposés pour la cause de la scission. Je teste les prédictions de certains de ces modèles. Je trouve que les forces générées par la dynamine et l'hydrolyse des lipides ne causent pas la formation de vésicules. Le moment de la scission est également indépendant du nombre de domaines BAR recrutés dans les tubes membranaires : la rupture membranaire n'est donc pas déclenchée par la concentration de BAR. Ce moment est plutôt réglé par la quantité d'actine au niveau des sites endocytaires, et donc par l'ampleur des forces générées sur la membrane. Il semble y avoir un seuil de force au-dessus duquel la membrane se rompt de manière fiable. La fonction de Rvs est de soutenir la membrane et d'empêcher la scission avant que cette force ne soit générée, permettant ainsi la formation fiable de vésicules.

Acknowledgements

Thank you Marko, for your patience and guidance while I discovered biology. I hope I acquired at least some of the deliberate and methodical way you think. I am grateful for your constant optimism, and I feel lucky to have been supervised by someone with whom I share a philosophy of science. Many thanks to the lab: Ori, Camilla, Hetty, Tanja, and Andrea, for getting me started on the messy details, your invaluable feedback throughout. The Geneva crew: Daniel, Mateusz, Serena, and Anne-Sophie, thanks for the many animated discussions. Daniel, thank you for your contribution to the trash under my desk.

Many thanks to Jonas and the rest of the Ries lab for shelter. Jonas, I appreciate that you suffer my lunch habits, I will keep trying to eat faster. Joran, Markus, Kostek, Jan, Jervis, Ulf, thank you for making limbo bearable. Markus, thank you for the many conversations, forcing me off starvation, and for annoying me into doing more thorough science. I truly (and grumpily) appreciate all of it, but biochemists do not own the word "regulate".

I would like to thank my TAC members Peter Lenart, Aurelien Roux, and John Briggs for their comments and suggestions through this project.

I am deeply indebted to some people for getting me through these years. Thibaut and Martina, thank you for existing. Paul, thanks for being a (mostly) fantastic flatmate, and an awful fake fiancé. Anastasia, for sharing your home and friendship. Many others who made leaving EMBL difficult: Marvin, Miguel, Phillippe, Ori, Filipa, Simone, thank you for the company.

My family has been supportive, frequently bemused, over the course of this PhD. Thank you for attempting to understand what I have been doing all these years.

Finally, the fact that this thesis exists is owed to Helke Hildebrand, Dean of the Graduate program at EMBL when I started my PhD. Thank you Helke, for the endless supply of support and chocolate.

Contents

Abstract	iii
Résumé	v
1 Introduction	1
1.1 Endocytosis and cellular trafficking pathways	1
1.2 Clathrin-mediated endocytosis	2
1.3 CME in mammalian versus yeast cells	4
1.3.1 Clathrin is required for mammalian CME	4
1.3.2 Actin forces are required for yeast CME	5
1.3.3 CME in yeast is highly regular	5
1.3.3.1 Early initiation phase	6
1.3.3.2 Coat module	7
1.3.3.3 Actin module	7
1.3.3.4 Scission module	10
1.3.4 Membrane scission in mammalian cells	11
1.3.4.1 Scission is dependent on dynamin	11
1.3.4.2 Dynamin is an oligomeric GTPase	11
1.3.4.3 Dynamin and BAR proteins interact via PRD and SH3 regions	12
1.3.5 Membrane scission in yeast	13
1.3.5.1 Yeast dynamin-like proteins	13
1.3.5.2 Yeast BAR domain proteins Rvs161/167 regulate scission timing	14
1.3.5.3 Forces needed for membrane invagination and scission	14
1.3.5.4 Proposed scission mechanisms	15
1.4 BAR domain proteins	17
1.4.1 N-BAR proteins and membrane shapes	18
1.4.2 N-BAR Amphiphysin	19

1.4.3	N-BAR Endophilin	20
1.4.4	N-BAR proteins in yeast: the Rvs complex	21
2	Aims of the study	23
3	Results	25
3.1	Tracking endocytic proteins in yeast	25
3.2	Rvs deletion reduces coat movement	29
3.3	Recruitment of Rvs and function of domains	31
3.3.1	BAR domains sense membrane curvature	32
3.3.2	SH3 domains can localize Rvs in an actin and curvature-independent manner	35
3.3.3	Loss of the SH3 domain affects membrane invagination	36
3.4	Function of Rvs	40
3.4.1	Hypothesis: Rvs is an interaction surface for membrane constriction by dynamin	40
3.4.1.1	Vps1 does not affect Sla1 or Rvs167 dynamics	41
3.4.2	Hypothesis: Rvs barrier causes line tension at lipid interphase, causing scission	43
3.4.2.1	Yeast synaptojanins do not affect coat and Rvs movement	44
3.4.3	Hypothesis: Rvs exerts frictional forces on the membrane, causing scission	49
3.4.3.1	Membrane scission is not influenced by Rvs molecule number	49
3.4.4	Hypothesis: BAR domains scaffold the membrane, preventing scission	55
3.4.4.1	Coat movement is influenced by recruitment of BAR domains	56
3.4.4.2	Hypothesis2: Rvs is a scaffold against turgor pressure	58
3.4.4.3	Requirement for Rvs is unchanged by reduced turgor pressure	59
4	Discussion	63
4.1	Recruitment of Rvs to endocytic sites	63

4.1.1	BAR domain senses membrane curvature	64
4.1.2	BAR domain times recruitment of Rvs	64
4.1.3	SH3 domain makes Rvs recruitment efficient . .	65
4.1.4	The SH3 domain can independently assemble and disassemble Rvs molecules	65
4.1.5	SH3 domain affects actin dynamics	66
4.1.6	What does the SH3 domain interact with?	66
4.1.7	Total number of Rvs recruited is independent of cell ploidy	67
4.1.8	Rvs recruitment rate increases with increasing gene copy number	68
4.2	Arrangement of Rvs dimers on the membrane	69
4.2.1	Rvs does not form a tight scaffold on membrane tubes	69
4.2.2	A limit for how much Rvs can be recruited to the membrane	70
4.2.3	Conclusions for Rvs localization	72
4.3	What causes membrane scission?	73
4.3.1	Dynamin does not drive scission	73
4.3.2	Lipid hydrolysis is not the primary cause of membrane scission	73
4.3.3	Protein friction does not drive membrane scission	75
4.3.4	Actin polymerization generates forces required for membrane scission	76
4.4	Function of the Rvs complex	76
4.4.1	Rvs scaffolds the membrane tube	76
4.4.2	A critical amount of Rvs is required to stabilize the membrane	77
4.5	Inp52 is likely involved in vesicle uncoating	79
4.6	Model for membrane scisison	80
5	Materials and Methods	83
5.1	Materials	84
5.1.1	Yeast strains	84
5.1.2	Buffers and plasmids	88
5.1.3	Media	89
5.1.4	Microscopes	90
5.2	Methods	91

5.2.1	Homologous recombination with PCR cassette insertion	91
5.2.2	Live-cell imaging	91
5.2.2.1	Live-cell image analysis	92
5.2.2.2	Cytoplasmic background quantification	93
5.2.2.3	CLEM	93
6	Appendix	95
	Bibliography	97

List of Figures

1.1	Endocytic pathways in cells	3
1.2	Clathrin lattices in CME	4
1.3	Actin network in yeast endocytosis	8
1.4	Endocytic pathway in mammalian and yeast cells	9
1.5	Dynamin-mediated membrane scission	12
1.6	Structures of BAR domain dimers	17
1.7	BAR domain scaffolds on membrane tubes	18
1.8	Schematic structure of Rvs and BAR protein domains .	22
3.1	Tracking yeast endocytic proteins	27
3.2	Coat movement in <i>rvs167Δ</i> cells	29
3.3	Localization of the Rvs167 BAR domain	34
3.4	Tracking endocytic proteins in BAR cells	38
3.5	Phenotype of <i>vps1Δ</i>	41
3.6	Tracking endocytic proteins in <i>vps1Δ</i> cells	42
3.7	Synaptojanin-like proteins in yeast	45
3.8	Effect of synaptojanin deletion	47
3.9	Overexpression of Rvs in haploid cells	51
3.10	Rvs molecule number titration in diploid cells	53
3.11	Molecule number in diploid cells	54
3.12	Overexpression of the Rvs BAR domain	57
3.13	Effect of sorbitol on <i>rvs167Δ</i> cells	59
4.1	Recruitment and cytosolic concentration of Rvs	67
4.2	Rate of recruitment of Rvs	68
4.3	Rvs decay time	72
4.4	Model for membrane scission in yeast	80
6.1	Scission failure rates	95
6.2	Lifetimes of proteins in WT and BAR cells	96

List of Tables

3.1 Molecule numbers of Rvs167 and Abp1	61
3.2 Cytoplasmic intensities	62

List of Abbreviations

3D	Three-dimensional
ATP	Adenosine triphosphate
ANTH	AP180 N-terminal homology
AP	Adaptor protein complex CME
Clathrin-mediated endocytosis	
ConA	Concanavalin A
CLEM	Correlative light and electron microscopy
DNA	Deoxyribonucleic acid
EMCCD	Electron multiplying charge-coupled device
ENTH	Epsin N-terminal homology
FCS	Fluorescence correlation spectroscopy
GPA	Glycine Proline Alanine-rich
GTP	Guanosine triphosphate
NPF	Nucleation promoting factor
OD₆₀₀	Optical density (600 nm)
PIP₂	Phosphatidyl inositole (4,5) diphosphate
PEG	Poly ethylene glycol
PCR	Polymerase chain reaction
PRD	Proline-rich domain
RT	Room temperature
SH3	Src homology 3
SC	Synthetic complete
TIRF	Total internal reflection fluorescence
WASP	Wiskott-Aldrich syndrome protein
WT	Wild-type
YPD	Yeast extract peptone dextrose
YPAD	Yeast extract peptone dextrose plus adenine

1 | Introduction

1.1 Endocytosis and cellular trafficking pathways

The plasma membrane serves as the defining barrier between the interior and exterior of the cell, thus creating cellular identity, and facilitating evolution out of the primordial soup into a defined structure that can regulate entry of signals into the cell. In eukaryotes, and with increasing complexity, in multicellular eukaryotes, tuning cellular response to external signals has resulted in a complex network of signalling pathways, and tight coupling of these pathways with the process of endocytosis. Endocytosis refers to the uptake of molecules too big to simply pass through the plasma membrane. It involves the bending of the plasma membrane into a cargo-filled invagination, and culminates in the severing of this invagination to form a vesicle. This vesicle and its contents are then targeted to other cellular organelles for degradation or recycling.

Apart from internalizing cargo, endocytosis allows regulation of the plasma membrane itself: its lipid and protein composition, and therefore many of its physical and biochemical properties like tension, rigidity, and surface-receptor composition. Cargo taken up by endocytic pathways include these surface-receptors and their ligands that are transported across the cell, forming the link between cell signalling and endocytosis. Endocytosis essentially forms the basis of all cellular responses, from incorporating external stimulus, to communication between different cellular compartments. This process arguably drove the development of organisms from single cell to multicellular eukaryotes.

Plasma membrane regulation and internalization of signalling molecules are critical for the function of the cell. Among the vast array of important cargo that are taken up via endocytosis are cholesterol (Goldstein and Brown, 1973; Anderson, Goldstein and Brown, 1976), insulin (Fan et al., 1982), and other hormones. Not surprisingly, many human diseases have been linked to defects in the endocytic pathway like familial hypercholesterolemia- the study of which established the field of endocytosis, Alzheimer's, and some types of cancer (Goldstein and Brown, 1973; Anderson, Goldstein and Brown, 1976, Maxfield, 2014, Mosesson, Mills and Yarden, 2008). The importance of the endocytic machinery as the entry portal into the cell is evident in the fact that it is hijacked by pathogens like viruses and bacteria to enter host cells (Mercer, Schelhaas and Helenius, 2010). Other components of the cellular signalling pathway transmit signals across the cell and between various organelles like the Golgi apparatus and endoplasmic reticulum. These membranes undergo similar transitions of the bounding membrane, and have mechanistic and biochemical similarities (McMahon and Mills, 2004; Traub, 2005), suggesting a universal principle of membrane deformation.

Although many early discoveries relating to endocytic pathways were identified in mammalian cell types (Hemmaplardh and Morgan, 1976; Karin and Mintz, 1981), description of endocytosis in *Saccharomyces cerevisiae* (Riezman, 1985) marked the beginning of the field of yeast endocytosis. Ease of genetic manipulation, availability of a completed genome sequence, and relative simplicity of endocytic pathways- there is only one- drove several discoveries that established yeast as a powerful model organism (Boettner, Chi and Lemmon, 2012; Payne, 2013).

1.2 Clathrin-mediated endocytosis

Many different endocytic pathways exist that facilitate the internalization of cargo at the plasma membrane, as depicted in Fig.1.1. These pathways select for differences in size and type of cargo. Of them, Clathrin-mediated endocytosis (CME), is universal among eukaryotes. In mammalian cells CME transports 90% of labelled surface protein

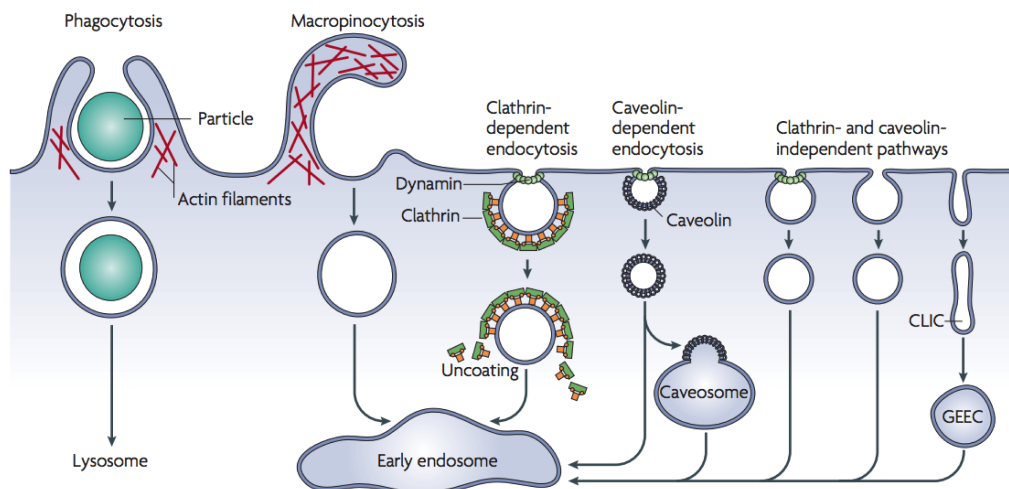


Figure 1.1 – Some of the endocytic pathways in mammalian cells. Large particles are incorporated by phagocytosis, bulk fluid by macropinocytosis. A large array of cargo is taken into the cell via CME and calveolin-dependent endocytosis. Vesicles formed by these pathways are targeted to the early endosome. Clathrin and calveolin-independent pathways incorporate cargo and involve different geometries, including tubular "clathrin- and dynamin-independent carriers" (CLIC), that arrive at "GPI-anchored protein enriched early endosomes" (GEEC), before they are transported to endosomes. *Reprinted by permission from Springer Nature: Nature Reviews Molecular Cell Biology (Mayor and Pagano, 2007), copyright (2007)*

into the cell (Bitsikas, Corrêa and Nichols, 2014). It was first identified when studying yolk uptake in mosquitos, and ultrastructural studies of their oocytes (where frequency of uptake events is high enough to be easily studied) identified a bristly coat formation inside the cell membrane and similarly bristly vesicles (Fig.1.2). These vesicles then lost the bristly coat and fused to eventually form yolk bodies in the mature oocyte (Roth and Porter, 1964). The bristle was noted in several cell types, and later identified as a lattice of a single highly conserved protein (Pearse, 1976). This protein was named Clathrin, derived from the latin word for lattice.

Clathrin is formed of light and heavy chains incorporated into a triskelion (Ungewickell and Branton, 1981) that assembles into closed hexagonal and pentagonal structures on the inner leaflet of the plasma membrane (Fig.1.2). CME has, since four decades ago, been recognized has an ubiquitous mechanism of membrane uptake in cell types ranging from the frog presynaptic membrane (Heuser and Reese, 1973) to rat vas deferens (Friend and Farquhar, 1967). Clathrin

also localizes to the trans-golgi network (TGN): these clathrin-coated vesicles mediate traffic from the TGN to the endosome. Specification of vesicle cargo and targeting to different cellular compartments is achieved by clathrin interaction with specialized adaptor proteins like the adaptor protein complexes (AP), which specifies Golgi-to-early endosome traffic, while Golgi-localized gamma-adaptin (GGA) complexes specify Golgi-to-late endosome traffic (Payne, 2013).

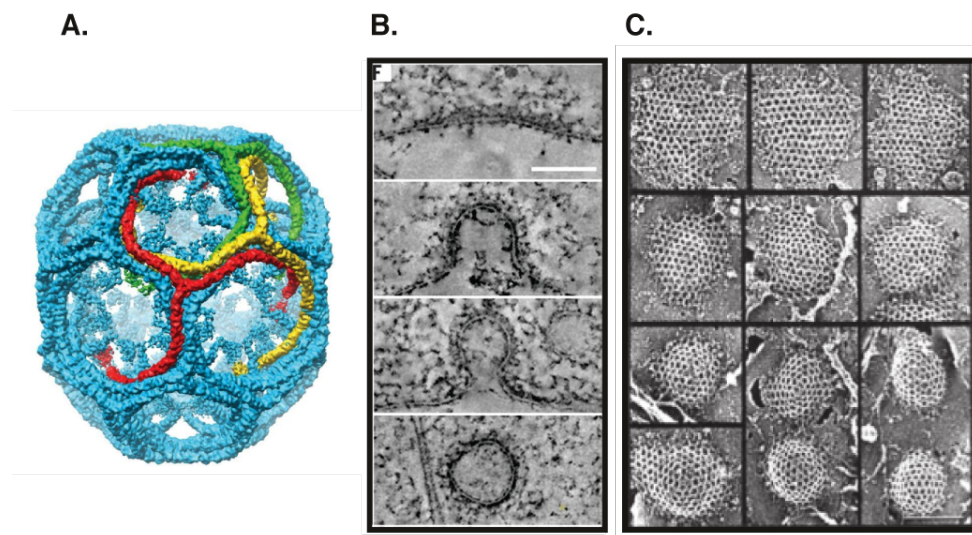


Figure 1.2 – A: Model for a clathrin-coated vesicle based on cryo electron microscopy. Three individual triskelions are highlighted. *Reprinted with permission from Springer Nature: Nature. Molecular model for a complete clathrin lattice from electron cryomicroscopy, Fotin et al., Copyright 2004.* B: Slices through tomograms of clathrin-coated pits in different stages of invagination. *From Avinoam et al, Science 2016. Reprinted with permission from AAAS.* C: Freeze-etch view of plasma membrane of mouse fibroblast showing a range of clathrin lattices. *Republished with permission from CCC, from Three-dimensional visualization of coated vesicle formation in fibroblasts, Heuser, JCB 84, 1980*

1.3 CME in mammalian versus yeast cells

1.3.1 Clathrin is required for mammalian CME

The clathrin lattice was speculated as responsible for remodelling the plasma membrane and selecting cargo in the first papers that noted the “bristly” coat (Roth and Porter, 1964; Kanaseki and Kadota, 1969). In multicellular organisms like *Caenorhabditis elegans*, clathrin depleted by RNAi results in decreased endocytic uptake in oocytes and dead progeny (Grant and Hirsh, 1999). In *Drosophila melanogaster*, deletion

of clathrin heavy chain results in embryonic lethality (Bazinet et al., 1993). Knock-down of the heavy chain by RNAi in Hela cells results in decrease in endocytosis by 80% (Huang et al., 2004). Essentially, endocytosis fails in the absence of clathrin in multicellular organisms. How exactly the clathrin coat shapes the progression of endocytosis has been heavily debated, but its involvement itself has not.

Early work in yeast revealed that clathrin is not necessary for endocytosis (Payne and Schekman, 1985). Loss of clathrin only changes the size of the vesicles formed and leads to decrease in the number of established endocytic sites (Kaksonen, Toret and Drubin, 2005; Kukulski et al., 2016). Clathrin appears to affect establishment of sites and regulation of scission, but is not necessary for membrane invagination. It is now apparent that though the mammalian and yeast systems are mechanistically similar and most of the yeast endocytic proteins have mammalian homologues (Weinberg and Drubin, 2012), there are some significant differences.

1.3.2 Actin forces are required for yeast CME

A single gene in yeast encodes the highly abundant actin protein, which is essential for cell survival (Koteliansky et al., 1979; Greer and Schekman, 1982). Organization of actin into axial filaments and cortical patches polarized to emerging buds was first described using phalloidin staining in fixed *S.cervisiae* (Adams and Pringle, 1984). These patches were later established as dynamic endocytic sites by observing co-localization with other endocytic proteins (Kübler et al., 1993). While the mammalian CME is heavily dependent on clathrin for invagination, the yeast system relies on actin filament polymerization and depolymerization for membrane invagination: disrupting actin filament dynamics blocks endocytosis (Kübler et al., 1993).

1.3.3 CME in yeast is highly regular

In yeast, over fifty proteins are recruited, interact, and disassemble during the endocytic process. In mammals as well as in yeast, proteins

that arrive at an endocytic site can be assigned into different modules according to their relative time of recruitment and function (Fig.1.4).

An initiation phase assembles coat proteins on the plasma membrane and establishes an endocytic site. The early proteins involved in the initiation phase are highly variable in both recruitment as well as time spent at sites. Initiation is followed by a very stereotypic sequence of events that assembles coat proteins, nucleates actin, organizes the actin network, invaginates a membrane tube, and finally severs the membrane to produce vesicles (Kaksonen, Toret and Drubin, 2005). While the entire process of initiation through scission occurs over a period of about a minute, once membrane invagination begins, inward movement and consecutive scission occurs in under fifteen seconds. This indicates tight regulation of the post-initiation sequence of events in the endocytic timeline.

Sterotypicity of the later stages of yeast endocytosis allows us to average the behaviour of a particular protein from multiple endocytic sites. Tracking the behaviour and organization of these proteins has led to a remarkably detailed understanding of the spatial and temporal regulation of endocytosis in yeast (Kaksonen, Toret and Drubin, 2005; Picco et al., 2015; Mund et al., 2017). The different stages of endocytosis are discussed below.

1.3.3.1 Early initiation phase

The initiation phase establishes endocytic sites and selects cargo (Brach et al., 2014). Deletion of an entire seven protein set of early endocytic proteins (Ede1, Syp1, Yap1801/1802, Apl1, Pal1, Pal2) does not prevent endocytosis. It seems that the initiation of endocytosis in yeast is independent of the recruitment of any one protein, and is likely a result of several different cooperative or independent factors (Brach et al., 2014). This could give the process robustness in the absence of alternate pathways for uptake of essential nutrients and signals. The variability in this phase could also provide a “checkpoint”, to ensure that sufficient cargo is loaded (Weinberg and Drubin, 2012) before later (energy consuming) phases are triggered.

1.3.3.2 Coat module

Coat proteins serve to template later-arriving proteins (Mund et al., 2017), as well as form the link between the actin network and membrane (Skruzny et al., 2012). Clathrin adaptors and the clathrin triskelion are not necessary for the progression of sites. Deletion of coat proteins Sla2 (Hip1R homologue) and Ent1 (Epsin homologue) results in what is known as an “uncoupling” phenotype. In these cells, actin polymerizes at the plasma membrane, but the membrane is decoupled from actin forces. This results in actin “flames” at cortical patches without membrane bending (Kaksonen, Sun and Drubin, 2003; Skruzny et al., 2012). A complex formed between Sla1, Pan1 and End3, which links the early coat to other coat proteins and polymerized actin, is involved in actin regulation itself, and connects vesicles to actin cables and endosomes (Wendland and Emr, 1998; Sun et al., 2015; Toshima et al., 2016). These proteins move inward into the cytoplasm with the membrane invagination.

1.3.3.3 Actin module

Once coat proteins are assembled, proteins that nucleate and organize a branched actin network are recruited. Actin filaments are nucleated by the Arp2/3 complex, acting in concert with actin nucleation promoting factors (NPFs): Wiscott-Aldrich syndrome protein (WASP) homologue Las17, type 1 myosins Myo3 and Myo5, intersectin homologue Pan1, and actin binding protein Abp1. Las17 is a potent actin nucleator, without which endocytosis essentially fails (Sun et al., 2006). Myo3/5 are non-processive motor proteins that interact with and can translocate actin filaments, but whose mechanistic contribution to endocytosis is unknown. Deletion of either Myo5 or Myo3 has subtle phenotypes, but deletion of both effectively blocked endocytosis (Sun et al., 2006). Abp1 binds actin filaments and is thought to activate the Arp2/3 complex. Without Abp1, cells are viable, but coat proteins persist on vesicles instead of disassembling after membrane scission. This suggests that Abp1 helps to dismantle the endocytic machinery. In support of this role, recruitment of late-stage enzymes like Ark1 and Prk1 that recycle endocytic proteins after scission to new endocytic sites require Abp1.

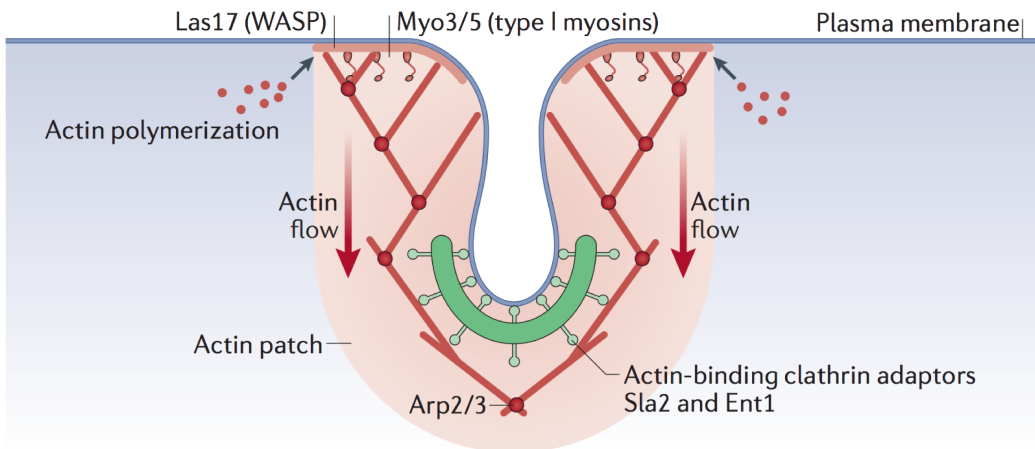


Figure 1.3 – The model for actin-driven membrane invagination in yeast. Actin filaments are nucleated around the base of the invagination by the Arp2/3 complex, which is activated by Las17 and Myo3/5. Actin polymerization at the base pushes the actin network inward into the cell (actin flow). The actin network is coupled to the membrane by Sla2 and Ent1, which is also pulled inward with the actin network as actin filaments polymerize. *Reprinted by permission from Springer Nature: Nature Reviews Molecular Cell Biology (Kaksonen and Roux, 2018), copyright (2018)*

Bbc1, Bzz1, and Vrp1 are other actin associated proteins that are recruited within the actin module. Bbc1 is known to inhibit Las17 NPF activity: its deletion accumulates actin at endocytic sites (Picco et al., 2018). Bzz1, an F-BAR protein, relieves Las17 of NPF activity inhibition by Sla1 (Sun et al, 2006). Vrp1 acts in concert with myosins and Las17 to stimulate the Arp2/3 complex (Anderson et al., 1998; Wong et al., 2010).

Once NPFs and WASP/Myo proteins are recruited, Arp2/3 is recruited and actin polymerization begins. Actin crosslinkers like Sac6 and Scp1, capping protein complexes like Cap1/Cap2, Aip1/Cofilin, Abp1/Aim3 are recruited at this time. This begins the invagination of membrane. Actin monomers are added at the base of the invagination, and the actin network is linked to the membrane via coat proteins Sla2 and Ent1. As actin polymerization progresses, the entire actin network is pushed inwards, taking the membrane along with it (Picco et al., 2015).

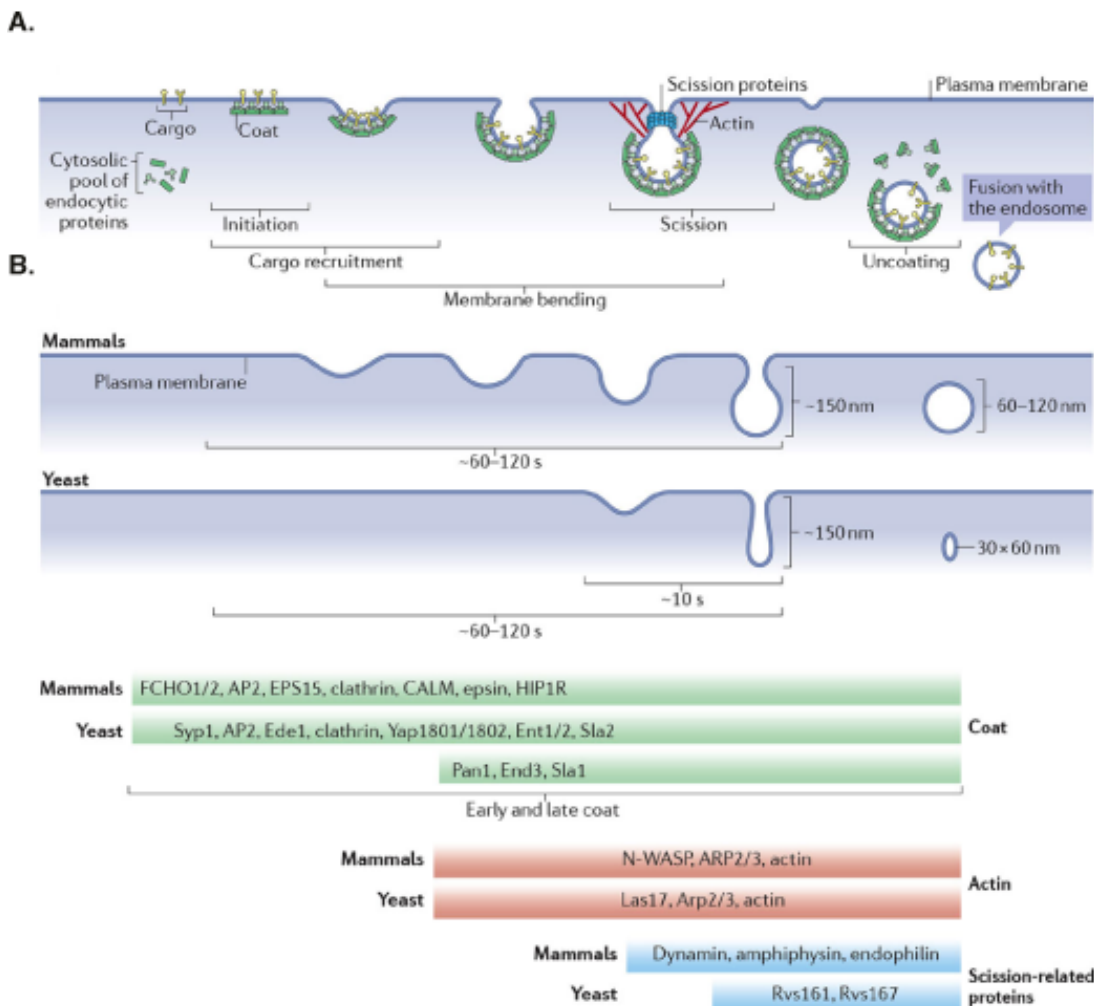


Figure 1.4 – A: Proteins involved in endocytosis are recruited from a cytosolic pool. Initiation of an endocytic event and cargo recruitment is followed by membrane bending. Membrane scission eventually forms a vesicle that releases its coat, allowing it to be transported down the trafficking pathway. **B:** Membrane invagination in mammalian cells results in wider vesicles than in yeast cells. Proteins that are involved in endocytosis can be grouped based on their function in the endocytic pathway. Shown here are the main proteins involved that are conserved between the two species. *Reprinted by permission from Springer Nature: Nature Reviews Molecular Cell Biology (Kaksonen and Roux, 2018), copyright (2018)*

1.3.3.4 Scission module

When the membrane invagination grows about 140nm, scission occurs, forming a vesicle. What actually causes scission in yeast is not yet determined (see Section 1.3.5). The role of the dynamin in yeast endocytosis is unclear so far. N-BAR domain complex Rvs161/Rvs167 (Rvs) is recruited in the late stage of invagination, and membrane scission occurs shortly after it arrives (Kukulski et al., 2012; Picco et al., 2015).

Coat proteins and the actin network are finally disassembled from the vesicle after scission and the nascent vesicle is transported into the cell. Disassembly of coat components are regulated by kinases Ark1/Prk1 that phosphorylate several coat proteins like Sla1, Sla2, and Pan1. Glc17 and its adaptor Scd5 likely dephosphorylate these proteins so that they can be incorporated into a new endocytic event. How the actin machinery is disassembled is not clear. The actin network is constantly assembled and disassembled throughout endocytosis, and growth of the actin network likely indicates that the rate of assembly of filaments is higher than rate of disassembly. NPFs Myosins and Las17 stop being recruited to endocytic sites seconds before scission occurs (Picco et al, 2015), so actin network disassembly is likely a result of a change in the ratio of assembly/ disassembly of the actin network. Disassembly is likely caused by increased rate of disassembly of actin, compared to assembly.

1.3.4 Membrane scission in mammalian cells

1.3.4.1 Scission is dependent on dynamin

In mammalian cells, endocytic membrane scission is primarily effected by the GTPase dynamin. Dynamin was originally discovered as mediating interactions between microtubules (Shpetner and Vallee, 1989). It is now known to play a pivotal role in membrane scission and fusion events at many different cellular organelles. The importance of dynamin in endocytosis was demonstrated in a temperature-sensitive mutant of the *Drosophila shibire* gene, which results in paralysis of flies at the non-permissive temperature. These flies fail to form synaptic vesicles (Grigliatti et al., 1973; Poodry and Edgar, 1979; van der Bliek and Meyerowitz, 1991). *Shibire* codes for multiple isoforms of dynamin that are differentially expressed across the organism (Chen et al., 1991). Knock-down of dynamin isoforms disrupts vesicle-formation after invagination, resulting in accumulation of a large number of long membrane tubes (Ferguson et al., 2009).

1.3.4.2 Dynamin is an oligomeric GTPase

Dynamins consist of a GTPase domain, a stalk region, a bundle signalling element that acts as the linker between the GTPase domain and stalk, a phosphatidylinositol (4,5)-bisphosphate (PtdIns(4,5)P₂, henceforth PIP₂)- binding pleckstrin homology domain (PH) domain and a proline rich domain (PRD) that extends beyond the GTPase domain (Antony et al., 2016). *In vitro*, dynamin oligomerizes into helical structures with the PH domain apposed against the membrane, and the GTPase domain facing away from the membrane (Sweitzer and Hinshaw, 1998; Zhang and Hinshaw, 2001). As depicted in Fig.1.5, dynamin within the helical structure undergoes conformation changes upon GTP hydrolysis that constricts the helix as well as the membrane tube under it, collapsing the inner leaflet of the bilayer membrane into a hemifission state, resulting in membrane fission (Zhao et al., 2016). Disruption of its GTPase activity results in membrane tubes that accumulate dynamin and fail to undergo scission (Takei et al., 1995; David et al., 1996; Ringstad, Nemoto and De Camilli, 1997).

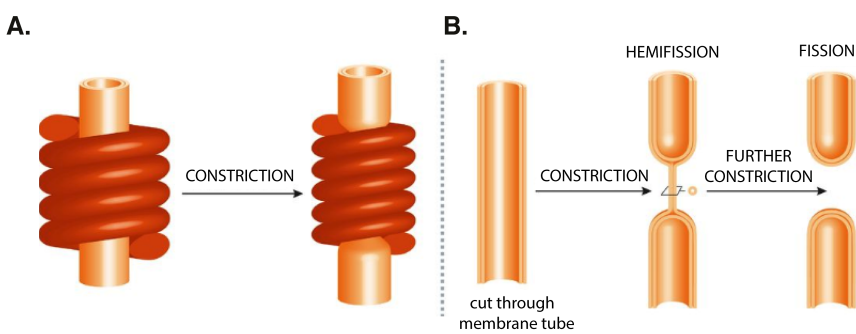


Figure 1.5 – Dynamin-mediated membrane constriction model. Dynamin forms a helical structure around the membrane. GTP hydrolysis constricts the helix and the membrane into first a hemifission state and then to fission. *Reproduced from Antonny et al., under Creative Commons Ctribution Non-Commercial No Derivatives Licence CC BY-NC-ND*

1.3.4.3 Dynamin and BAR proteins interact via PRD and SH3 regions

In vivo, dynamin arrives at clathrin-coated pits via interaction with BAR proteins endophilin and amphiphysin (Ferguson et al., 2009). In addition to the BAR domain, most BAR proteins have additional motifs that mediate their interaction with membranes or other proteins. Some BAR proteins have an N-terminal amphiphatic helix (N-helix) that is inserted into the membrane bilayer. Others have phosphoinositide binding motifs like phox or pleckstrin homology (PH) domains, which direct BAR proteins to specific lipids within membranes. Some BAR proteins contain Src homology 3 (SH3) domains that mediate protein-protein interaction. These SH3 regions act as a scaffold for the proline-rich domains (PRD) of dynamin (Grabs et al., 1997).

Dynamin's PRD interacts with the SH3 domains of BAR proteins endophilin and amphiphysin (Grabs et al., 1997; Cestra et al., 1999; Farsad et al., 2001; Meinecke et al., 2013). Endophilin and dynamin appear to help recruit each other: endophilin recruitment is reduced in the absence of dynamin, and vice-versa. Interaction with the endophilin BAR domain is also known to inhibit the GTPase action of dynamin (Farsad et al., 2001; Meinecke et al., 2013; Hohendahl et al., 2017). Meanwhile, amphiphysin levels are unchanged in absence of dynamin, while deletion of amphiphysin results in increased recruitment and prolonged lifetimes of dynamin and absence of membrane

scission (Meinecke et al., 2013). These results suggest a role for amphiphysin for disassembly of dynamin involving GTP hydrolysis, and a role for endophilin in dynamin assembly. The mechanistic interplay between the two BAR proteins with dynamin is still debated, and the sequence of events that leads to membrane scission remains unclear (Neumann and Schmid, 2013; Hohendahl et al., 2017). Dynamin localization to clathrin-coated pits is not entirely dependent on BAR proteins, but both GTP hydrolysis and interaction with BAR proteins is necessary for efficient vesicle scission in mammalian cells (Shupliakov et al., 1997; Meinecke et al., 2013).

1.3.5 Membrane scission in yeast

1.3.5.1 Yeast dynamin-like proteins

In yeast, three dynamin-like large GTPases have been identified: Vps1, Dnm1, and Mgm1. Dnm1 and Mgm1 are involved in mitochondrial fission and fusion (Cerveny et al., 2007). Vps1 is essential for vacuolar protein sorting (Rothman et al., 1990). It is also involved in fission and fusion of vacuoles (Peters et al., 2004) and peroxisomes (Hoepfner et al., 2001), and is required for regulation of golgi to endosomal trafficking (Gurunathan, David and Gerst, 2002). Vps1 may also arrive at early endocytic events (Nannapaneni et al., 2010). None of the three yeast dynamins have the typical PH domain (Bui et al., 2012; Mousaq et al., 2016) that in mammals interacts with the lipid bilayer. Instead, an “InsertB” region likely performs the same function. Although yeast dynamins also do not have PRDs that could interact with the SH3 domains of yeast BAR proteins, Vps1 has been shown to interact with clathrin and other endocytic proteins (Yu, 2004; Nannapaneni et al., 2010; Goud Gadila et al., 2017), while other work has failed to observe localization of Vps1 at endocytic sites (Kishimoto et al., 2011; Goud Gadila et al., 2017). The role of Vps1 in endocytosis is thus not clear, but it is a candidate for the role of the canonical dynamin in CME.

1.3.5.2 Yeast BAR domain proteins Rvs161/167 regulate scission timing

In yeast, the Amphiphysin and Endophilin homologue is the heterodimeric complex Rvs161/167 (Friesen et al., 2006) (Rvs). Apart from an N-BAR domain, Rvs167 has a C-terminal SH3 domain. Rvs arrives at endocytic sites in the last stage of the endocytosis, and disassembles rapidly at the time of membrane scission (Picco et al., 2015). Deletion of Rvs results in failure of membrane scission in nearly 30% of endocytic events (Kaksonen, Toret and Drubin, 2005). Scission failure is identified by the movement inwards of the endocytic protein coat into the cytoplasm, followed by its retraction back towards the cell wall, indicating a failure to form vesicles. No mutation of other endocytic proteins exhibits this phenotype. Electron microscopy has shown that in *rvs167Δ* cells, vesicles formed are smaller than in wild-type (WT) cells. This profile suggests that although Rvs is not necessary for scission, localization of the complex makes scission more efficient, and influences the invagination length at which scission occurs. Some mutations like that of the yeast syndapin Bzz1 and synaptojanin Inp52 in the background of *rvs167Δ* exacerbates the retraction phenotype (Kishimoto et al., 2011), suggesting that Rvs might act in concert with other proteins.

1.3.5.3 Forces needed for membrane invagination and scission

Forces are required to deform the membrane and pull it inward. In yeast, estimates of these forces are in the order of 1000 - 5000pN (Dmitrieff and Nédélec, 2015), influenced largely by the high turgor pressure within the cells. Intracellular forces of this magnitude are typically provided by components of the cytoskeletal network like microtubules and actin filaments. Disrupting formation of actin filaments completely disassembles the actin network and stops endocytosis (Kübler and Riezman, 1993; Aghamohammazadeh and Ayscough, 2009). A substantial amount of the force required to pull up the membrane therefore comes from actin filament polymerization.

Actin monomers polymerize into filaments at the base of endocytic

invaginations (Picco et al., 2015). Polymerization of actin filaments against a membrane can generate forces that push away this membrane, a mechanism that is employed across many organisms and cell types to produce movement. For example, the bacterium Listeria propels itself across its host cell by high-jacking the actin machinery of its host, and polymerizing an actin “comet tail” behind it.

Simulations show that the highest force requirement for membrane deformation occurs at the beginning of membrane invagination (Dmitrieff and Nédélec, 2015). After a tubular structure is formed, a constant force can continue to pull the tube into the cytoplasm. At the time of scission, rather than a constantly growing actin network, NPF activity has essentially already plateaued (Picco et al., 2015), indicating there is likely less force exerted on the membrane at the time of scission than before scission. It is not clear what causes the final shape transition from membrane tube to vesicle.

Rvs deletion appears to affect this transition, but its mechanistic contribution to this process has not been determined. Since yeast dynamins do not have PRDs, there is probably no interaction between dynamin and Rvs. A mechanism that does not involve PRD-SH3 interactions like in mammalian cells is therefore likely. Several scission models have been presented in the literature so far. They are described briefly below and in more detail in the results section (see Section 3).

1.3.5.4 Proposed scission mechanisms

Although none of the three dynamin-like proteins has a proline-rich domain, increased membrane retractions have been seen in *vps1Δrvs167Δ* cells compared to *rvs167Δ* cells (Rooij et al., 2010), indicating that Vps1 might affect scission.

Another hypothesis is that lipid hydrolysis by yeast synaptojanin-like proteins can cause vesicle scission (Liu et al., 2006). Synaptojanins dephosphorylate PIP₂, a lipid subtype enriched at endocytic sites. In this model, Rvs would form a scaffold on the membrane tube,

protecting the underlying PIP₂. Hydrolysis of unprotected PIP₂ causes a boundary between hydrolyzed PIP₂ at the bud tip and BAR-covered PIP₂ at the tube. This lipid boundary produces a line tension at the interphase between the lipids that could generate enough force to pinch off a vesicle.

In vitro experiments have recently suggested protein friction as a mechanism by which membrane scission could occur (Simunovic et al., 2017). In this model, a BAR domain scaffold exerts a frictional force on a membrane that is pulled under it. In yeast, this pulling force would be generated by actin polymerization, while Rvs scaffolds the membrane tube. Steric pressure exerted on the membrane by disordered protein domains that typically follow the BAR region has also been proposed as a mechanism for scission (Snead et al., 2018). In these experiments, the amphiphysin BAR domain is able to drive scission, but scission efficiency increases three- to four-fold because of the disordered protein regions. These regions do not need to have any specific biochemical properties: they can be replaced by any other disordered protein region. It has also been proposed that BAR domains scaffold membrane tubes and stabilize them, preventing scission (Boucrot et al., 2012; Dmitrieff and Nédélec, 2015). For a more detailed discussion on these models, see Section 3.4.

Many of these models are based on *in vitro* data using mammalian BAR proteins, at protein concentrations orders of magnitude higher than physiologically relevant levels, and without the context of interaction partners, relevant membrane tension, native lipid composition and intracellular turgor pressure. The mechanism for membrane scission in yeast is yet to be determined.

1.4 BAR domain proteins

Proteins in the BAR protein superfamily have a highly conserved BAR domain structure named after their founding members, metazoan BIN/ Amphiphysin and yeast proteins Rvs161/ Rvs167. These proteins are involved in a range of cellular processes including endocytosis, actin organization, cell polarity, transcription and tumor suppression (Sakamuro et al., 1996; Ren et al., 2006).

Of the mammalian isoforms of the founding members, Bin1 (AmphiphysinII) and Bin3 are ubiquitously expressed, while AmphiphysinI is expressed only in neurons. The conserved portion of these proteins, as well as of Rvs161 and Rvs167, is an N-terminal region that forms the BAR domain. This domain typically forms dimers that have an intrinsic curvature defined by the dimerization angle. This curvature categorizes BAR proteins to classical BAR (high curvature), Fer–Cip4-homology-BAR (F-BAR, shallow curvature), and I-BAR (inverted curvature) (FigBARstructure). Membrane-binding is mediated by cationic clusters that bind via non-specific electrostatic interactions to anionic lipids like phosphatidyl serine (PS) or PIP₂.

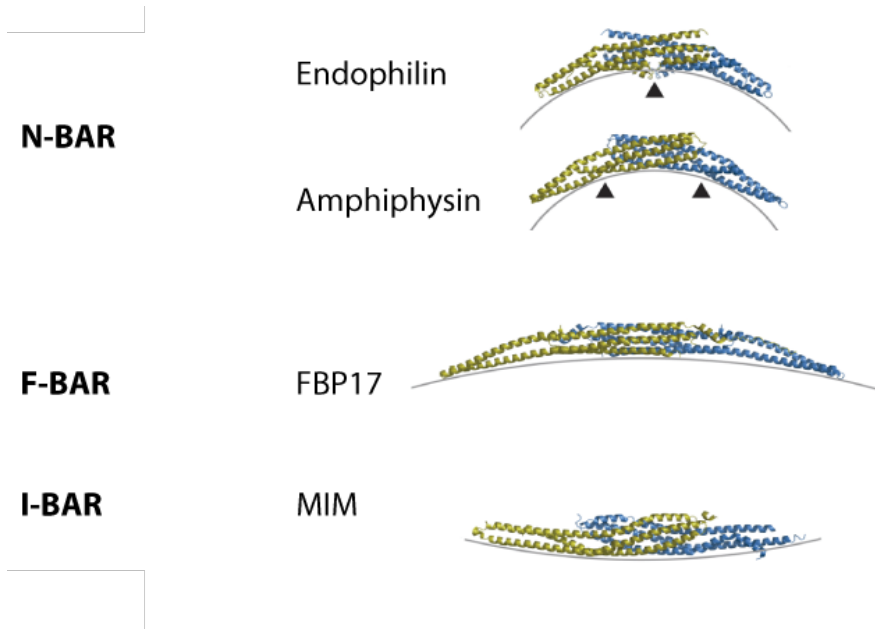


Figure 1.6 – Domain structures from different families of BAR proteins. One monomer is depicted in yellow, the other in blue. Arrow heads indicate positions on the BAR domain that are inserted hydrophobically into the membrane. Adapted with permission from John Wiley & Sons, Inc.: *The EMBO Journal* (Qualmann, Koch, and Kessels, 2011), copyright (2011)

BAR dimers are able to oligomerize and scaffold large areas of membrane. These scaffolds can tubulate and generate curvature across membrane regions much larger than the dimensions of a single BAR dimer (Farsad et al., 2001; Peter et al., 2004) (Fig.1.7). BAR scaffolds can also bind membranes in a curvature-dependent manner. Correlation between the membrane shapes that they bind *in vivo* and their intrinsic curvature has been shown for many BAR proteins. At membranes, they are thought to induce, stabilize, or generate specific curvature.

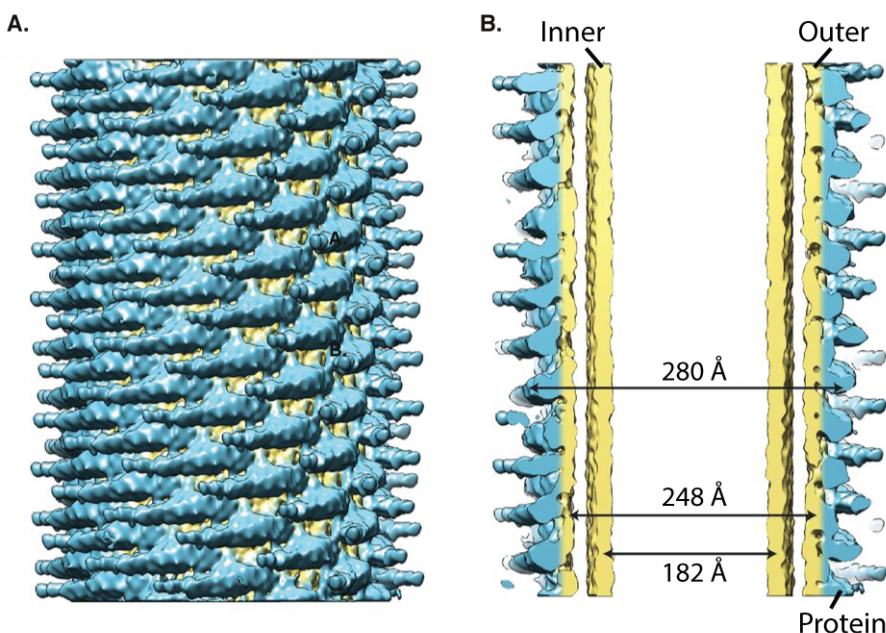


Figure 1.7 – A: 3D reconstruction of amphiphysin-mediated tube from cryo-EM. Protein densities in blue, lipid densities in yellow. B: Inner and outer leaflet of membrane is indicated. Numbers correspond to total diameter, and diameter of inner and outer membrane tubes. *Figure reprinted from (Adam et al., 2015) under creative commons licence CC BY 4.0*

1.4.1 N-BAR proteins and membrane shapes

Classical BAR domain proteins form a crescent-shaped structure. Some of them have an N-terminal helix (N-helix), forming a subclass of classical BAR called N-BAR domains. Two significant endocytic BAR proteins, endophilins and amphiphysins, are both N-BAR proteins. 35-40 residues at the N-terminal region of the genes form the N-helix that acts as an amphiphatic wedge (Peter et al., 2004). This wedge is unstructured until it is inserted into the one leaflet of a membrane (Gallop et al., 2006). Insertion of the wedge into the one leaflet of a membrane

bilayer causes displacement of lipids. This results in a change in the area of one lipid layer compared to the other, which in turn results in bending of the membrane. This indicates that N-helix insertion into a membrane bilayer could favour bending and scission (Kozlovsky and Kozlov, 2003; Boucrot et al., 2012). BAR domains lacking this helix are not able to efficiently tubulate liposomes (Gallop et al., 2006). The N-helix also increases efficiency of binding to liposomes (Farsad et al., 2001) in a curvature-sensitive manner, suggesting that the N-helix likely interacts with membrane curvature additionally to the BAR mechanism.

High-resolution structural data has shown that N-BAR proteins can form helical scaffolds on tubular membranes (Peter et al., 2004; Shimada et al., 2007; Mim et al., 2012). An energetically favourable arrangement of BAR domains consists of dimers parallel to each other, apposed to the membrane. This scaffold favours membrane tubulation and prevents scission by stabilizing the membrane tube (Boucrot et al., 2012). N-helices on the other hand appear to favour vesicle formation. N-helices combined with BAR scaffolds can therefore allow coexistence of both vesicles and tubules, with preference for one or the other depending on the ratio between number of N-helices that favour vesiculation, and BAR generated scaffold stability (Boucrot et al., 2012). Amphiphysin and endophilin can both tubulate membranes (Peter et al., 2004; Gallop, 2006; Mim et al., 2012).

1.4.2 N-BAR Amphiphysin

Two mammalian isoforms of Amphiphysins (Amph) exist. AmphI is enriched in neurons in mammals, while AmphII (Bin1) is expressed in other tissue types, with one isoform enriched in muscle T-tubule junctions (Lee et al., 2002). The only Amphiphysin in flies (d-Amph) is expressed in various tissues, and enriched at muscle T-tubule junctions. The d-Amph dimer forms a coiled coil, with each BAR domain made of three long, kinked alpha-helices (Peter et al., 2004). *In vitro*, liposome tubulation activity of Amphiphysin is concentration dependent. At very high concentrations, Amphiphysin is also able to sever tubular membrane to form vesicles (Peter et al., 2004).

AmphI and II both have BAR domains, a proline rich region, and C-terminal SH3 domain. AmphI binds clathrin and its clathrin adaptor AP2 (Razzaq et al., 2001) and can polymerize clathrin into invaginated lattices in a BAR domain dependent manner (Peter et al., 2004). Both AmphI and AmphII also bind dynamin, and the lipid phosphatase Synaptojanin (Cestra et al., 1999).

1.4.3 N-BAR Endophilin

The EndophilinA1-A3 (EndoA) family of genes were discovered in a screen for SH3 domain containing proteins (Giachino et al., 1997). EndophilinA were subsequently found to co-localize with dynamin, interact with Synaptojanin (Ringstad, Nemoto and De Camilli, 1997) and amphiphysin (Micheva et al., 1997): all three already identified as important regulators of synaptic vesicle recycling by endocytosis. A second mammalian protein was later discovered as related to endophilin, and termed EndophilinB (EndoB).

EndoA1 isoform is found in neurons, EndoA2 is expressed ubiquitously, and EndoA3 is enriched in the brain and testes. All three are found at presynaptic membranes. Crystal structure of EndoA1 shows the same overall structure as that of amphiphysin, with an additional amphiphatic helix similar to the N-helix, located at the centre of the crescent-shaped dimer (Weissenhorn, 2005; Gallop, 2006) (Fig.1.6). This helix is thought to insert into the membrane in the same way as the N- helix, potentially increasing membrane tubulation efficiency. EndoA1 and 2 may interact with calcium channels at synapses, and may be involved in lipid modification (Huttner and Schmidt, 2000; Gallop, Butler and McMahon, 2005), suggesting different roles for the two BAR domain proteins in membrane interaction. Endophilin interacts with dynamin, NWASP and Synaptojanin proteins via its SH3 domain (Cestra et al., 1999; Otsuki, Itoh and Takenawa, 2003; Hohendahl et al., 2017)

1.4.4 N-BAR proteins in yeast: the Rvs complex

RVS161 and RVS167 (Reduced Viability upon Starvation) genes were discovered in a screen that tested yeast cells for survival under starvation conditions (Crouzet et al., 1991). Cells without Rvs genes cannot grow under high salt conditions. They are also sensitive to increased sphingolipid levels, and have random instead of bipolar budding pattern (Bauer et al., 1993; Sivadon et al., 1995; Lombardi and Riezman, 2001; Toume and Tani, 2016). Rvs deleted cells also have aberrations in actin localization: instead of actin patches polarized to emerging buds, patches are homogenously distributed across mother and daughter cells. Loss of Rvs therefore affects localization of actin, and heightens sensitivity of yeast cells to stressful growth conditions.

Rvs161 and Rvs167 are both N-BAR domain proteins that are thought to form obligate heterodimeric complexes (Rvs) *in vivo* (Sivadon, Crouzet and Aigle, 1997; Lombardi and Riezman, 2001). There is some evidence of heterodimerization: loss of one destabilizes the other, deletion phenotypes of Rvs167 is the same as that of Rvs161, and FCCS measurements indicate that they dimerize (Lombardi and Riezman, 2001; Kaksonen, Toret and Drubin, 2005; Boeke et al., 2014). However, Rvs161 functions that do not overlap with those of Rvs167 have been reported. For instance, Rvs161 interacts with Fus2 in cell-cell fusion, while Rvs167 does not (Brizzio, Gammie and Rose, 1998). It is likely that at endocytic sites the Rvs proteins function as heterodimers, while Rvs161 also forms heterodimers with Fus2 during its involvement in different processes.

Rvs161 and Rvs167 are very similar in structure at the N-terminus. Both contain N-BAR domains that are 42% similar, and 21% identical, but are not interchangeable (Sivadon, Crouzet and Aigle, 1997). In addition to the BAR domain, Rvs167 has a Glycine-Proline-Alanine rich (GPA) region and a C-terminal SH3 domain. The GPA region is thought to act as a linker with no known other function, while loss of the SH3 domain affects budding pattern and actin morphology. Most Rvs deletion phenotypes can however, be rescued by expression of the BAR domain alone (Sivadon, Crouzet and Aigle, 1997), suggesting that the BAR domains are the main functional unit of the complex.

Homology modelling has shown that the BAR domain of Rvs167 is similar to amphiphysin and endophilin (Youn et al., 2010), and is therefore likely to function similarly to the mammalian homologues. In keeping with this theory, Rvs has been shown to tubulate liposomes *in vitro* (Youn et al., 2010). While it is known to be involved in the last stages of endocytosis, how the Rvs complex affects scission, and what eventually causes membrane scission are the major questions addressed in this work

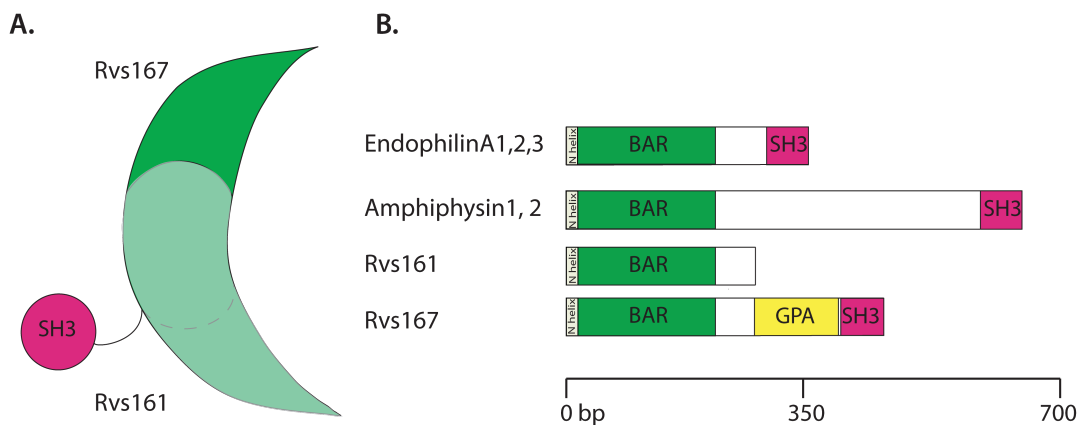


Figure 1.8 – A: Schematic of Rvs dimer. **B:** domain structures of endocytic BAR domain proteins

2 | Aims of the study

The final stage of endocytosis involves breaking a tubular membrane invagination into a vesicle. Over fifty different proteins are involved in establishing endocytic sites and forming an actin network that pulls up the membrane. Only two proteins are definitively involved in the scission stage, Rvs161 and Rvs167, that form the BAR domain protein complex Rvs. Rvs arrives at invaginated membranes. As BAR domains have curved structures, Rvs likely interacts with membrane curvature, but whether it is recruited by membrane curvature is not known. The first part of this thesis address the question of BAR-membrane interaction, and addresses the question:

- How is Rvs recruited to endocytic sites?

Rvs deletion results in a high rate of scission failure, and formation of smaller vesicles than in cells with Rvs, indicating that localization of the complex likely prevents premature membrane scission. In the second portion of this thesis I test several proposed scission mechanisms that could explain the influence of Rvs on scission dynamics. The purpose is to determine, specifically:

- What is the function of Rvs?
- What causes membrane scission?

3 | Results

3.1 Tracking endocytic proteins in yeast

The process of endocytosis can be tracked by following the dynamics of coat, actin, and scission module proteins. Sla1 is a late-stage coat protein. Since coat proteins moves inward with the membrane as it invaginates, Sla1 serves as a marker for membrane invagination and is used throughout this work to track coat movement. In Fig.3.1B, a kymograph of a Sla1-GFP patch at the plasma membrane shows that it arrives at endocytic sites, and then moves inward into the cytoplasm. Abp1, which labels the actin network, moves inward as soon as it arrives at endocytic sites. Rvs167, the scission-stage protein, has a relatively short lifetime, and jumps into the cytoplasm instead of moving gradually.

Averaged centroid tracking in live cells, as described in Picco et al., 2015, can quantify the dynamics of endocytic proteins. Briefly described, yeast cells expressing fluorescently-tagged endocytic proteins are imaged at the equatorial plane. Since membrane invagination progresses perpendicularly to the plane of the plasma membrane, protein patches that move inward with invagination do so in the imaging plane. Centroids of a protein patch at endocytic sites are thus tracked in time. Between 40-50 centroids of each protein are averaged. This provides an averaged centroid that can be followed with high spatial and temporal resolution. When different endocytic proteins are simultaneously imaged with Abp1, Abp1 provides a frame of reference to which all the other proteins can be aligned. Abp1 is used because it is an abundant at endocytic sites and easily imaged.

Averaged centroid tracking, and correlating these centroid movements with membrane shapes acquired by correlative light and electron microscopy (CLEM) allows us to understand the dynamics of these proteins in the context of shape transitions of the membrane (Picco et al., 2015). Correlating membrane shapes acquired from CLEM and centroid movements from live-cell imaging has shown that Sla1 starts to move into the cytoplasm when Abp1, and therefore actin, arrives at sites (Kaksonen, Toret and Drubin, 2005; Kukulski et al., 2012; Picco et al., 2015). Sla1 moves inward with the membrane and follows it through endocytosis. As movement of the coat begins, the Sla1 patch is disassembled, inferred from the decay of the fluorescent intensity of Sla1-GFP (Picco et al., 2015) (Fig.3.1D,E).

Rvs167 localizes to endocytic patches after a membrane tube is formed (Kukulski et al., 2012). Membrane scission occurs at around 60% of its lifetime at sites (Kukulski et al., 2012). At the time of scission, the Rvs167 centroid shows a sharp jump into the cytoplasm, while fluorescent intensity shows a sudden decay, a profile that is unique among endocytic proteins (Kukulski et al., 2012; Picco et al., 2015). The Rvs complex is proposed to form a scaffold at the membrane tube. At scission time, this scaffold is thought to disassemble, resulting in an inward jump of the Rvs167 centroid to protein localized at the newly formed vesicle (Fig.3.1).

Abp1 intensity peaks at scission time and consequently drops, indicating disassembly of the actin network upon vesicle formation. At scission time, the Sla1 centroid has moved about 140nm into the cytoplasm. Sla1 can be tracked about for 2-3 seconds after scission occurs. This portion of the centroid movement is marked by an increase in variability in fluorescent signal, and corresponds to diffusion of the vesicle after scission.

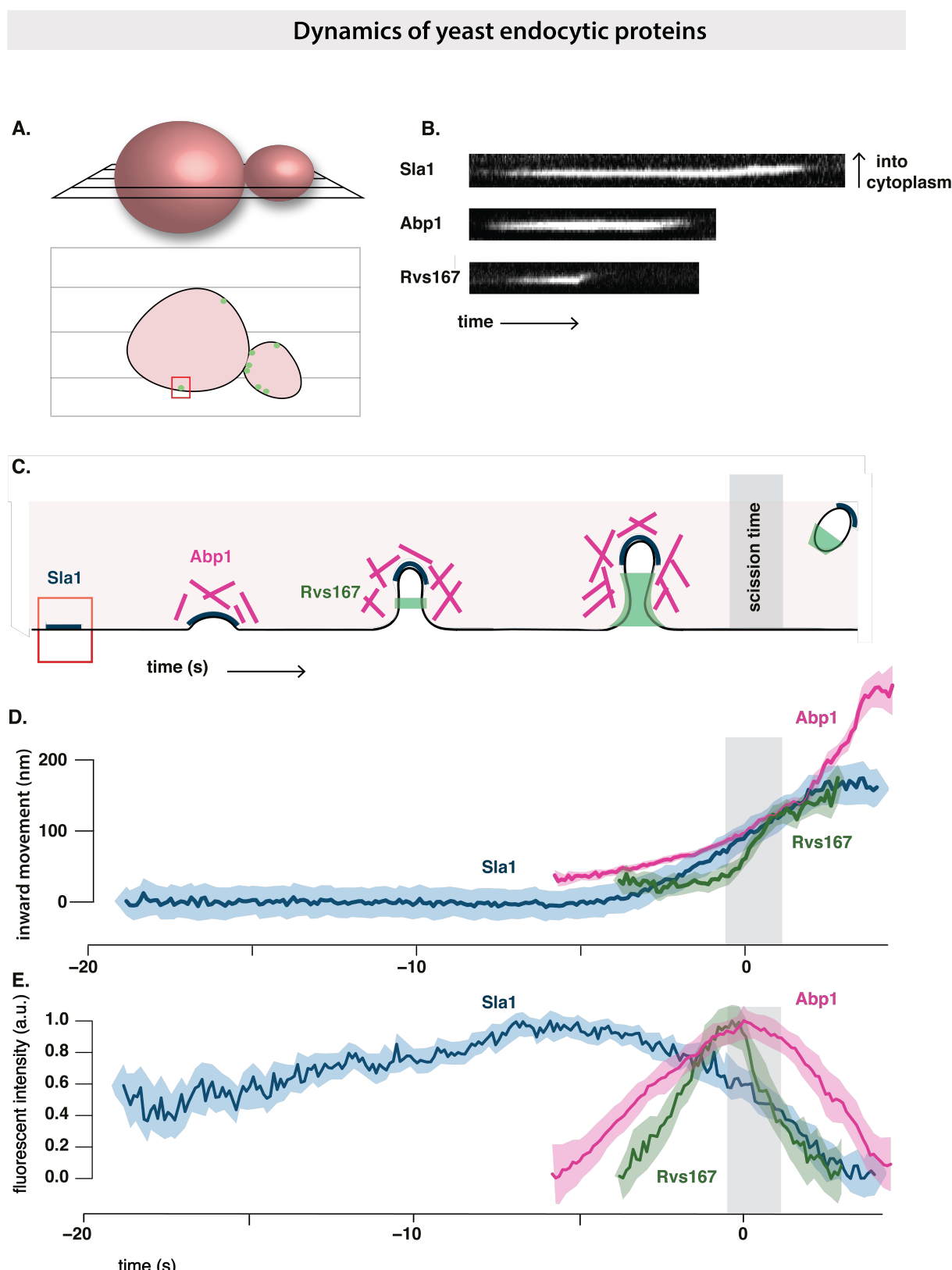


Figure 3.1 – A: Above, schematic of a yeast cell, showing the equatorial plane. Below, cross section of the cell at the equatorial plane, with fluorescently-tagged endocytic protein at the plasma membrane. B: Kymographs of Sla1-GFP, Abp1-GFP and Rvs167-GFP at endocytic sites. Exposure time 80ms. C: Schematic of the timeline of membrane invagination during endocytosis, with Sla1, Abp1, Rvs167 and scission time indicated. D, E: Averaged centroid movement and normalized fluorescent intensity for GFP-tagged Sla1, Abp1 and Rvs167. D and E are aligned in time so that time=0 (s) corresponds to the maximum of fluorescent intensity of averaged Abp1 patches. This corresponds to scission time.

Centroid tracking as in Picco et al., 2015, is used throughout this work to quantify the movement of endocytic proteins. Averaged centroid movement is referred to as just “movement”. Unless indicated otherwise, “scission time” refers to the fluorescent intensity maximum of averaged Abp1 patches. The protein of interest is aligned in the endocytic timeline to “scission time” by simultaneous dual-colour imaging of this protein and Abp1, as in Picco et al., 2015.

Averaging fluorescent intensities from tracking a protein at multiple endocytic sites allows us to also follow the assembly and disassembly of proteins as the membrane inaginates. Scaling fluorescent intensities with a known marker can then provide numbers of molecules of a specific protein (Picco et al., 2015).

3.2 Rvs deletion reduces coat movement

The Rvs complex, as has been discussed in Section 1.3.5.2, is known to have an influence on membrane scission efficiency. Recruitment in the final stage of membrane invagination, localization to the membrane tube, and disassembly concomitant with scission all indicate that Rvs could mechanistically influence the scission process.

In order to quantify what happens in the absence of Rvs, I tracked the Sla1-GFP centroid in *rvs167Δ* cells and compared its movement against WT Sla1-GFP movement. Since Rvs161 and Rvs167 form dimers, deletion of Rvs167 effectively removes both proteins from endocytic sites. 27% of Sla1 patches that begin to move inward retract, consistent with retraction rates measured in other experiments (Kaksonen, Toret and Drubin, 2005). These retractions suggest failed invagination events. Movement of the remaining 73% Sla1 patches were quantified. Sla1 movement in *rvs167Δ* cells and WT look similar up to about 60nm (Fig.3.2).

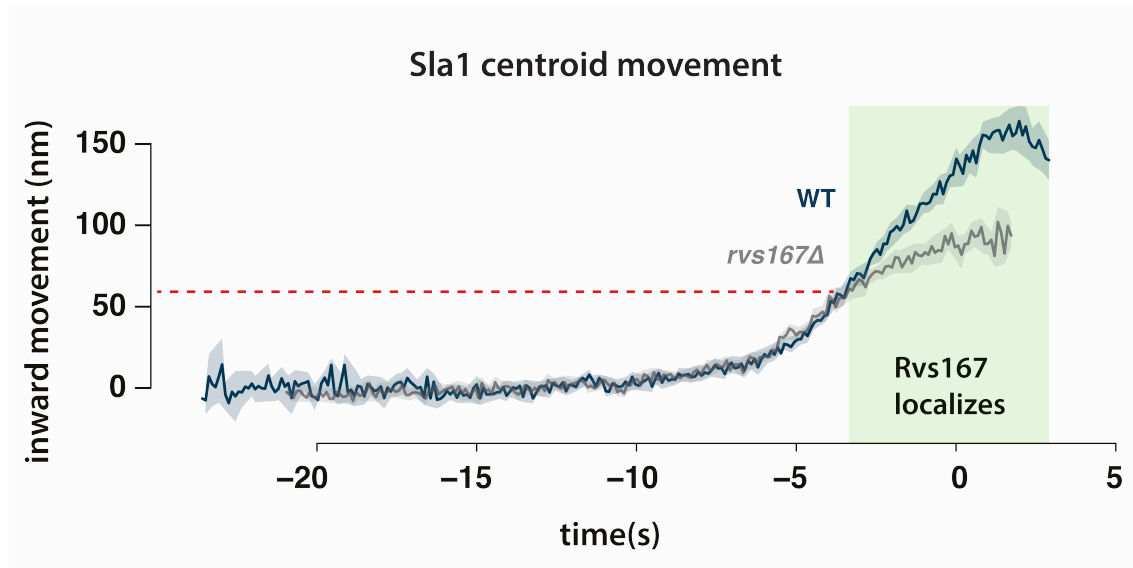


Figure 3.2 – Movement of Sla1 in WT and *rvs167Δ* cells. WT Sla1 is aligned so that time=0 (s) corresponds to scission time. Sla1 centroid in *rvs167Δ* is shifted in time so that it moves inwards at the same time as WT Sla1. Red line indicates approximate start of deviation of *rvs167Δ* from WT.

CLEM has shown that Rvs167 localizes to endocytic sites after the invaginations are about 60nm long (Kukulski et al., 2012). Sla1 movement in *rvs167Δ* shows therefore that membrane invagination is unaffected till Rvs is supposed to arrive. Sla1 in *rvs167Δ* then continues to move at a much slower rate to about 80nm. That membrane scission occurs at shorter invagination lengths than in WT is corroborated by the smaller vesicles formed in *rvs167Δ* cells (Kukulski et al., 2012). Variability in fluorescence intensity of the Sla1 centroid in *rvs167Δ* also increases, similar to WT Sla1 after scission. In WT cells, Sla1 continues to move inward to 140nm. This indicates that first, membrane scission can occur at invagination lengths of 80nm. Then, that the arrival of Rvs prevents membrane scission at 80nm and allows further membrane invagination.

3.3 Recruitment of Rvs and function of domains

Curvature-sensing / generation by BAR proteins

Cellular membrane shape is a result of properties like membrane rigidity, tension, and intracellular pressure, that are all influenced by lipid composition and the proteins embedded in it (Stachowiak, Brodsky and Miller, 2013; Dmitrieff and Nédélec, 2015). Since these properties oppose membrane deformation, energy is required to deform and bend it. BAR domains localize to curved membranes, but they have also been shown to generate membrane tubes and induce vesicle formation, leading to some discussion on the interplay between these functions.

Generating curvature

BAR domains are thought to generate membrane curvature by either scaffolding the membrane or inserting an N-terminal amphipathic helix (N-helix) into the lipid bilayer. Scaffolding refers to interaction between the positively charged concave surface of BAR domains with negatively charged lipids. By attracting lipids to the positive surface, BAR domains are thought to induce membrane curvature. Curvature-generation by scaffolding has been proposed as a function for I-BAR, F-BAR as well as N-BAR domains (Shimada et al., 2007; Frost et al., 2008; Arkhipov, Yin and Schulten, 2009; Saarikangas et al., 2009; Pykäläinen et al., 2011).

N-helices similar to that of NBAR domains can generate curvature independently of the BAR scaffold mechanism (Varkey et al., 2010; Boucrot et al., 2012). Shallow insertion of the N-helix into one leaflet of a lipid bilayer causes the lipids to rearrange, and results in a difference in membrane surface area between the two leaflets (Gallop et al., 2006). This results in membrane curvature.

Sensing curvature

BAR domains show preferential binding to membranes that correlate to their intrinsic curvature: flat F-BAR domain proteins are found at flat membranes, N-BAR domains are found at tubular structures (Henne et al., 2010; Picco et al., 2015). That BAR domains are able to generate curvature does not imply that this is their function. *In vivo*, the significance of curvature-generation is not determined. Tracking over thirty different endocytic proteins in mouse fibroblasts by TIRF imaging showed that Endophilin and Amphiphysin arrive late in the endocytic timeline right before scission (Taylor, Perrais and Merrifield, 2011), suggesting they arrive when membrane tubes are already formed.

Curvature-generation and sensing are likely intrinsically coupled mechanisms. BAR proteins that can induce curvature could also sense curvature: there could be feedback between curvature-sensing and generation. In the case of Rvs, the complex localizes to sites once membrane curvature is established. Whether this localization is dependent on membrane curvature, recognized by the BAR domain is not known.

3.3.1 BAR domains sense membrane curvature

To test whether Rvs is recruited because of membrane curvature, I looked at the recruitment of Rvs167 without the SH3 domain, that is only the BAR domain. Cells that contain only the Rvs167 BAR domain are referred to as BAR cells. I use BAR-GFP to test first whether Rvs167 can localize without the SH3 domain, and then if it does, whether the localization is dependent on membrane curvature.

BAR domains are recruited to endocytic sites

BAR-GFP forms cortical patches (Fig.3.3A) in cells with curvature, so the BAR domain alone is able to localize to the plasma membrane. In yeast cells expressing both BAR-GFP and Abp1-mCherry, BAR-GFP co-localizes with Abp1-mCherry, indicating that BAR domains are recruited to endocytic patches (Fig.3.3A, C).

BAR domains sense membrane curvature *in vivo*

In order to test the curvature dependence of this localization, I compared the dynamics of Rvs167-GFP against BAR-GFP in *sla2Δ* cells (Fig.3.3D-F). Sla2 is a coat protein that acts as a linker between the membrane and actin cytoskeleton. It binds membrane via its N-terminal ANTH domain and actin by the C-terminal THATCH domain. This allows forces generated by the actin network to be transmitted to the membrane (Skruzny et al., 2012). In *sla2Δ* cells, rather than cortical actin patches that transiently co-localize with endocytic coat proteins, an “uncoupling phenotype” is observed (Kaksonen, Sun and Drubin, 2003; Skruzny et al., 2012). Although endocytic coats are formed, and actin is polymerized continuously at these sites, the membrane is not pulled inward, and vesicles are not formed. Forces generated by the actin network are not transmitted to the membrane and the membrane is not curved (Fig.3.3E) . If the BAR localized to endocytic sites by sensing curvature, BAR-GFP would not form cortical patches in *sla2Δ* cells.

Full-length Rvs167 is recruited to the plasma membrane in *sla2Δ* cells (Fig.3.3D,F), along with Abp1. Some Rvs167 patches persist at the plasma membrane, while many are assembled and disassembled. In *sla2Δ* cells expressing BAR-GFP, localization is removed except for rare transient patches at the plasma membrane. This shows that the BAR domain requires membrane curvature to localize. Full-length Rvs167 is able to localize to *sla2Δ* cells, indicating that the SH3 domain helps Rvs localization. This is discussed further in the following section.

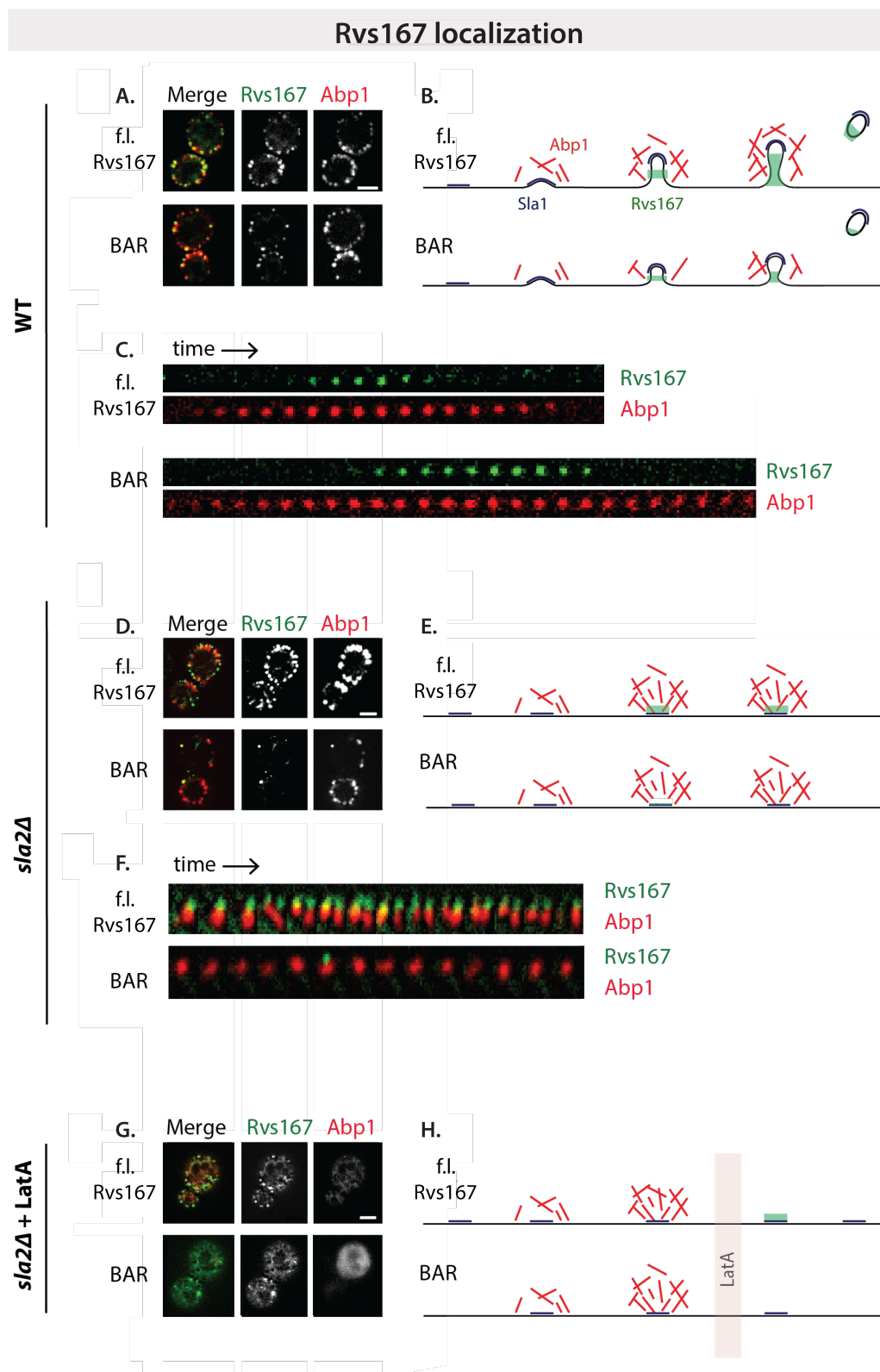


Figure 3.3 – A: Maximum intensity projection of Rvs167-GFP or BAR-GFP, and Abp1-mCherry. Exposure time 250ms. B: Schematic of membrane progression in WT and BAR. C: Montage of Rvs167-GFP and BAR-GFP and Abp1-mCherry. Time between frames 750ms. D: Max. int. projection of Rvs167-GFP or BAR-GFP and Abp1-mCherry in *sla2Δ* cells. E: Schematic of membrane invagination in *sla2Δ*. F: Montage of Rvs167-GFP or BAR-GFP and Abp1-mCherry. Exposure time 1000ms for GFP, 800ms for RFP. G: Max. int. projection of Rvs167-GFP or BAR-GFP and Abp1-mCherry in *sla2Δ* cells after treatment with LatA for 10'. Exposure time 1000ms for GFP, 800ms for RFP. H: Schematic of membrane invagination in *sla2Δ* cells treated with LatA. All scale bars = 2um.

3.3.2 SH3 domains can localize Rvs in an actin and curvature-independent manner

As I show in Section 3.3.1, full-length Rvs167 is able to localize to endocytic patches in *sla2Δ* cells. This localization must be dependent on the SH3 domain, since the BAR domain alone does not localize in *sla2Δ* cells. SH3 domains of Rvs167 are known to interact with many actin associated proteins: an interaction with Abp1 has been shown, as well as with Las17, type I myosins, and Vrp1 (Lila and Drubin, 1997; Colwill et al., 1999; Madania et al., 1999; Liu et al., 2009).

In order to test whether it interacts with an actin binding protein, I imaged BAR-GFP and full-length Rvs167-GFP in *sla2Δ* cells treated with the actin sequestering agent LatrunculinA (LatA). LatA is a sea-sponge toxin that binds monomeric actin and prevents incorporation of actin into filaments. Since high actin turnover is required at endocytic sites, LatA effectively disassembles the actin network, and blocks endocytosis. In *sla2Δ* cells treated with LatA, membrane curvature as well as actin and actin-binding proteins are removed from endocytic sites. Removal of the actin network with LatA is confirmed by imaging Abp1 after treatment.

Surprisingly, full-length Rvs167 is transiently localized to the plasma membrane in *sla2Δ* cells treated with LatA (Fig. 3.3G, H). This localization does not depend on BAR-membrane interaction, since BAR-GFP patches are not seen in similarly treated cells. This suggests that the SH3 domain is able to recruit Rvs to the plasma membrane in the absence of curvature and actin network components. Rvs167-GFP patches are transient, so assembly and disassembly of an Rvs patch can be mediated by the SH3 domain. Localization of Rvs161, which does not have an SH3 domain, is removed by LatA treatment in WT cells (Kaksonen, Sun and Drubin, 2003), supporting the conclusion that the SH3 domain drives the localization of full-length Rvs167 in *sla2Δ* cells, as well as in *sla2Δ* cells with LatA.

3.3.3 Loss of the SH3 domain affects membrane invagination

The BAR domain was expected to act as the functional module of the Rvs complex: phenotypes of *rvs167Δ* such as non-viability on starvation, and mis-localization of actin can be effectively rescued by expression of the BAR domain alone (Sivadon, Crouzet and Aigle, 1997). Since the SH3 domain unexpectedly influences localization of Rvs, I investigated its effect further.

The SH3 domain generally mediates protein-protein interaction by binding to proline-rich sequences that contain a core PXXP motif (Mayer, 2001; Verschueren et al., 2015) (where X is any amino acid). These domains are ubiquitous in cellular interaction pathways, and several endocytic proteins have at least one SH3 domain. Although SH3 domains are abundant, they appear to have specific binding partners. For Rvs167, neither binding partner, nor function of the SH3 domain is clear.

Rvs recruitment and inward movement is reduced in BAR cells

In order to probe the contribution of the Rvs SH3 domain to endocytosis, I compared movement of Rvs167 and BAR centroids, and quantified the number of molecules recruited to endocytic sites. Rvs167 refers to the full-length protein, BAR refers to Rvs167 without the SH3 domain. Fig.3.4C shows that recruitment of BAR is reduced to half that of Rvs167 (57 ± 9.9 for BAR compared to 113.5 ± 5.3 for Rvs167). Cytoplasmic concentration of Rvs167 and BAR are not different (see 3.2). This indicates that although the BAR is expressed at the same level at WT Rvs167, it is recruited less efficiently. The inward jump of BAR is less than that of full-length Rvs167 (Fig.3.4A). The decrease in inward jump indicates that the position of the newly formed vesicle in BAR cells is lower than in WT. This would imply that invagination lengths are reduced in BAR cells compared to WT.

Coat movement and actin recruitment is reduced in BAR cells

Movement of the coat protein Sla1 is similarly reduced (Fig.3.4A). Sla1 moves into the cytoplasm approximately 60nm instead of the 140nm found in WT invaginations. Tubular invaginations are formed in BAR cells, and qualitatively resemble that in WT cells, as seen by CLEM (Fig.3.4E). Invagination lengths in BAR cells measured by CLEM are around $35\text{nm} \pm 13$ (mean \pm standard deviation), compared to WT $107.6\text{nm} \pm 30$. Short invaginations with a maximum of 60nm have been observed in *rvs167Δ* cells by CLEM (Kukulski et al., 2012), which is about the same length as those observed in the BAR cells. Abp1 recruitment in BAR cells is reduced to 50% of WT recruitment, to 172.6 ± 12.9 from 347 ± 30.6 molecules in WT (Fig.3.4C). This data shows that loss of the SH3 domain is detrimental to the progress of endocytic sites.

Rvs recruitment in BAR cells is delayed

To check if there was a change in the timing of endocytic progression, I quantified the lifetimes of BAR, Sla1 and Abp1 in BAR cells using total internal reflection fluorescence (TIRF) microscopy and compared these against WT Sla1, Abp1, and Rvs167. Unlike epifluorescence microscopy at the equatorial plane, in TIRF only fluorophores up to a depth of about 100nm from the glass-sample interphase are excited. This reduces fluorescent signal from the cytoplasm, allowing detection of low intensity fluorescent signal, and is a better method for quantification of protein lifetime than epifluorescence microscopy. Although this method is sensitive to low fluorescent intensity, as the proteins start to move inward into the cytoplasm, fluorescent intensity rapidly drops, because of the limited excitation depth. Therefore, rather than a quantification of the entire lifetime of the protein, this is a quantification of the non-motile lifetime of a protein that arrives at endocytic sites. Non-motile lifetimes of Rvs167, Bar, Sla1 and Abp1 are thus compared between cell types.

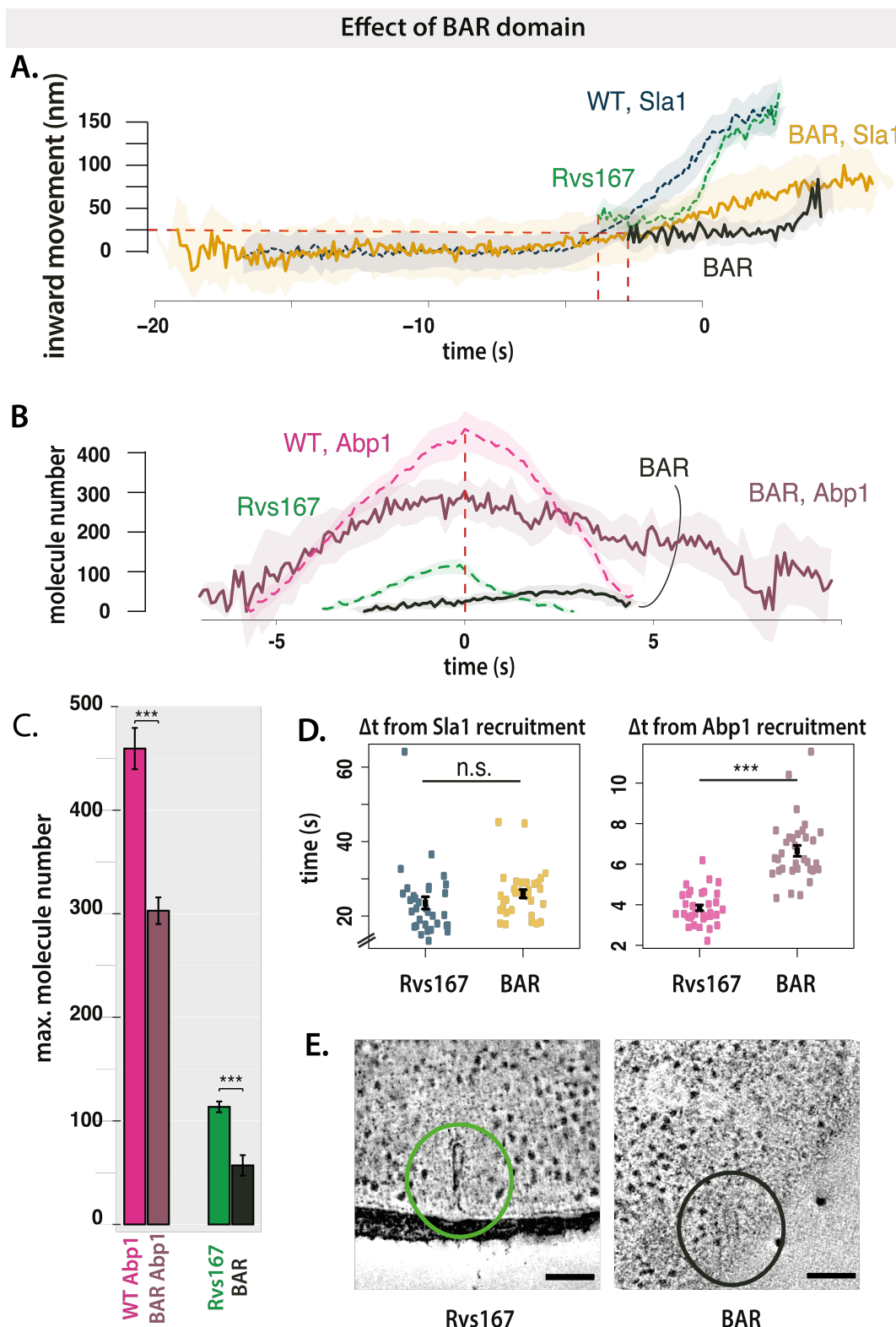


Figure 3.4 – A: Movement of WT Sla1, Rvs167, BAR Sla1 and BAR. All movements are aligned so that time=0 (s) corresponds to scission time. **B:** Molecule numbers in WT and BAR cells. **C:** Maximum molecule numbers and standard error of mean in WT and BAR cells. P-values from two-sided z test, * = $p \leq 0.05$, ** = $p \leq 0.01$, *** = $p \leq 0.001$. **D:** Time between arrival of Sla1 or Abp1 and Rvs167 or BAR. Mean and standard error of the mean are shown. p-values of two-sided t test, * = $p \leq 0.05$, ** = $p \leq 0.01$, *** = $p \leq 0.001$. **E:** Z-stack of slices from reconstructed tomograms of WT and BAR cells expressing Rvs167-GFP or BAR-GFP and Abp1-mCherry. Scale bar=100nm

While lifetimes of Rvs167 and Sla1 are similar in both cell types, there is a significant increase in the lifetime of Abp1 in BAR cells (6). Comparable increase in lifetime of Abp1 is also seen by epifluorescence microscopy (Fig.3.4B). I then looked for differences in the sequence of recruitment of these proteins by looking at the difference in time between recruitment of Sla1 and Rvs167, and the difference in time between recruitment of Abp1 and Rvs167. Time differences are measured from TIRF images of cells expressing Rvs167-GFP and Sla1-mCherry, and BAR cells expressing BAR-GFP and Sla1-mCherry, and similarly for Abp1-mCherry. The time difference between recruitment of Sla1 and Rvs167 is unchanged between WT and BAR cells, while the difference in time between recruitment of Abp1 and Rvs167 is increased in BAR cells (Fig.3.4D).

Taken together these data suggest that the BAR domain alone cannot reproduce the function of the Rvs167 at endocytic sites: recruitment of Rvs, coat and actin dynamics are all affected by the absence of the SH3 domain.

3.4 Function of Rvs

While work in mammalian cells has converged on the idea that membrane scission is caused by dynamin acting in concert with BAR domain proteins, in yeast what causes the final shape-transition from tubes to vesicles is not determined. Several scission mechanisms for yeast endocytosis have been proposed in the last years, in the absence of conclusive mechanistic evidence. We know that Rvs plays a major role in determining the efficiency of membrane scission, and that in its absence membrane invaginations are shorter than in WT. I have therefore focused of models of membrane scission that assign a central role to BAR domain proteins. In the following pages, I discuss their propositions, describe experiments that have tested these mechanisms, and the conclusions they propose.

3.4.1 Hypothesis: Rvs is an interaction surface for membrane constriction by dynamin

Yeast dynamin is the obvious solution to membrane scission. None of the three dynamin-like yeast proteins has a proline-rich domain that typically binds BAR domains, but one of them- Vps1 has been suggested to function like the mammalian dynamin in endocytic scission (Nannapaneni et al., 2010; Rooij et al., 2010). Rooij et al., 2010 propose that Vps1 localizes to endocytic sites at scission stage, and report that in *vps1Δrvs167Δ* cells, rates of coat retraction after invagination increases. Coat retraction after invagination is an indication of membrane scission failure (Kaksonen, Toret and Drubin, 2005). Vps1-GFP does not localize to endocytic sites in Gadila et al., 2017, but localizes to the golgi body and to vacuoles. Kishimoto et al., 2011, do not find a co-localization between Vps1 and Abp1, and find that the *vps1Δrvs167Δ* cells do not show increased coat retraction rates. Vps1 tagged with GFP as well as superfolder GFP, and imaged by TIRF microscopy, fails to co-localize with Abp1 (data from Andrea Picco, not shown). The debate concerning the involvement of Vps1 in membrane scission has been compounded by the possibility that the GFP tag on Vps1 could interfere with its localization to endocytic

sites, and/or its interaction with the Rvs complex. If Vps1 is required for membrane scission, Sla1 would undergo delayed or failed scission in its absence, and Rvs dynamics would be affected.

3.4.1.1 Vps1 does not affect Sla1 or Rvs167 dynamics

I investigated the role of Vps1 by studying coat and scission proteins in *vps1Δ* cells in order to avoid the question of whether fluorescently tagging Vps1 affects its function.

vps1Δ phenotype

vps1Δ cells exhibit a growth defect at 37°C, as has been reported (Rooij et al., 2010). In *vps1Δ* cells, Sla1 accumulates in patches at the plasma membrane, moves inward, and disassembles like in WT. *vps1Δ* does not increase the rate of membrane retraction (Fig.3.5C).

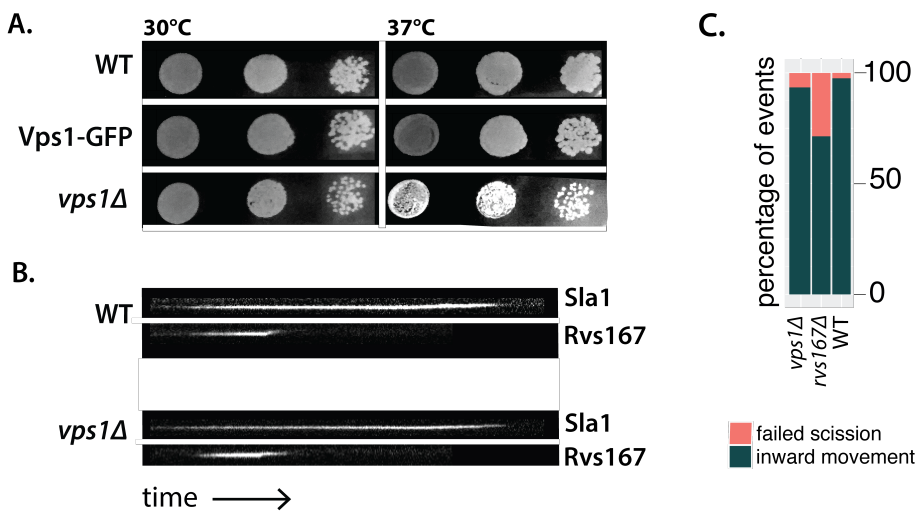


Figure 3.5 – A: Dot spots of yeast cells in WT, Vps1-GFP (diploid), and *vps1Δ* cell at 30°C and 37°C. B: Kymographs of Sla1-GFP and Rvs167-GFP in WT and *vps1Δ* cells. Exposure 80ms. C: Failure rate of membrane scission, in WT, *vps1Δ*, and *rvs167Δ* cells.

Sla1 and Rvs167 in *vps1Δ* cells are unchanged

Centroid movements and intensities of Sla1 and Rvs167 in time are plotted in Fig.3.6A,B. WT Sla1 is aligned so that time=0 (s) corresponds to scission time. Sla1 for *vps1Δ* in Fig.3.5 is shifted in time so that it starts to move inward at the same time as WT. The lifetime

of Sla1-GFP appears to be slightly shortened in *vps1Δ* compared to the WT. However, this shortening occurs early in the lifetime of the protein at endocytic patches, when the molecule numbers of Sla1 are low, and therefore is not likely to be a directly related to the scission process. Later, similar to WT, Sla1 in *vps1Δ* moves into the cytoplasm about 140nm before membrane scission occurs. Sla1 moves inward at the same rate, and to similar maxima as WT, suggesting that membrane invagination is not affected in *vps1Δ* cells.

Dynamics of Rvs167 also remains the same as in WT (Fig.3.5C,D). Magnitude of centroid movement is unchanged, indicating that the base of the vesicle formed is likely at the same position as in WT. Fluorescent intensity shows the typical sharp drop. These data indicate that Vps1 is not involved in regulating membrane scission in *S. cerevisiae*.

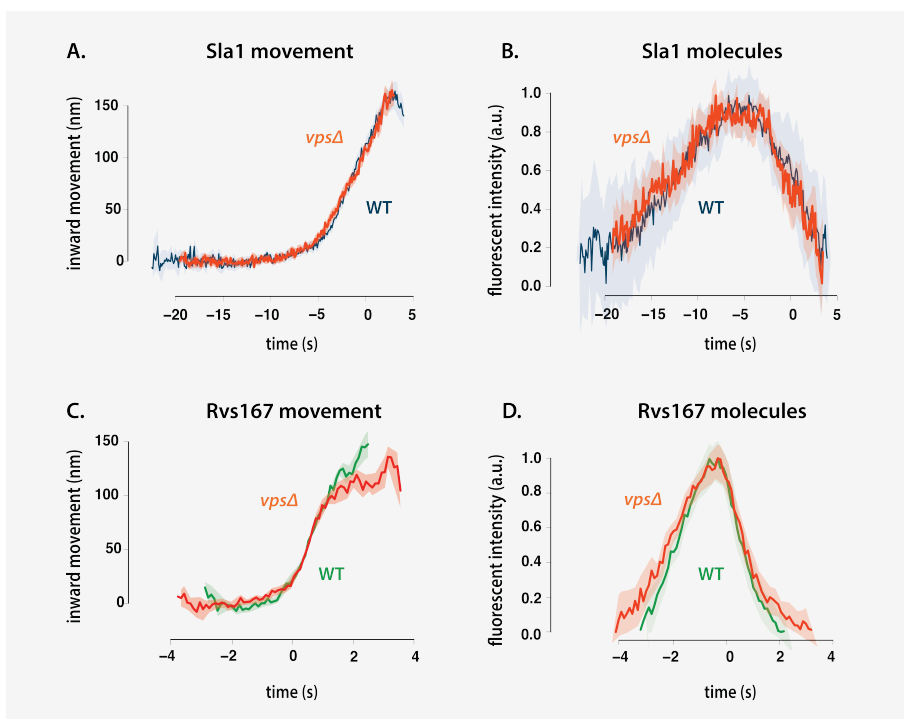


Figure 3.6 – A, B: Movement and normalized fluorescent intensity of Sla1 in WT and *vps1Δ* cells. Time =0 (s) for WT Sla1 centroid corresponds to scission time. Sla1 in *vps1Δ* is shifted in time to begin inwards movement at the same time as WT. C, D: Movement and normalized fluorescent intensity of Rvs167-GFP in WT and *vps1Δ* cells. Time =0 (s) for WT Rvs167 centroid corresponds to scission time. Rvs167 for *vps1Δ* is shifted so that fluorescent intensity maxima is at time=0 (s).

3.4.2 Hypothesis: Rvs barrier causes line tension at lipid interphase, causing scission

Phosphatidylinositols (PIs) and their lipid derivatives play important roles in many cellular processes including membrane trafficking and cell signalling. Conversion between lipid types is driven by kinases, lipases, and phosphatases and controlled throughout the membrane trafficking pathway.

Phosphatidylinositol (4,5)-biphosphate (PIP₂) is an important lipid type found at the cell surface, and is enriched and depleted from endocytic sites at the plasma membrane in concert with the assembly and disassembly of the endocytic machinery. Synaptojanins form a subset of inositol polyphosphate 5-phosphatases that hydrolyze PIP₂ to PI(4)P by removing the phosphate at the 5' position of the inositol ring. They are known to take part in CME and intracellular signalling, as well as in modulating the actin cytoskeleton (McPherson et al., 1996).

In mammalian cells, disruption of Synaptojanin genes results in cellular accumulation of PIP₂ at endocytic sites. Coated vesicles gather at the plasma membrane, suggesting a role for lipid hydrolysis in releasing coat proteins from nascent vesicles. Synaptojanins contain an N-terminal homology domain with the cytoplasmic domain of the yeast SAC1 gene that is implicated in lipid metabolism, actin morphology, and vesicle transport in the secretary pathway (Kearns et al., 1997). A central catalytic domain is then followed by a proline-rich C-terminal region that is the canonical interaction partner of SH3 domains. Synaptojanins interact with actin binding proteins and BAR domain proteins, potentiating also a role in membrane invagination and scission.

The yeast genome encodes for three Synaptojanin-like proteins- Inp51, Inp52 and Inp53- that regulate phospholipid metabolism. In *inp51Δinp52Δ* cells, increased lifetimes of endocytic proteins and produce aberrant membrane invaginations that could indicate scission

failure and defective endocytosis (Srinivasan et al., 1997; Singer-Krüger et al., 1998). *inp52Δ rvs167Δ* cells have increase membrane retraction rates, supporting a possible role for Inp52 in membrane scission (Kishimoto et al., 2011). Loss of Inp51 leads to an increase in bulk PIP₂ level. Changes in PIP₂ levels have not been reported for mutations of Inp52, and are lipid levels not measured locally at the endocytic sites, so the effects of synaptojanin deletion to PIP₂ levels at yeast endocytic sites not established (Stolz et al., 1998; Stefan, Audhya and Emr, 2002).

In a model proposed by Liu et al, 2006, Synaptojanins and BAR proteins interact to regulate PIP₂ hydrolysis, which in turn drives membrane scission. Here, Rvs forms a scaffold on the membrane tube, and protects the underlying PIP₂ from hydrolysis. Synaptojanin arrives at invaginated membranes, and hydrolyses unprotected PIP₂. This generates a boundary between BAR-protected PIP₂ at the tube and hydrolyzed PIP₂ at the bud tip. This lipid boundary produces line tension at the interphase that could generate enough force to pinch off a vesicle.

3.4.2.1 Yeast synaptojanins do not affect coat and Rvs movement

Localization of yeast synaptojanin

Of the three yeast synaptojanins, only Inp52-GFP localizes to cortical patches (Fig.3.7A). Inp51-GFP exhibits a diffuse cytoplasmic signal, while Inp53 localizes to patches within the cytoplasm, likely to the trans-golgi network, as has been noted in other work (Bensen, Costaguta and Payne, 2000). Time alignment with other endocytic proteins, as in Picco et al., 2015 , shows that Inp52 localizes to endocytic sites at the late stage of scission, similar to Rvs. The centroid of Inp52-GFP is localized to the tip of the invaginated tube (Fig.3.7D): spatial and temporal localization is consistent with influence on scission.

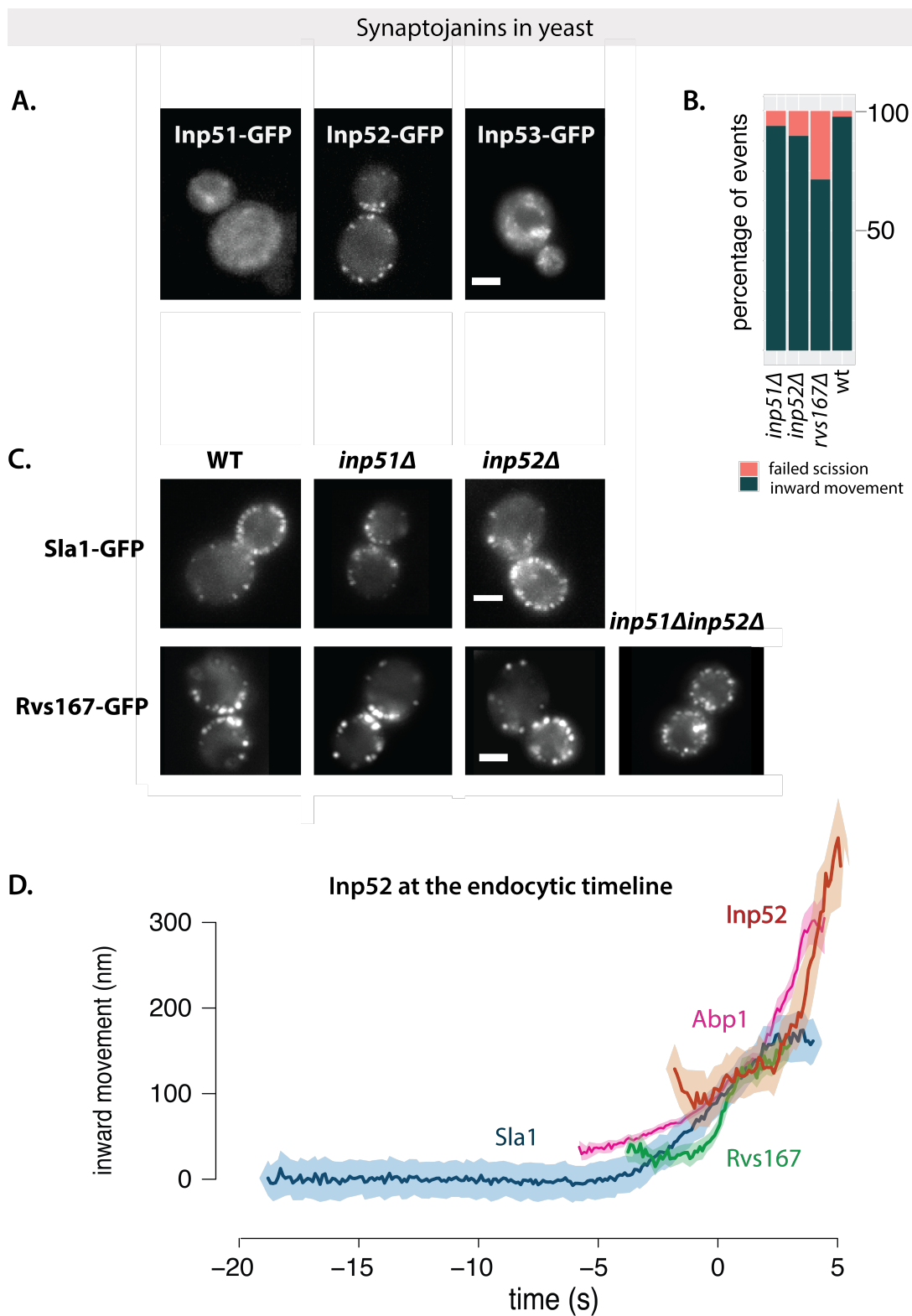


Figure 3.7 – A: Maximum intensity projections of cells expressing GFP-tagged Inp51, Inp52, and Inp53. Exposure time 80ms. B: Retraction rate of Sla1 in WT, *rvs167 Δ* , *inp51 Δ* and *inp52 Δ* strains. C: Maximum intensity projection of Sla1-GFP in WT, *inp51 Δ* , *inp52 Δ* and *inp51 Δ inp52 Δ* cells. Max. int. projection of Rvs167-GFP in WT, *inp51 Δ* , *inp52 Δ* and *inp51 Δ inp52 Δ* cells. D: Localization of Inp52-GFP in endocytic timeline in WT cells. Time=0 (s) is scission time. All scale bars =2um.

Sla1 movement in synaptojanin deleted cells is unchanged

I tested the lipid hydrolysis model described above by studying the effect of synaptojanin deletion on Sla1 and Rvs167. In both *inp51Δ* and *inp52Δ* cells, Sla1-GFP patches are assembled and disassembled, as are Rvs167-GFP patches. Sla1 retraction rates are slightly increased to 12% in *inp52Δ*, compared to 2% in WT, and 6% in *inp51Δ* (Fig.3.7B). In Fig.3.8A, Sla1 movement in *inp51Δ* and *inp52Δ* cells is compared against WT. WT Sla1 is aligned in time so that time=0 (s) corresponds to scission time. Sla1 centroids for *inp51Δ* and *inp52Δ* are shifted so that they begin to move inward at the same time as WT Sla1. All three Sla1 centroids have the same rate of inward movement. While Sla1 in *inp51Δ* moves inward to about the same distance as WT, in *inp52Δ*, the centroid of Sla1 persists for nearly 5 seconds longer than WT (arrowhead in Fig.3.8A). This centroid movement is noisier than the inward movement preceding it, and is likely from post-scission movement of the vesicle, suggesting a delay in the disassembly of Sla1 from the vesicle.

Rvs patches persist after scission in *inp52Δ* cells

Rvs167 dynamics are similar to WT in both *inp51Δ* and *inp52Δ* cells (Fig.3.8C, D). Rvs167 centroids move inward to about the same distance into the cytoplasm as WT when they jump inward. In *inp52Δ* cells, however, Rvs167 patches appear to not disassemble completely (arrowhead in Fig.3.8C) unlike in the WT. Since the delay is at the end of decay in fluorescent intensity, this change in Rvs167 dynamics is likely after vesicle formation. This indicates that there is a delay in the disassembly of Rvs from vesicles in *inp52Δ* cells, similar to the Sla1 delay. Assembly of Rvs167 in the *inp51Δ* takes about 2 seconds longer compared to WT. The implication of this delay is not thus far clear.

The Liu et al., 2006 model predicts that if line-tension from lipid hydrolysis is removed, membrane scission should be delayed or fail. Since the differences in Sla1 and Rvs167 centroid dynamics for *inp52Δ* are post-scission, I find that the data is consistent with a role for Inp52 in removing Sla1 and Rvs167 from vesicles, rather than a primary role in membrane scission.

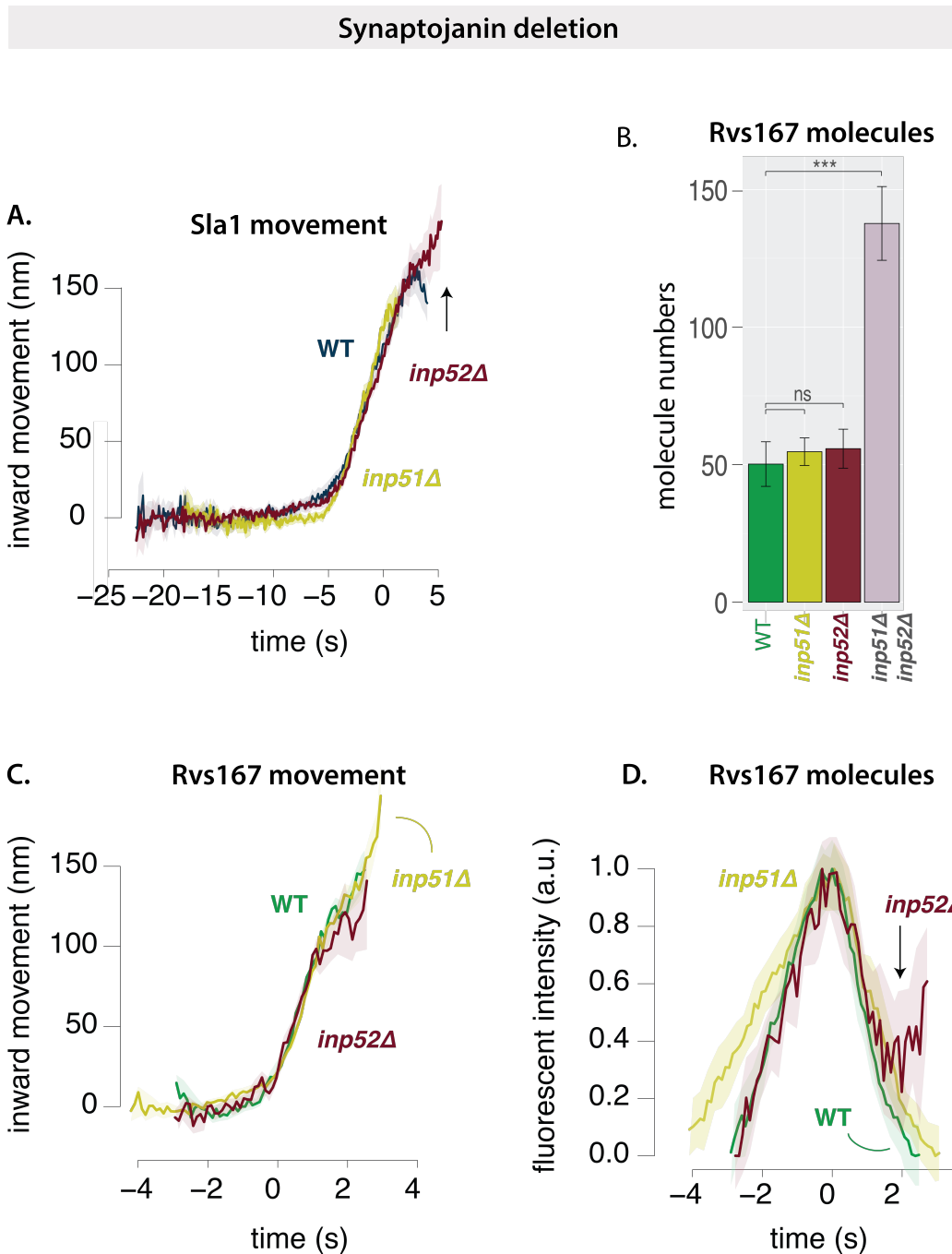


Figure 3.8 – A: Movement of Sla1 in WT, *inp51Δ* and *inp52Δ* cells. Time=0 (s) for WT Sla1 centroid corresponds to scission time. Sla1 centroids for *inp51Δ*, *inp52Δ* are shifted to move inwards at the same time as WT. B: Median number of Rvs167 molecules recruited and standard error of mean in WT, *inp52Δ*, *inp51Δ* and *inp51Δ*/*inp52Δ* cells. P-values from two-sided z test, * = $p \leq 0.05$, ** = $p \leq 0.01$, *** = $p \leq 0.001$. C: Movement of Rvs167 in WT, *inp51Δ* and *inp52Δ*. D: Normalized fluorescent intensity of averaged Rvs167 patches in WT, *inp51Δ*, *inp52Δ* cells.

Rvs accumulates in *inp51Δinp52Δ* cells

I then quantified the number of Rvs167 molecules recruited to endocytic patches in *inp51Δ*, *inp52Δ*, and *inp51Δinp52Δ* cells. WT levels of Rvs167 are recruited in both *inp51Δ* and *inp52Δ* cases. In *inp51Δinp52Δ* cells however, nearly three times as much Rvs is recruited to sites as in WT (Fig.3.8B). Some Rvs167-GFP patches in these cells assemble and disassemble, although the majority persist throughout the imaging time. Many large clusters of Rvs167 are present, and the regular inward jump observed in WT cells is not seen in these mutant cells. Some Rvs167 patches are also seen inside the cell far from the plasma membrane, consistent with observations of Sla1 patches deep within the cytoplasm (Sun et al., 2007). These cytoplasmic Rvs167 patches are likely formed on aberrant membrane invaginations continuous with the plasma membrane. These membranes are able to assemble and disassemble endocytic patches (Sun et al., 2007). Some Sla1 patches are motile in *inp51Δinp52Δ*, and uptake of extracellular membrane appears to proceed in spite of the morphological aberrations (Sun et al., 2007). This means that endocytic membrane scission can occur in these cells.

Analysis of the *inp51Δinp52Δ* phenotype is compounded by the retention of endocytic proteins on vesicles. If Rvs, coat, and other components are not recycled from vesicles, I cannot distinguish between newly forming invaginations and vesicles that remain in the vicinity of these invaginations. Further, this failure to recycle proteins affects recruitment of protein to new endocytic sites and I cannot separate the effect due to failure to recruit protein from a direct effect on scission. That the *inp51Δinp52Δ* phenotype results in more aberrations in Rvs dynamics than single deletions suggests that the two proteins function in separate but partially overlapping pathways (Stolz et al., 1998). Defects caused by *inp51Δ* are then partially compensated for by Inp52, and vice-versa, but deletion of both results in large irregularities in cellular processes.

3.4.3 Hypothesis: Rvs exerts frictional forces on the membrane, causing scission

Recent *in vitro* experiments have proposed BAR-mediated protein friction as a mechanism for membrane scission (Simunovic et al., 2017). In this model, a BAR domain scaffold on a membrane tube forms a frictional barrier to lipid diffusion. Forces that pull on the membrane increase the frictional force exerted by the scaffold on the underlying membrane tube. This leads to membrane thinning in the region not covered by the BAR scaffold, since there is no lipid influx. In turn, this leads to increased membrane tension in this region. Eventually, membrane pores form in this portion of the tube and rupture the tube, forming a vesicle. *In vivo*, the forces pulling the membrane could be provided by actin polymerization. This model predicts that if more BAR proteins are added, and at a faster rate, to the membrane, frictional force would increase. If frictional force increases, scission would occur faster: that is, at shorter invagination lengths compared to a membrane with fewer BAR proteins.

3.4.3.1 Membrane scission is not influenced by Rvs molecule number

To test whether protein friction could effect membrane scission in yeast, I duplicated the RVS161 and RVS167 genes using a method described in Huber et al., 2014. Gene duplication was performed in haploid cells to produce strains that have two copies in tandem of both RVS161 and RVS167 genes (2xRvs complex in haploid, or 2xh). These haploid strains were then mated to generate diploid strains that have four copies of RVS161 and RVS167 genes (4xd). WT diploid strains have two copies of RVS genes (2xd). Cells containing 1x copy of RVS161 and RVS167 (1xd) were generated by crossing an *rvs167Δ* strain with an *rvs161Δ* strain. The diploid strains allows us to compare the effects of a wider range of variation in Rvs gene copy number than haploid cells.

Rvs duplication in haploid cells

Recruitment of Rvs is increased in Rvs duplicated haploid cells

I measured the number of Rvs molecules recruited to endocytic sites in 1xh and 2xh strains. The maximum number of Rvs molecules recruited in the 2xh strain is 178 ± 7.5 , compared to 113.5 ± 5.3 in WT (Fig.3.9C): 1.6x more Rvs is recruited to endocytic sites in the gene duplicated strain. In Fig.3.9C, fluorescent intensity of Rvs167 in 1xh and 2xh cells are shown. Both Rvs167 fluorescent intensity plots are aligned so that time=0 (s) corresponds to their respective maxima. Rvs accumulation takes the same amount of time in 1xh as in 2xh, so rate at which Rvs molecules is recruited to endocytic sites is 1.6x in Rvs duplicated cells (Fig.3.9B, Fig.4.2). A much higher number of Rvs molecules can therefore be recruited to endocytic sites than is recruited in WT cells, indicating that the recruitment of Rvs is influenced by the amount of available protein.

Rvs disassembly is delayed with increased recruitment of Rvs

However, the dynamics of Rvs disassembly are quite different. Fig.3.9C shows that disassembly is slowed by about 1.5 seconds in 2xh compared to 1xh cells. When comparing Rvs movement, (Fig.3.9B), instead of the sharp jump seen in WT, there is a delay in movement into the cytoplasm in 2xh cells. In WT cells, the sharp disassembly of Rvs indicates that all the protein is bound to the membrane: after scission, there is no tubular membrane, so all the Rvs is released at once. The delay in disassembly in the 2xh case then suggests that all the protein is not directly on the membrane, so all the protein is not realeased at once. The change in movement of 2xh Rvs likely also comes from a delay in disassembly, and would suggest that the vesicle has moved some distance by the time the Rvs around the invagination has diassembled.

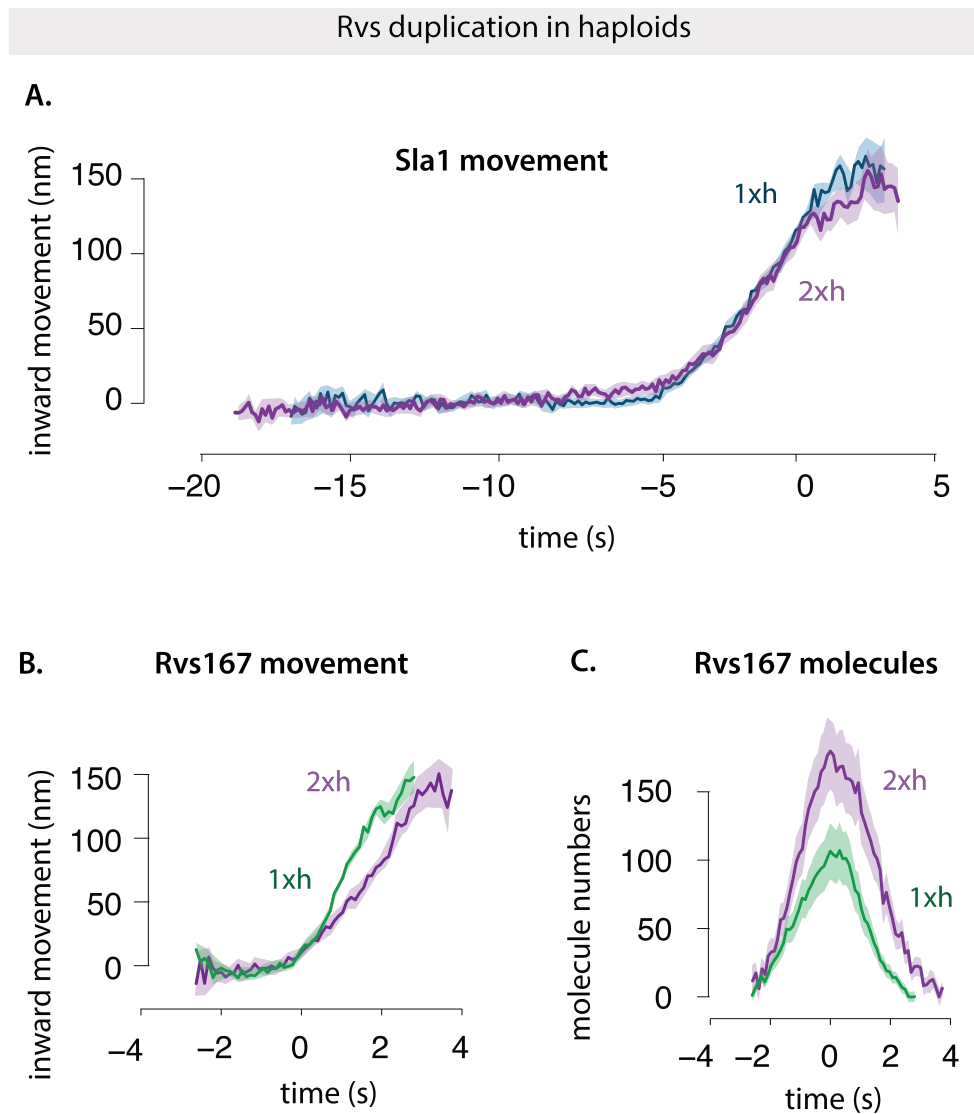


Figure 3.9 – A. Movement of Sla1 in haploid cells containing 1 (WT, 1xh) and 2 copies (2xh) of RVS161, RVS167 genes. Sla1 centroid in 1xh is aligned so that time=0 (s) corresponds to scission time. Centroid of 2xh Sla1-GFP is shifted to move inwards at the same time. **B. C** Movement and molecule numbers of Rvs167 recruited in 1xh and 2xh cells. In B and C, 1xh is aligned to scission time. 2xh is shifted to move inwards at the same time as 1xh

Sla1 dynamics does not change with increased recruitment of Rvs

In Fig.3.9A, Sla1 movement in WT (1xh) and duplicated (2xh) haploids are presented. WT Sla1 is aligned so that time= 0 (s) corresponds to scission time. Sla1 for 2xh is shifted so that it moves inward at the same time as WT. Both Sla1 centroids move inward at the same rate, and to the same distance of 140nm, suggesting that membrane progression is unchanged even if more Rvs is recruited.

Rvs duplication in diploid cells

Rvs dynamics and recruitment changes with Rvs gene copy number

Compared to WT haploid strains, WT diploid strains appear to have more Rvs167-GFP patches (Fig.3.10A). Recruitment dynamics of Rvs in all three are different: in the 4xd strain, Rvs is recruited at a rate of about 51 molecules/second, which is reduced to 27.5 molec./sec. for 2xd and 13.6 molec./sec. for the 1xd. Recruitment of Rvs is not directly proportionate to gene copy number: maximum number of Rvs recruited increases from 101 ± 4.6 in the 2x Rvs strain to 143 ± 5.5 in the 4x strain (Fig.3.10C). In the 1x Rvs strain, a maximum of 80 ± 4.7 molecules of Rvs are recruited. In order to determine whether this is a reflection of protein availability or if something else limits recruitment of Rvs, I quantified the cytoplasmic intensities of Rvs167-GFP in the respective strains, and compared them to the WT intensity. The number of molecules recruited to endocytic sites scales with the amount of protein in the cytoplasm (see3.2, Fig.4.1).

Rvs167 movement and fluorescent intensities are shown in Fig.3.10B,C. Magnitude of inward movement of the Rvs is similar for the 4xd, 2xd and 1xd. In the 1x strain, however, the centroid disappears immediately after scission, suggesting that there is reduced Rvs at the base of the newly formed vesicle compared to the 2xd and 4xd.

Sla1 movement decreases with reduced recruitment of Rvs

In Fig.3.10A, Sla1 in the three cell types are shown. In all cases time=0 (s) corresponds to scission time. Sla1 movement is the same in 4xd and 2xd cells: they move at the same rate, and to the same lengths of about 140nm. In 1xd strain, Sla1 movement rate is the same till about 110nm, and is then slightly reduced. Sla1 movement in 1xd suggests that vesicle scission occurs at invagination lengths about 10nm shorter than that in 2xd and 4xd.

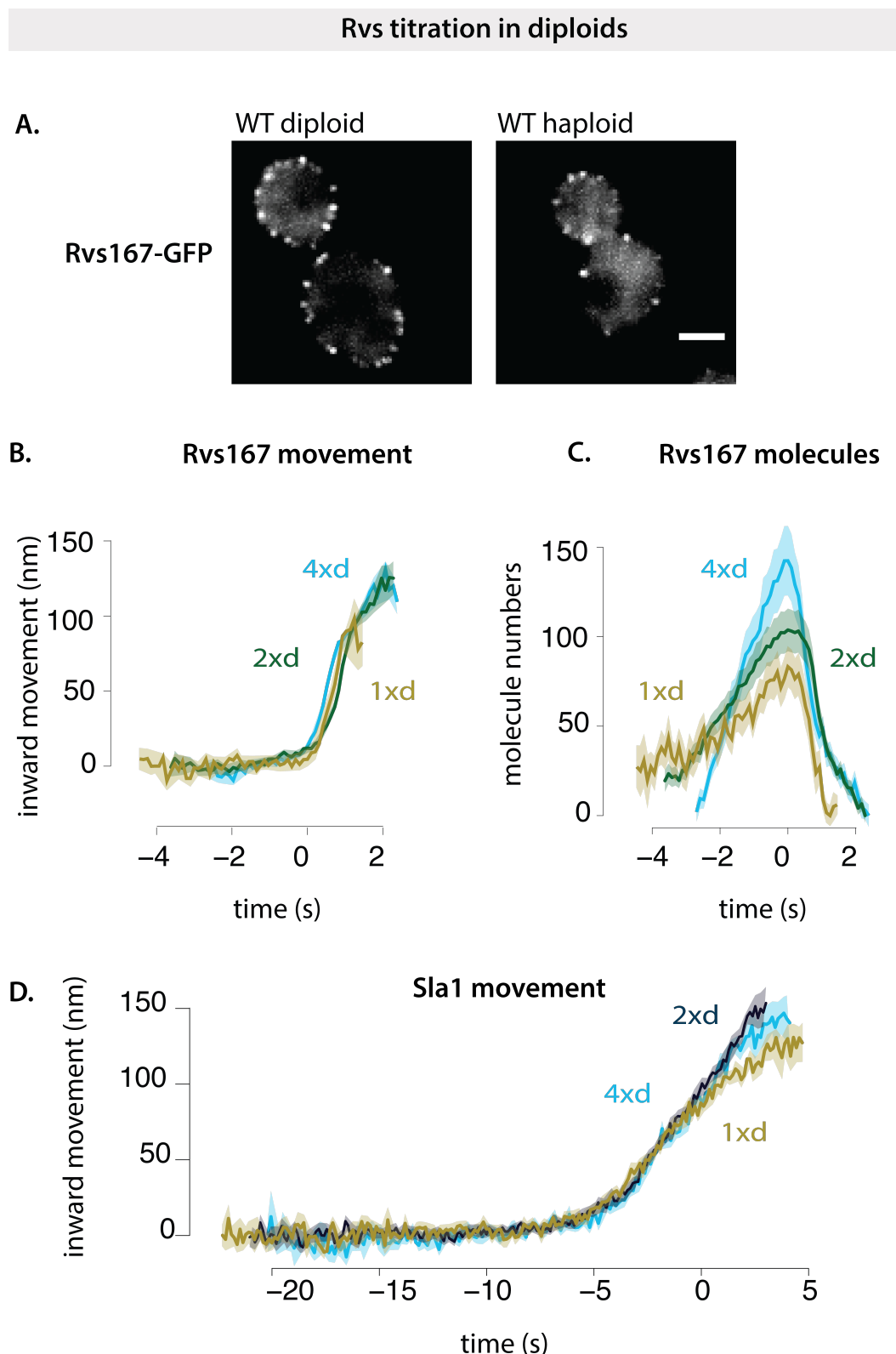


Figure 3.10 – A. Maximum intensity projection of WT haploid and diploid cells expressing Rvs167-GFP. Scale bar =2um. B. Rvs167 movement in diploid cells 1xd, 2xd and 4xd. All are aligned so that time=0 (s) corresponds to maximum molecules recruited. C. Number of molecules of Rvs167 in 1xd, 2xd, 4xd cells. Time=0 (s) corresponds to maximum molecules. D. Movement of Sla1 in 1xd, 2xd and 4xd. Sla1 centroids for 2xd, 4xd are aligned so that Time=0 (s) corresponds to scission time. 1xd Sla1-GFP centroid is shifted to move inwards at the same time as the other two.

Abp1 amount do not change with increasing Rvs recruitment

I measured the amount of Abp1 at endocytic sites in 4xd, 2xd, and 1xd diploid cells. Abp1 numbers provided in Fig.3.11 are quantified in cells containing Rvs167-GFP and Abp1-mCherry. Abp1-mCherry signal was then scaled to Nuf2-mCherry, like in Picco et al., 2015. Fig.3.11 shows that even though the number of Rvs molecules recruited varies depending on the number of Rvs gene copies, the same amount of Abp1 is recruited to endocytic sites in all three cases. In the Abp1 quantification in this case, only one allele of Abp1 is tagged with mCherry, the total amount of Abp1 is therefore likely to be double the numbers reported, although this assumes that labelled and unlabelled Abp1 are recruited at the same rate to endocytic sites.

Rvs gene duplication data suggests that even if Rvs is recruited up to 1.6x faster than in WT cells, the maximum lengths of membrane invaginations do not change. The same amount of Abp1 is recruited irrespective of amount of Rvs, suggesting that membrane invagination is sensitive to amount of Abp1, and therefore actin, rather than Rvs. Sensitivity to the amount of actin suggests that scission timing is likely to be determined by the amount of force generated by the actin network.

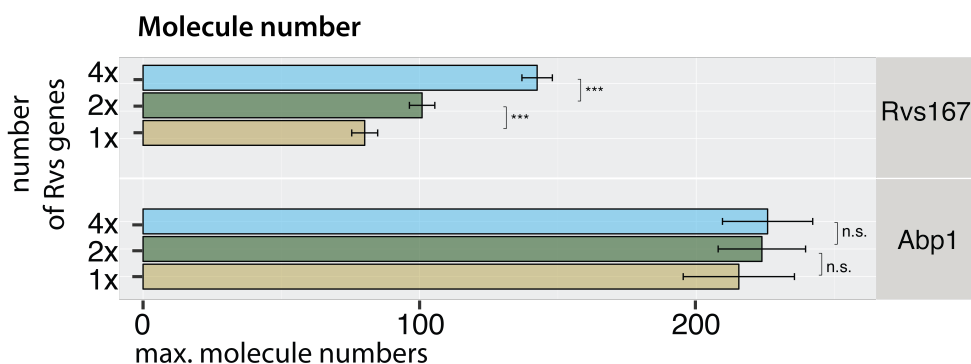


Figure 3.11 – Maximum molecule numbers and standard error of mean of Rvs167-GFP and Abp1-mCherry in diploid strains. Only one allele of Abp1 is tagged with m-Cherry, so double the amount shown here is expected to be recruited. P-values from two-sided z test, * = $p \leq 0.05$, ** = $p \leq 0.01$, *** = $p \leq 0.001$.

3.4.4 Hypothesis: BAR domains scaffold the membrane, preventing scission

As mentioned earlier in Section 3.3, based on the capacity for BAR domains to oligomerize and tubulate liposomes, it has been proposed that membrane scaffolding is their *in vivo* function. As membrane scaffolds, they would impose their own curvature on the underlying membrane and stabilize this shape. There are some requirements for a protein to act as a scaffold (Qualmann, Koch and Kessels, 2011):

1. it must have a defined membrane interface
2. it must have an intrinsic curvature
3. it must be rigid in structure, and
4. its membrane binding surface must be large enough to induce curvature

BAR domains present a curved shape as the membrane interacting surface (Peter et al., 2004; Weissenhorn, 2005; Gallop et al., 2006), and have the capacity to oligomerize into large assemblies on tubes (Takei et al., 1999; Arkhipov, Yin and Schulten, 2009; Mim and Unger, 2012). It has also been shown that the central BAR region is rigid and is required for tubulation (Masuda et al., 2006). BAR domains therefore meet all of these requirements.

It has been shown that BAR domains can prevent membrane scission by scaffolding the membrane, allowing formation of stable tubular structures and preventing vesiculation of these structures (Boucrot et al., 2012). In simulations, adding BAR domains to an invaginating tube removes membrane shape instabilities. Actin forces, membrane rigidity and tension, and turgor pressure result in a wide invagination tip and shrinking tubular region that result in membrane shape instability and therefore scission. Adding curved BAR domains that have a preferred radius of curvature results in stabilization of the membrane shape and prevents scission (Dmitrieff and Nédélec, 2015).

3.4.4.1 Coat movement is influenced by recruitment of BAR domains

As observed in the previous section, Sla1 movement is decreased by reduced recruitment of Rvs, although adding excess protein (compared to the WT protein level) does not affect it. In BAR cells, Sla1 movement is reduced from WT to close to that of *rvs167Δ*. However, Rvs recruitment is also decreased in BAR cells compared to WT. Reduced coat movement therefore could result from loss of the SH3 domain, or from reduced BAR recruitment. To test this, I duplicated, as described before, the BAR domain alone in haploid yeast cells (2xBAR). I then compared Sla1 and Rvs in 2xBAR against BAR (1xBAR), WT Rvs (1xh), duplicated Rvs (2xh), and *rvs167Δ*

Overexpressing BAR domain increases its recruitment

As shown in Fig.3.12B-D, 1x BAR is recruited at low copy numbers compared to WT. Maximum molecules recruited is 57 ± 9.9 , about 50% that of WT. Recruitment of the BAR domain in 2x BAR is 90.58 ± 9.6 , 62% of the WT levels.

Increased BAR recruitment increases Sla1 inward movement

In WT cells Sla1 moves inward at a rate of about 26nm/s. While duplication of the full-length Rvs genes does not change the rate of inward movement of Sla1, total rate of inward movement is reduced to 13.3nm/s in 1x BAR case. This rate increases to about 18nm/s in the 2x BAR case. Adding BAR domain increases the rate of inward movement, as well as the distance Sla1 moves. Movement of Sla1 centroids in *rvs167Δ* cells is similar to 1x BAR case. Increasing the amount of BAR domain recruited to endocytic sites therefore shifts the movement of Sla1 from near *rvs167Δ* lengths to WT lengths (Fig.3.12). Shallow invaginations of the *rvs167Δ* can be rescued by adding Rvs molecules, whether BAR or full-length Rvs. In the 1xBAR case, since less Rvs is recruited, invaginations remain shallow, and the BAR domain has to be overexpressed to be recruited at near WT molecule numbers. This shows that the coat movement is sensitive to the amount of Rvs, and needs only the BAR domain interaction.

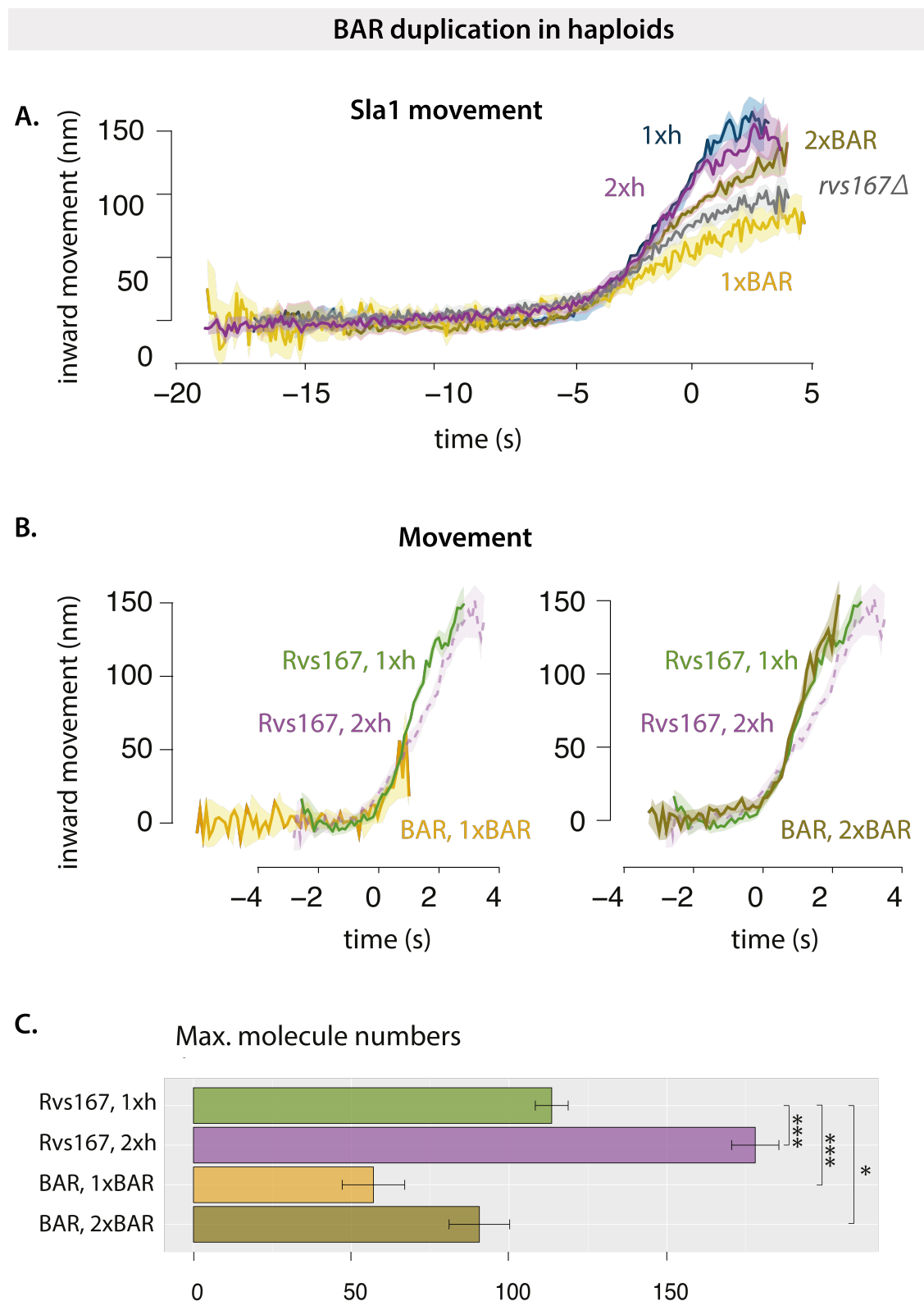


Figure 3.12 – A: Movement of Sla1 in haploid cells consisting of 1 (1xh) and two copies (2xh) of Rvs genes, 1 (1xBAR) and 2 copies of BAR domain (2xBAR) and *rvs167Δ* cells. Time=0 (s) for WT Sla1 is scission time. Other centroids shifted to move inwards at the same time as WT. **B,C:** Movement of Rvs167 in 1xh, 2xh, BAR in 1xBAR, 2XBAR cells. Time= 0 (s) for WT corresponds to scission time. Other centroids shifted to move inwards at the same time as WT. **D:** Maximum molecule number and standard error of mean of Rvs167 and BAR recruited. P-values from two-sided z test, * = $p \leq 0.05$, ** = $p \leq 0.01$, *** = $p \leq 0.001$.

3.4.4.2 Hypothesis2: Rvs is a scaffold against turgor pressure

Intracellular pressure, membrane tension, and rigidity influence the shape of membrane invaginations. In yeast, turgor pressure has been estimated around 0.6 - 0.8 MPa. This pressure pushes the plasma membrane against the cell wall. The endocytic machinery must exert forces to bend and pull the plasma membrane away from the cell wall into the cytoplasm. Large forces from actin polymerization are hence necessary to overcome this resistance to membrane invagination. In Dmitrieff and Nédélec, 2015, simulations show that membrane tension has a negligible influence on forces required to pull the membrane. Shape of the membrane is primarily influenced by membrane rigidity and turgor pressure. Membrane rigidity, which is influenced by the properties of the lipids and proteins embedded in it, influences the shape of the top of the invagination that is pulled up. Actin forces are coupled to the top of the invagination, pulling it up, and turgor pressure pushes against the invagination, constricting the membrane neck.

Turgor pressure can be controlled by osmoregulating agents like sorbitol. Sorbitol treatment causes cells to expel water and increase the internal concentration of osmolytes to match that of the environment. When the cell expels water, it shrinks in size, resulting in a brief decrease of turgor pressure as well as membrane tension. Loss of turgor pressure is compensated by increased glycerol production in cells within 10 minutes of sorbitol treatment.

In *Saccharomyces pombe*, treatment with sorbitol shortens the time between arrival of the coat protein Sla1 and actin-binding protein App1, but does not affect the inward movement of the coat (Basu, Munteanu and Chang, 2014). Sorbitol rescues the invagination defect of partially blocking actin with low doses of LatA. At 0.2M sorbitol, 90% of Sla1 patches in these cells move inward for 50nm instead of 300nm, but retract back to the plasma membrane. These experiments show that some defects in the force generation system can be compensated by lowering turgor pressure.

An extension of the scaffold hypothesis for Rvs is that it protects the

membrane tube against the high turgor pressure inside yeast cells. Reducing turgor pressure could then remove the requirement for Rvs scaffolding.

3.4.4.3 Requirement for Rvs is unchanged by reduced turgor pressure

In order to test if the role of the Rvs scaffold is to counter the membrane constricting effect of turgor pressure, I studied Sla1 and Rvs in WT and *rvs167Δ* cells treated with 0.2M sorbitol. At higher concentrations of sorbitol, cells shrivel and do not recover from turgor pressure loss (Basu, Munteanu and Chang, 2014).

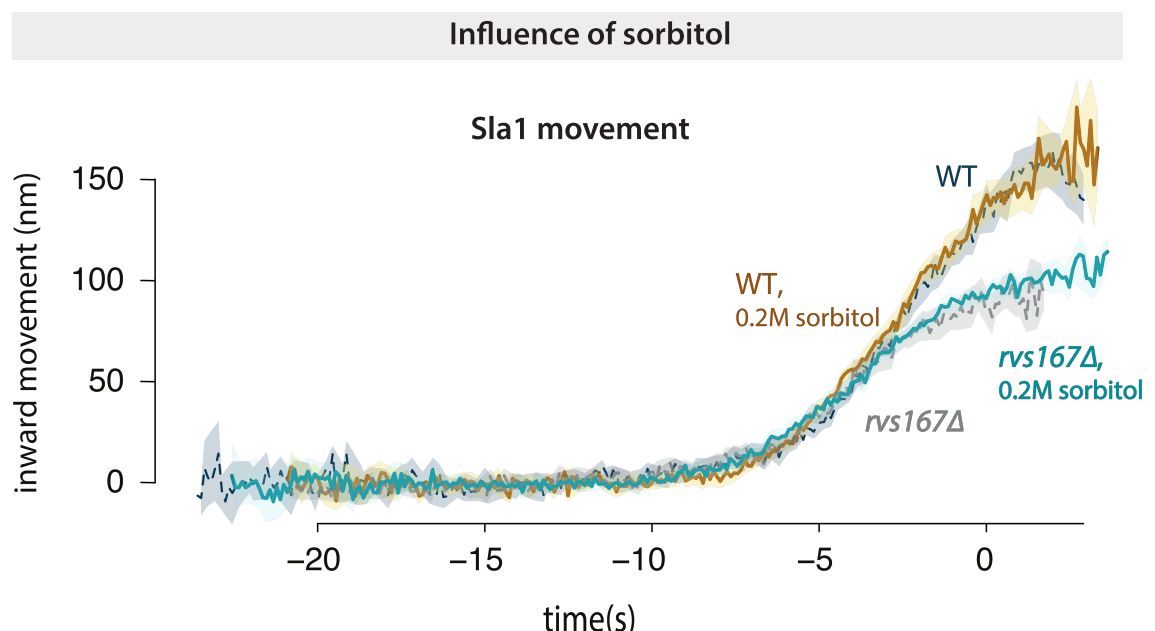


Figure 3.13 – Movement of Sla1-GFP in WT, WT cells treated with 0.2M sorbitol, *rvs167Δ* and *rvs167Δ* cells treated with 0.2M sorbitol. WT Sla1-GFP is aligned to scission time, other centroids moved to move inwards at the same time as WT.

In Fig.3.13, Sla1 movement in WT and *rvs167Δ* cells with and without sorbitol treatment is shown. WT Sla1 is aligned so that time=0 (s) corresponds to scission time. The other three centroid movements are shifted so that they move inward at the same time as the WT. WT cells treated with sorbitol do not show any change in inward movement of Sla1. Both centroids move to the same lengths of 140nm at the same rate, consistent with *S.pombe* data from Basu et al. In *rvs167Δ* cells,

Sla1 moves to about 80nm. In *rvs167Δ* cells treated with sorbitol, there is no difference in Sla1 movement. Both Sla1 centroids move at the same rate, and to the similar invagination lengths. This suggests that the Rvs scaffold does not function to counter turgor pressure.

PLOIDY	PROTEIN	GENOTYPE	MEDIAN NUMBER	S.E.M
Haploid	Abp1	WT	253.1	19.9
	Abp1-mCh	WT	347	30.6
	Abp1	BAR	172.6	12.9
	Abp1-mCh	2x RVS	260.7	21.3
	Rvs167	WT	53.2	5.2
	Rvs167	BAR	30.1	9.9
	Rvs167	<i>inp51Δ</i>	54.7	5
	Rvs167	<i>inp52Δ</i>	55.8	7.1
	Rvs167	<i>inp51Δ inp52Δ</i>	137.7	13.4
	Rvs167	<i>bzz1Δ</i>	49.2	4.8
	Rvs167	2x RVS167	57.3	7.5
	Rvs167	2x RVS	82.7	7.5
	Rvs167	2x BAR	43.6	9.6
	Rvs167	2x BAR, 2x RVS161	41.3	8.4
Diploid	Abp1-mCh*	WT (2x RVS)	131.4	15.8
	Abp1-mCh*	4x RVS	124.1	16.3
	Abp1-mCh*	1x RVS	126.5	20.1
	Rvs167	WT (2x RVS)	55.9	4.6
	Rvs167	4x RVS	63.7	5.5
	Rvs167	1x RVS	44.8	4.7
	Rvs167	Rvs mismatch**	31.1	8.6

Table 3.1 – Median molecule numbers of Rvs167 and Abp1 measured in different yeast strains. *= Number of molecules was quantified in cells containing one tagged allele of Abp1-mCherry. **= 3 copies of RVS167, 2 copies of RVS161

	STRAIN	Rvs167 CYTOPLASMIC INTENSITY (a.u.)	ST.DEV
Haploid	WT (1x RVS)	2633.166	346.67
	2x RVS	4175.517	735.466
	WT (1x RVS)*	1951.611	299.56
	BAR*	2058.02	322.249
Diploid	WT (2x RVS)	3231.935	421.68
	4x RVS	5126.167	607.57
	1x RVS	2503.667	690.38

Table 3.2 – Cytoplasmic intensities measured in different strains.

4 | Discussion

Recruitment and function of the Rvs complex in has been explored in this work, as well as several models for how membrane scission could be effected in yeast endocytosis. I propose that Rvs localizes to endocytic sites by interactions of the BAR domains of the Rvs complex with invaginated membrane, and that the SH3 domain mediated protein-protein interactions are required for efficient recruitment of Rvs to sites. Arrival of Rvs on membrane tube scaffolds the membrane and prevents premature membrane scission,till actin forces rupture the membrane, causing vesicle scission. Effective scaffolding depends on recruitment of a critical number of Rvs molecules. Here I discuss the main findings of this thesis in support of these propositions.

4.1 Recruitment of Rvs to endocytic sites

Rvs is relatively short-lived protein at endocytic sites. It is recruited only once membrane tube is formed (Kaksonen, Toret and Drubin, 2005; Kukulski et al., 2012; Picco et al., 2015). Fluorescence correlation spectroscopy (FCS) measurements have shown that the cytosolic concentration of Rvs167 and Rvs161 is quite high compared to other endocytic proteins (Boeke et al., 2014). Many endocytic proteins like Las17, Vrp1, type1 myosins, are measured at 80-240nM, while cytosolic concentration of Rvs161 and 167 is 721nM and 354nM respectively. In spite of this, relatively few numbers of Rvs are recruited to endocytic sites, suggesting that cytosolic concentration does not determine recruitment. Comparison between FCS measurements of cytoplasmic concentration for different endocytic proteins, and their recruitment to the endocytic sites indicates low correlation between

the two, perhaps unsurprisingly, requiring that other directed mechanisms recruit proteins in a timed and efficient manner. In the case of Rvs, both timing and efficiency appear crucial to its function, the question is what confers both.

4.1.1 BAR domain senses membrane curvature

The curved structure of BAR dimers (Peter et al., 2004; Mim et al., 2012) has suggested that Rvs is recruited by its preference for some membrane shapes over others, supported by its arrival at curved membrane tubes. In the absence of membrane curvature, in *sla2Δ* cells, the BAR domain alone does not localize to cortical patches (Fig.3.3D-F). This demonstrates for the first time that the BAR domain does indeed sense and requires membrane curvature to localize to cortical patches. Work on BAR domains have proposed that electrostatic interactions at the concave surface and tips of the BAR domain structure mediate membrane binding (Qualmann, Koch and Kessels, 2011). Mutations in these lipid-binding surfaces would clarify the interaction with underlying lipids, and test if Rvs relies on similar interactions.

4.1.2 BAR domain times recruitment of Rvs

BAR is able to localize to endocytic sites, and has a similar lifetime in WT cells (Fig.3.3, Fig.3.3.3). In Fig.3.3.3B we see that while the full-length Rvs167 arrives about 4 seconds after the arrival of Abp1, BAR arrives only 6 seconds after Abp1 arrives. There is a time delay between Abp1 recruitment and BAR arrival, compared to the arrival of full-length Rvs167, confirmed by the TIRF measurement in 3.3.3D.

The delay in recruitment could occur because the membrane has not acquired the required invagination length or because the loss of the SH3 domain causes delayed recruitment. That the delayed recruitment occurs because the invagination takes longer to reach a particular length is supported by the fact that Sla1 moves inwards at a slower rate in BAR cells. It takes longer for the membrane in BAR cells to reach the same length as WT. Rvs167 arrives in BAR cells when

Sla1 has moved inwards 25-30nm (dashed red lines in Fig.3.3.3A), which is also the distance Sla1 has moved when Rvs167 arrives in WT. By the time Sla1 has moved this distance, the membrane is already tubular (Kukulski et al., 2012; Picco et al., 2015), consistent with Rvs arrival at invaginated tubes. This suggests Rvs recruitment is timed to specific membrane invagination length- therefore to a specific membrane curvature- and that this timing is provided by the BAR domain.

4.1.3 SH3 domain makes Rvs recruitment efficient

As seen in Fig.3.3.3C, Rvs167 in BAR cells accumulates to about half the WT number, even though the same cytoplasmic concentration is measured. This indicates that the SH3 domain increases the efficiency of recruitment of Rvs. Either SH3 domain helps recruitment to endocytic sites, or it stabilizes interaction with sites. In *sla2Δ* cells, full-length Rvs can assemble on the membrane (Fig.3.3D-F). Since BAR domains alone do not localize to patches in *sla2Δ* cells, full-length localization must be mediated by the SH3 domain, supporting a role for the SH3 domain in increasing recruitment of Rvs by clustering protein molecules.

4.1.4 The SH3 domain can independently assemble and disassemble Rvs molecules

As mentioned above, in *sla2Δ* cells, full-length Rvs167 is able to assemble and disassemble at cortical patches without the curvature-dependent interaction of the BAR domain (Fig.3.3D-F). This unexpected finding indicates that the SH3 domain is able to mediate both the recruitment and the disassembly of Rvs at the endocytic site.

In *sla2Δ* cells treated with LatA (Fig.3.3G-H), actin-based membrane curvature is inhibited, and the actin patch proteins are removed from the plasma membrane. Full-length Rvs167 in these cells still shows transient localizations at the plasma membrane (Fig.3.3A). In *sla2Δ* cells treated with LatA, the localization of BAR is lost. This suggests that localization of the full-length Rvs167 in LatA treated

cells is dependent on an SH3 domain interaction, and that this is independent of both actin and membrane curvature.

4.1.5 SH3 domain affects actin dynamics

In WT cells, the Abp1 and Rvs167 fluorescent intensities reach maxima concomitantly, and the consequent decay of both also coincide. That this occurs at the same time indicates that upon vesicle scission, the actin network is immediately disassembled. Membrane scission essentially occurs around the intensity peak of the two proteins. This coincident peak is lost in BAR cells. Rvs in these cells peaks several seconds after Abp1 intensity starts to drop, and the decay of Abp1 is prolonged, taking nearly double the time as in WT. As we see in Fig.3.3.3C, the number of Abp1 molecules recruited is decreased to about two thirds the WT number. Although it is not clear what the decoupling of Abp1 and Rvs peaks means, the changes in Abp1 dynamics suggests a strong disruption of the actin network. SH3 domains are known to interact with components of the actin network like Abp1 and Las17 (Lila and Drubin, 1997, Madania et al., 1999), but study of other components of the actin machinery will be required to understand how exactly loss of the SH3 has changed the progression of endocytosis.

4.1.6 What does the SH3 domain interact with?

SH3 interaction with an endocytic binding partner could help recruit Rvs to endocytic sites. Many such interaction partners have been proposed. Abp1 interaction with the Rvs167 SH3 domain has been shown (Lila and Drubin, 1997; Colwill et al., 1999), as has one with WASP protein Las17 (Madania et al., 1999; Liu et al., 2009), yeast Calmodulin Cmd1 (Myers et al., 2016), type I myosins (Geli et al., 2000), and Vrp1 (Lila and Drubin, 1997). These proteins are currently being studied as potential targets of the Rvs167 SH3 domain. All of these suggested binding partners localize to the base of the invagination (Yidi Sun, 2006; Picco et al., 2015), and do not follow the invaginating membrane into the cytoplasm. If one of these is the SH3 interaction partner, SH3 domains interact with the endocytic network at the base of the invagination. Centroid tracking however,

suggests that Rvs is accumulated all over the membrane tube without bias towards the base of the invagination. If Rvs was recruited to the base and pulled up as the invagination grows, the centroid would move continuously upwards rather than remain relatively non-motile before the jump at scission time. It is possible that the SH3 initially helps cluster near the base, and as the membrane invaginations grow longer, BAR-membrane interactions dominate.

4.1.7 Total number of Rvs recruited is independent of cell ploidy

When ploidy is doubled from haploids to diploids, we could expect that double the protein amount is expressed and recruited, but it does not appear so. The amount of Rvs recruited in WT haploid (1xh) and diploids (2xd) remains about the same, and cytoplasmic signal is similar (Fig.4.1). This invariance between accumulated protein in haploids and diploids shows that Rvs recruitment is not determined by the number of alleles of Rvs. Haploid and diploid cells appear to tune the amount of Rvs recruitment to get a specific amount to endocytic sites.

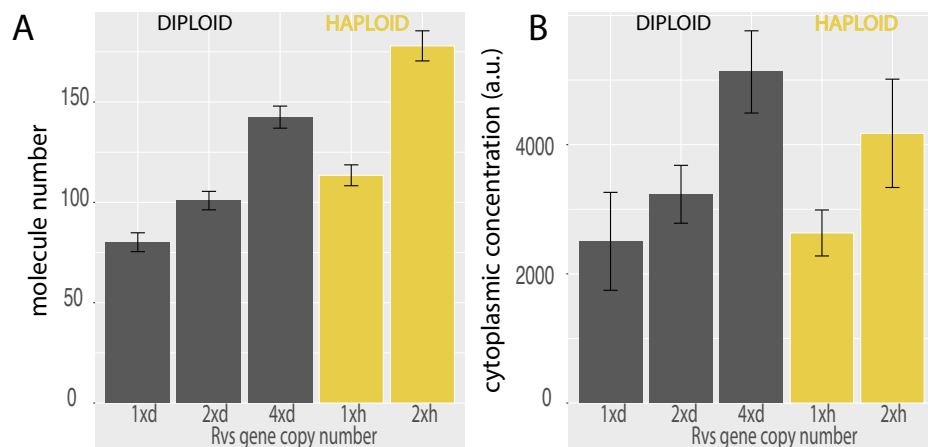


Figure 4.1 – A. Maximum molecule number of Rvs167-GFP recruited with S.E.M in haploid and diploid cells with different gene copies of Rvs. B. Cytoplasmic signal of Rvs167-GFP with standard deviation in haploid and diploid cells with different gene copies of Rvs.

4.1.8 Rvs recruitment rate increases with increasing gene copy number

WT diploids (2xd) contain two copies each of RVS161 and RVS167 genes. Rvs duplicated diploids, which contain four copies each of RVS167 and RVS161 (4xd) could be expected to express and recruit to sites twice the amount of Rvs as 2xd. However, compared to 2xd, cytoplasmic signal in 4xd increases by 1.6x and recruitment of Rvs167 to endocytic sites increases only by 1.4x. Doubling the gene copy number increases, but does not double protein expression or recruitment in the case of Rvs. Similarly, duplicating Rvs genes in haploid cells results in an increase in number of molecules recruited, but not in doubling (1xh, 2xh). Although the rate of adding Rvs is different in haploids and diploids, in both cases, it increases by gene copy number (yellow line in Fig.4.2).

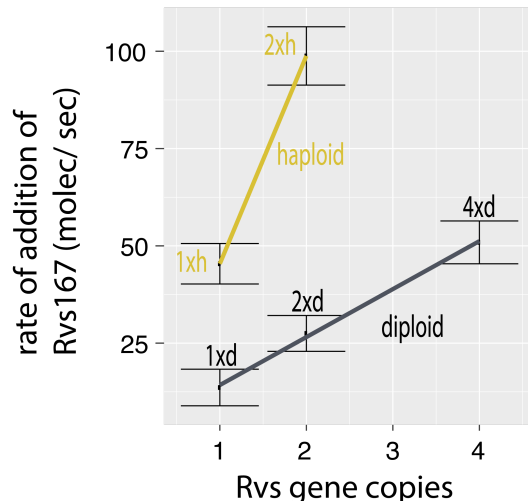


Figure 4.2 – Rate of Rvs molecules added to endocytic sites vs. gene copy number in haploids and diploids. Standard error of mean of the molecule numbers recruited, and linear fit through the data is shown.

Cytoplasmic protein concentration is increased when gene copy number is increased, and recruitment to endocytic sites is increased by the increase in cytoplasmic concentration. These data suggest that the amount of Rvs that is recruited scales with available concentration of protein. Comparing across ploidy however, the rate of Rvs recruitment is lower in WT diploid compared to WT haploid (2xd vs 1xh, Fig.4.1)

in spite of the same cytosolic concentration of Rvs in both. The reason for this is not clear.

4.2 Arrangement of Rvs dimers on the membrane

A homology model of the Rvs BAR dimer structure based on Amphiphysin suggests that it has the concave structure typical for N-BAR domains. Rvs is a hetero- rather than homodimer unlike Amphiphysin, and a high-resolution structure will be necessary to clarify the interaction and arrangement of Rvs on endocytic tubes. There are some indications from the experiments in this thesis however, regarding its interaction with the membrane.

4.2.1 Rvs does not form a tight scaffold on membrane tubes

In vitro helices of BAR domains have suggested that Rvs might form a similar helical scaffold. The number of Rvs molecules recruited to endocytic sites is high enough to cover the surface area of the tubular invagination, so it has been proposed that an Rvs scaffold covers the entire membrane tube up to the base of the future vesicle (Picco et al., 2015).

In Rvs duplicated diploid cells (4xd), Rvs can be recruited at a much faster rate than in the WT (2xd) (Fig.3.10B-C, Fig.4.2) while disassembly dynamics is the same in both (Fig.3.10C, Fig.4.3). The exponential decay of fluorescent intensity in WT haploid and diploid cells (1xh, 2xd, Fig.4.3) indicates that all of the protein is suddenly disassembled from the endocytic site. When the membrane tube undergoes scission, there is no more tubular curvature for the Rvs to bind to. The sharp decay is therefore consistent with a BAR scaffold that breaks upon vesicle scission because there is no more membrane interaction, releasing all the membrane-bound protein at once.

A similar decay in the 4xd strain suggests that all the Rvs in this case is also bound to the membrane: if the protein was not bound to the membrane, fluorescent intensity would not decay sharply. Since the membrane is able to accommodate 1.4x the amount of BAR protein as the WT, it would suggest that at lower protein amounts, a tight helix that covers the entire tube is not likely. Adding molecules to a tube already completely covered by a scaffold would result in a change in Rvs assembly and disassembly dynamics.

Further, additional molecules would have to be added at the top or base of a tight scaffold. At the top, the radius of curvature is decreased compared to the tube since this is the rounded vesicle region. At the base, the plasma membrane is nearly flat, and the Rvs BAR domain is similarly unlikely to favour interactions here. Otherwise the scaffold would have to be disrupted to add new molecules, which would likely slow down recruitment rate rather than speed it up. Molecules could also be added concentric to an existing scaffold. However, the concave surface of Rvs is known to interact with lipids, and multiple layers of BAR domains on the membrane tube would probably not show the sudden disassembly seen here.

I assume that the membrane surface area does not change in the 4xd compared to 2xd from the identical movement of Sla1 in both cases (Fig.3.10A). It is possible that a wider tube is formed, which would increase the membrane surface area for BAR binding. This would, however, require the BAR domains to interact with a lower radius of curvature than in WT. This seems unlikely, and in the absence of any indication otherwise, I assume that the membrane tubes in all diploid and haploid cases have the same width.

4.2.2 A limit for how much Rvs can be recruited to the membrane

In the case of Rvs duplication in haploids (2xh), a change in disassembly dynamics is seen (Fig.3.9C, Fig.4.3). In 2xh, the maximum number of molecules recruited is 178 ± 7.5 compared to the maximum of 113.505 ± 5.2 in WT (1xh). This means that nearly 1.6x the WT

amount of protein is recruited to membrane tubes in the 2xh case. The Rvs167 fluorescent intensity in 2xh shows a delay in disassembly. This suggests that the excess protein may not be directly on the membrane, since if the protein was membrane bound, when the membrane breaks, the protein must be released. The excess Rvs could either interact with the actin network via the SH3 domain, or interact with other Rvs dimers. By a similar argument as in 4.2.1 above, I do not expect that multiple layers of BAR domains are formed, and that the excess protein is recruited by the interaction of the SH3 domain.

Another explanation for the delayed disassembly is that at high concentrations of Rvs like in the 2xh case, a tight BAR scaffold is formed, and the BAR domains interact with adjacent BAR domains. When the membrane undergoes scission, the protein is no longer membrane-bound, but lateral interactions delay disassembly of the scaffold. Lateral interactions between neighbouring BAR dimers have been shown in the case of Endophilin (Mim et al., 2012). It is not currently clear where the Rvs molecules are added in the 2xh case: superresolution microscopy could clarify whether it is added at the membrane tube.

Whatever the arrangement of the Rvs complex on the membrane, disassembly dynamics is changed in the case of 2xh, compared to the other haploid and diploid strains. Since the number of Rvs molecules is highest in this strain, this suggests that there is a limit to how much Rvs can assemble on the tube without altering interaction with the endocytic protein network.

5mm

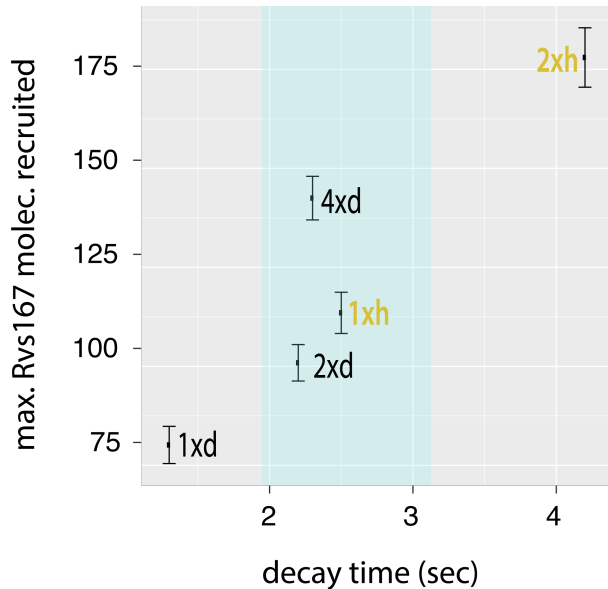


Figure 4.3 – Time from peak of Rvs167 fluorescent intensity to minimum intensity, against maximum molecule numbers recruited. Coloured region highlights similar disassembly time for increasing amounts of molecules recruited.

4.2.3 Conclusions for Rvs localization

All of these data support the idea that Rvs recruitment rate and total numbers are determined by concentration of protein in the cell. The maximum number of molecules that can interact with the membrane is limited by the surface area of the invagination. Although more can be recruited, Rvs molecules over a certain threshold interact in a different way with endocytic sites, possibly via the SH3 domain. Timing of recruitment to sites is by curvature-recognition via the BAR domain, while efficiency of recruitment and interaction with the actin network is established via the SH3 domain.

4.3 What causes membrane scission?

4.3.1 Dynamin does not drive scission

Some studies have suggested that dynamin-like Vps1 localizes to endocytic sites, and affects the scission mechanism: Nannapaneni et al (Nannapaneni et al., 2010), find that the lifetimes of Las17, Sla1, Abp1 increase in the absence of Vps1. Rooij et al (Rooij et al., 2010), find that Rvs167 lifetimes increase, and are recruited in fewer patches to the cell cortex. On the other hand, *vps1Δ* did not increase the scission failure rate of *rvs167Δ* in other studies (Kishimoto et al., 2011), and did not co-localize with endocytic proteins (Goud Gadila et al., 2017). If Vps1 was to affect scission, the number of failed scission events should increase in *vps1Δ* cells, but I do not find so, confirming other studies (Kishimoto et al., 2011). Vps1 tagged with GFP and imaged in TIRF does not form cortical patches that co-localize with Abp1-mCherry (data from Andrea Picco, not shown). GFP-tagging could affect the recruitment of Vps1 to endocytic sites while maintaining its role in other pathways of vesicular trafficking. Membrane movement and scission dynamics are however, unchanged in the absence of Vps1. If loss of Vps1 prevented or delayed scission, the membrane would continue to invaginate longer than WT lengths, and Sla1 movements of over 140nm should be observed. Rvs centroid movement would likely also be affected: a bigger jump inwards could indicate that a longer membrane has been cut. My observation that there are no changes in the behaviour of coat and scission markers indicates that even if Vps1 is recruited to endocytic sites, it is not necessary for Rvs localization or function, and is not necessary for scission.

4.3.2 Lipid hydrolysis is not the primary cause of membrane scission

In this model, synaptojanins hydrolyze PIP₂ that are not covered by BAR domains, resulting in a boundary between hydrolyzed and non-hydrolyzed PIP₂. The model predicts that interfacial forces generated at the lipid boundary causes scission (Liu et al., 2006). Inp51 is not seen in patches at the cellular cortex, but this could be because protein

recruitment is below our detection threshold. Inp52 localizes to the top of invaginations right before scission, consistent with a role in vesicle formation (Fig.3.7D). Some predictions of the lipid hydrolysis model are inconsistent with our data, however.

First, vesicle scission is expected to occur at the interphase of the hydrolyzed and non-hydrolyzed lipid. Since the BAR scaffold covers the membrane tube, this interphase would be at the top of the area covered by Rvs. Kukulski et al., 2012 have shown that vesicles undergo scission at 1/3 the invagination length from the base: that is, vesicles generated by the lipid boundary would be smaller than have been measured. Second, removing forces generated by lipid hydrolysis by deleting synaptojanins should increase invagination lengths, since scission would be delayed or it would fail without those forces. Deletion of neither Inp51 nor Inp52 changes the invagination lengths: Sla1 movement does not increase. That the position of the vesicle formed is also unchanged compared to WT is indicated by the similar magnitude of the jump into the cytoplasm of the Rvs centroid.

There are some changes in the synaptojanin deletion strains (Fig.3.8). In *inp51Δ* cells, Rvs assembly is slightly slower than that in WT. Therefore, Inp51 could play a role in Rvs recruitment. In the *inp52Δ* strain, about 12% of Sla1-GFP tracks retract, indicated that scission fails in those cases. Although this is low compared to the failed scission rate of *rvs167Δ* cells (close to 30%), this data could suggest a moderate influence of Inp52 on scission. Rvs centroid persists after scission for about a second longer in *inp52Δ* cells than in WT, indicating that disassembly of Rvs on the base of the newly formed vesicle is delayed.

In *inp51Δinp52Δ* cells, Rvs is accumulated at patches, but majority of Rvs patches do not show the typical sharp jump into the cytoplasm. Membrane morphology is hugely aberrant in these cells, complicating interpretation of this data (Srinivasan et al., 1997). Electron microscopy shows long, undulating membrane invaginations (Srinivasan et al., 1997). Fluorescence microscopy shows that multiple endocytic sites that are assembled and disassembled at these long invaginations,

and fail to undergo scission (Sun et al., 2007). Where on these long membranes Rvs localizes could be clarified by CLEM or super-resolution microscopy. Large clusters of Rvs seen in the *inp51Δinp52Δ* strain could be multiple Rvs patches on same membrane tube. Pooling signal from multiple endocytic sites would influence the molecule numbers acquired by our analysis, and yield a higher number than at a single site. Rvs does, interestingly, assemble and disassemble in these mutants. If no vesicles are formed at these membranes, it would indicate that Rvs disassembly is not caused by membrane scission.

4.3.3 Protein friction does not drive membrane scission

Protein-friction mediated membrane scission proposes that BAR domains induce a frictional force on the membrane, causing scission. In Rvs duplicated haploid cells (2xh), adding up to 1.6x the WT (1xh) amount of Rvs to membrane tubes does not affect the length at which the membrane undergoes scission (Fig.3.9). The model introduced in Section 3.4.3 predicts that if more BAR domains were added to the membrane tube, frictional force generated as the membrane is pulled under it will increase, and the membrane would rupture faster. That is, membrane scission occurs as soon as WT forces are generated on the tube. Since BAR domains are added at a faster rate in the 2xh cells, these forces would be reached at shorter invagination lengths. In 2xh cells, WT amount of Rvs is recruited at about 1.8 seconds before maximum fluorescent intensity, but scission does not occur at this time. Instead, Rvs continues to accumulate, and the invagination continues to grow. In diploid strains, adding 1.4x the WT amount of Rvs in the 4x Rvs case also does not change length of membrane that undergoes scission. Therefore, protein friction due to Rvs does not appear to contribute significantly to membrane scission in yeast endocytosis.

4.3.4 Actin polymerization generates forces required for membrane scission

Maximum amount of Abp1 measured in all the diploid strains is about 220 molecules (Fig.3.11). In this case, only one allele of Abp1 is fluorescently tagged, so half the amount of Abp1 recruited is measured. The maximum amount of Abp1 recruited is then double that measured, which is about 440 ± 20 molecules (assuming equal expression and recruitment of tagged and untagged Abp1). In WT haploid cells, the maximum number of Abp1 measured is 460 ± 20 molecules. That the same number of molecules of Abp1 is recruited in all cases before scission indicates that scission timing depends on the amount of Abp1, and hence, on the amount of actin recruited.

This data is consistent with actin supplying the forces necessary for membrane scission. The membrane invagination continues until the “right” amount of actin is recruited. At this amount of actin, enough forces are generated to rupture the membrane. The amount of force necessary is determined by the physical properties of the membrane like membrane rigidity, tension, and proteins accumulated on the membrane (Dmitrieff and Nédélec, 2015). Vesicle scission releases membrane-bound Rvs, resulting in release of the SH3 along with BAR domains. Release of the SH3 domains could indicate to its binding partner in the actin network that vesicle scission has occurred, beginning disassembly of actin components. In BAR strains, a low amount of actin is recruited (Fig.3.4C). Although the absence of the SH3 domain severely perturbs the actin network, the mechanistic effect of this perturbation is unclear.

4.4 Function of the Rvs complex

4.4.1 Rvs scaffolds the membrane tube

Invaginations in *rvs167Δ* cells undergo scission at short invagination lengths of about 80nm (Fig.3.2), compared to the WT lengths of 140nm. This shows that first, enough forces are generated at 80nm

to cause scission. Then, that Rvs167 is required at membrane tubes to prevent premature scission.

Prevention of scission at short invagination lengths can be explained by Rvs stabilizing the membrane invagination via membrane interactions of the BAR domain (Boucrot et al., 2012; Dmitrieff and Nédélec, 2015). Rvs preventing membrane scission could also be explained by the SH3 domain mediating actin forces to the invagination neck: one can imagine that the SH3 domain somehow decouples actin forces from the neck, and that this delays scission. Since invagination lengths of *rvs167Δ* cells are increased towards WT by overexpression of the BAR domain alone (Fig.3.12A), I propose that localization of Rvs BAR domains to the membrane tube stabilizes the membrane. This allows deep invaginations to grow until actin polymerization produces enough forces to overcome this stabilization and sever the membrane. Stabilization of the membrane tube increases with increasing amounts of BAR domains recruited to the membrane tube (Fig.3.12). The requirement for Rvs scaffolding cannot be removed by reducing turgor pressure (Fig.3.13), suggesting that the function of the scaffold is not to counter turgor pressure.

4.4.2 A critical amount of Rvs is required to stabilize the membrane

Scission efficiency decreases with decreased amounts of Rvs: in diploids, lowering the amount of Rvs by 20 molecules decreases scission efficiency to about 90% from 97% (see Chapter6. This indicates that a particular coverage of the membrane tube is required for effective scaffolding by BAR domains. In support of this, in BAR strains, fewer numbers of Rvs are recruited, and scission efficiency is similarly reduced. At low concentrations of Rvs like in the 1xd cells, it is likely that some membrane tubes recruit the critical number of Rvs, in which case the invaginations grow to near WT lengths. Over a certain amount of Rvs, adding more BAR domains does not increase the stability of the tube: in 4xd, the same amount of actin is recruited before scission as in the 2xd and 1xd strains.

If enough forces are generated at 80nm, why is scission efficiency decreased in *rvs167Δ* compared to WT? Forces from actin may be at a threshold when the invagination is at 80nm. There could be enough force to sever the membrane, but not enough to sever reliably. The Rvs scaffold then keeps the network growing to accumulate enough actin to reliably cause scission. Controlling membrane tube length could also be a way for the cell to control the size of the vesicles formed, and therefore the amount of cargo packed into the vesicle.

4.5 Inp52 is likely involved in vesicle uncoating

Deletion of synaptojanin-like Inp52 does not affect the movement of the invagination. In spite of this, Sla1 patches persist for longer after scission in the *inp52Δ* than in WT cells, as does Rvs167, indicated by the arrows in Fig.3.8A,D. Persistence of both suggests that rather than the scission timepoint, post-scission disassembly of proteins from the vesicle is inhibited in *inp52Δ* cells. Inp52 then plays a role in recycling endocytic proteins from the vesicle to the plasma membrane. The slower assembly of Rvs in *inp51Δ* and the increase in coat retraction rates of *inp52Δ* could indicate that there is a slight effect on Rvs recruitment, and that lipid hydrolysis could play a small role in scission.

4.6 Model for membrane scission

I propose that Rvs is recruited to sites by two distinct mechanisms. SH3 domains cluster Rvs at endocytic sites. This SH3 interaction increases the efficiency with which the BAR domains sense curvature on tubular membranes. BAR domains bind to endocytic sites by sensing tubular membrane. BAR domains are recruited over the entire membrane tube, but do not form a tight helical scaffold. Membrane shape is stabilized against fluctuations that could cause scission by the BAR-membrane interaction. This prevent actin forces from rupturing the membrane, and the invaginations continue to grow in length as actin continues to polymerize.

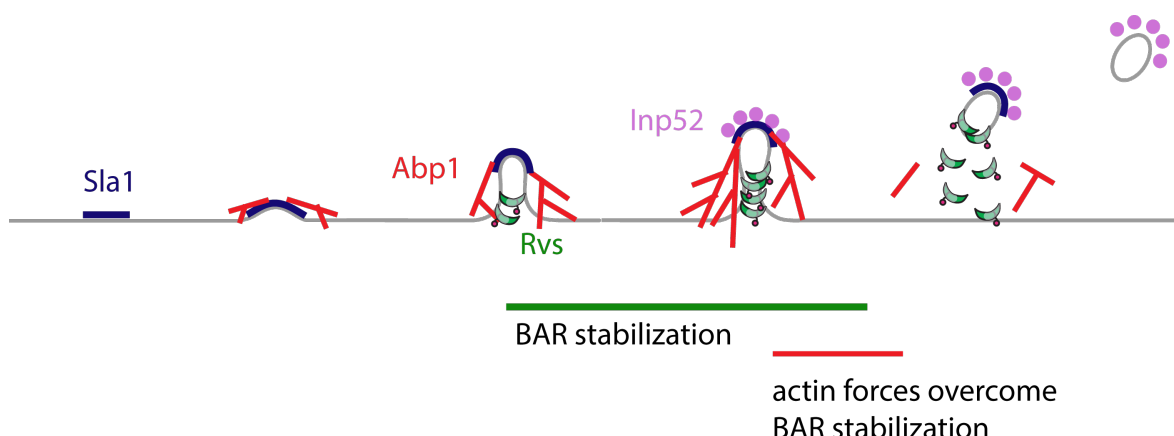


Figure 4.4 – Schematic model for membrane scission in yeast endocytosis. BAR domains are recruited to tubular membranes, and scaffold them, preventing scission. Recruitment to the membrane is increased by the SH3 domain. Actin filaments meanwhile continue to polymerize and eventually exert enough forces to overcome the influence of the BAR scaffold, causing membrane scission. Inp52 is recruited to the top of the invagination right before scission and is involved in uncoating the vesicle.

BAR recruitment to membrane tubes is restricted by the surface area of the tube: after a certain amount of Rvs, the excess interacts with endocytic sites via the SH3 domain. Adding over a certain amount of Rvs also does not increase the stabilization effect on the tube. As actin continues to polymerize, at a certain amount of actin, enough forces are generated to overcome the resistance to membrane scission provided by the BAR scaffold. The membrane ruptures, and vesicles are formed. Synaptotjanins may help recruit Rvs at

endocytic sites: Inp51 and Inp52 have proline rich regions that could act as binding sites for Rvs167 SH3 domains. They are involved in vesicle uncoating post-scission, likely by dephosphorylating PIP₂ and inducing disassembly of PIP₂-binding endocytic proteins. Eventually phosphorylation regulation allows endocytic proteins to be reused at endocytic sites, while the vesicle is transported elsewhere into the cell.

5 | Materials and Methods

5.1 Materials

5.1.1 Yeast strains

STRAIN	GENOTYPE
MKY0100	MAT α , his3 Δ 200, leu2-3,112, ura3-52, lys2-801
MKY0102	MAT α , his3 Δ 200, leu2-3,112, ura3-52, lys2-801 MAT α /MAT α , his3 Δ 200/his3 Δ 200, leu2-3,112/leu2-3,112, ura3-52/ura3-52,
MKY0105	lys2-801/lys2-801
MKY0122	MAT α , his3 Δ 200, leu2-3,112, ura3-52, lys2-801, ABP1-EGFP::HIS3MX6
MKY0123	MAT α , his3 Δ 200, leu2-3,112, ura3-52, lys2-801, ABP1-EGFP::HIS3MX6
MKY0216	MAT α his3 Δ 200, leu2-3,112 ura3-52, lys2-801 NUF2-EGFP::HIS3MX6
MKY0217	MAT α his3 Δ 200, leu2-3,112 ura3-52, lys2-801 NUF2-EGFP::HIS3MX6
MKY0224	MAT α , his3 Δ 200 leu2-3,112, ura3-52, lys2-801 NUF2-mCherry::KANMX4
MKY0225	MAT α his3 Δ 200, leu2-3,112 ura3-52, lys2-801 NUF2-mCherry::KANMX4 MAT α , his3 Δ 200, leu2-3,112, ura3-52, lys2-801,SLA1-EGFP::HISMX, ABP1-
MKY0822	mCherry::kanMX MAT α , his3 Δ 200, leu2-3,112, ura3-52, SLA1-EGFP::HISMX, ABP1-
MKY0823	mCherry::kanMX
MKY0141	MAT α , his3 Δ 200, leu2-3,112, ura3-52, lys2-801, SLA1-EGFP::HIS3MX6
MKY2832	Mat a, his3 Δ 200, leu2-3,112, ura3-52, lys2-801, Rvs167-EGFP::HIS3MX6 MAT α , his3 Δ 200, leu2-3,112, ura3-52, lys2-801, Abp1-mCherry::KANMX4,
MKY3131	Rvs167-EGFP::HISMX6 MAT α , his3 Δ 200, leu2-3,112, ura3-52, lys2-801, Abp1-mCherry::KANMX4,
MKY3132	Rvs167-EGFP::HISMX6 Mat a, his3 Δ 200, leu2-3,112, ura3-52, lys2-801, rvs167- Δ SH3-
MKY3154	EGFP::HIS3MX6 MAT α , his3 Δ 200, leu2-3,112, ura3-52, lys2-801, rvs167- Δ SH3::natNT2, ABP1-
MKY3201	EGFP::HIS3MX6

	Mat a/α, his3Δ200/his3Δ200, leu2-3,112/leu2-3,112, ura3-52/ura3-52, lys2-
MKY3258	801/lys2-801,Vps1-EGFP::HIS3MX6/Vps1, Abp1-mCherry::KANMX/Abp1
MKY3260	Mat a, his3Δ200, leu2-3,112, ura3-52, lys2-801, Vps1-sfGFP::URA3
	MAT α , his3Δ200, leu2-3,112, ura3-52, lys2-801, sla2::natNT2, rvs167-ΔSH3-
MKY3280	EGFP::HIS3MX6, SLA1-mcherry::kanMX5
	MAT α , his3Δ200, leu2-3,112, ura3-52, lys2-801, sla2::natNT2, rvs167-ΔSH3-
MKY3281	EGFP::HIS3MX6, SLA1-mcherry::kanMX5
	MAT α , his3Δ200, leu2-3,112, ura3-52, lys2-801, sla2::natNT2, RVS167-
MKY3282	EGFP::HIS3MX6, ABP1-mcherry::kanMX5
	MAT α , his3Δ200, leu2-3,112, ura3-52, lys2-801, sla2::natNT2, RVS167-
MKY3283	EGFP::HIS3MX6, ABP1-mcherry::kanMX5
	MAT α , his3Δ200, leu2-3,112, ura3-52, lys2-801, sla2::natNT2, rvs167-ΔSH3-
MKY3284	EGFP::HIS3MX6, ABP1-mcherry::kanMX5
	MAT α , his3Δ200, leu2-3,112, ura3-52, lys2-801, sla2::natNT2, rvs167-ΔSH3-
MKY3285	EGFP::HIS3MX6, ABP1-mcherry::kanMX5
	MAT α , his3Δ200, leu2-3,112, ura3-52, lys2-801, rvs167-ΔSH3-
MKY3286	EGFP::HIS3MX6, ABP1-mCherry::KANMX4
MKY3287	MAT α , his3Δ200, leu2-3,112, ura3-52, lys2-801 rvs167-ΔSH3::natN2
MKY3288	MAT α , his3Δ200, leu2-3,112, ura3-52, lys2-801, rvs167-ΔSH3::natNT2
	MAT α , his3Δ200, leu2-3,112, ura3-52, lys2-801, rvs167-ΔSH3::natNT2, SLA1-
MKY3289	EGFP::HIS3MX6
	MAT α , his3Δ200, leu2-3,112, ura3-52, lys2-801, rvs167-ΔSH3::natNT2, SLA1-
MKY3290	EGFP::HIS3MX6
	MAT α , his3Δ200, leu2-3,112, ura3-52, lys2-801, rvs167-ΔSH3::natNT2, ABP1-
MKY3291	EGFP::HIS3MX6
	MAT α , his3Δ200, leu2-3,112, ura3-52, lys2-801, rvs167-ΔSH3::natNT2, SLA1-
MKY3292	EGFP::HIS3MX, ABP1-mcherry::kanMX4
	Mat α his3Δ200, leu2-3,112, ura3-52, lys2-801, SLA1-mCherry::KANMX4,
MKY3295	sla2::NAT, RVS167-EGFP::HIS3MX6
MKY3339	MAT α , his3Δ200, leu2-3,112, ura3-52, lys2-801 vps1::natNT2
	MAT α , his3Δ200, leu2-3,112, ura3-52, lys2-801, vps1::natNT2, RVS167-
MKY3341	EGFP::HIS3MX6
	MAT α , his3Δ200, leu2-3,112, ura3-52, lys2-801, vps1::natNT2, RVS167-
MKY3342	EGFP::HIS3MX6
	MAT α , his3Δ200, leu2-3,112, ura3-52, lys2-801, vps1::natNT2, RVS167-
MKY3343	EGFP::HIS3MX6 , ABP1-mCherry::kanMX4
	MAT α , his3Δ200, leu2-3,112, ura3-52, lys2-801, vps1::natNT2, RVS167-
MKY3344	EGFP::HIS3MX6 , ABP1-mCherry::kanMX4

	MAT α , his3 Δ 200, leu2-3,112, ura3-52, lys2-801, vps1 Δ ::natNT2, SLA1-
MKY3345	EGFP::HIS3MX6
	MAT α , his3 Δ 200, leu2-3,112, ura3-52, lys2-801, vps1 Δ ::natNT2, SLA1-
MKY3346	EGFP::HIS3MX6
	MAT α , his3 Δ 200, leu2-3,112, ura3-52, lys2-801, vps1 Δ ::natNT2, SLA1-
MKY3347	EGFP::HIS3MX6 , ABP1-mCherry::kanMX4
MKY3559	MAT α , his3 Δ 200, leu2-3,112, ura3-52, lys2-801, Inp51-EGFP::HIS3MX6
MKY3560	MAT α , his3 Δ 200, leu2-3,112, ura3-52, lys2-801, Inp52-EGFP::HIS3MX6
MKY3561	MAT α , his3 Δ 200, leu2-3,112, ura3-52, lys2-801, inp51 Δ ::URA
	MAT α , his3 Δ 200, leu2-3,112, ura3-52, lys2-801, inp51 Δ ::URA, Sla1-
MKY3562	EGFP::HIS3MX6, Abp1-mCherry::KANMX4
MKY3586	MAT α his3 Δ 200, leu2-3,112, ura3-52, lys2-801 inp52 Δ ::hphNT1
MKY3587	MAT α his3 Δ 200, leu2-3,112, ura3-52, lys2-801 inp52 Δ ::hphNT1
	MAT α , his3 Δ 200, leu2-3,112, ura3-52, lys2-801, Rvs167-EGFP::HISMX6,
MKY3620	inp51 Δ ::URA
	MAT α , his3 Δ 200, leu2-3,112, ura3-52, lys2-801, Rvs167-EGFP::HISMX6,
MKY3621	inp51 Δ ::URA
	MAT α , his3 Δ 200, leu2-3,112, ura3-52, lys2-801, Rvs167-EGFP::HISMX6,
MKY3622	inp51 Δ ::URA
	MAT α , his3 Δ 200, leu2-3,112, ura3-52, lys2-801, Inp52-EGFP::HISMX6, Abp1-
MKY3623	mCherry::KANMX4
	MAT α , his3 Δ 200, leu2-3,112, ura3-52, lys2-801, Inp52-EGFP::HISMX6 Abp1-
MKY3624	mCherry::KANMX4
MKY3702	MAT α his3 Δ 200, leu2-3,112, ura3-52, lys2-801 RVS161::URA::RVS161
	MAT α , his3 Δ 200, leu2-3,112, ura3-52, lys2-801, RVS161::URA::RVS161,
MKY3703	RVS167::HPH::RVS167
	MAT α , his3 Δ 200, leu2-3,112, ura3-52, lys2-801, RVS161::URA::RVS161,
MKY3704	RVS167::HPH::RVS167
	MAT α his3 Δ 200, leu2-3,112, ura3-52, lys2-801 RVS167::HPH::RVS167, SLA1-
MKY3705	EGFP::HISMX6
	MAT α his3 Δ 200, leu2-3,112, ura3-52, lys2-801 RVS161::URA::RVS161
MKY3706	RVS167::HPH::RVS167 SLA1-EGFP::HISMX6 ABP1-mCherry::KANMX4
MKY3707	MAT α his3 Δ 200, leu2-3,112, ura3-52, lys2-801 RVS167::HPH::RVS167
	MAT α his3 Δ 200, leu2-3,112, ura3-52, lys2-801, Rvs167-
MKY3708	EGFP::his3MX6::hphNT1::Rvs167-EGFP::his3MX6
	MAT α his3 Δ 200, leu2-3,112, ura3-52, lys2-801 RVS167-EGFP::HPH::RVS167-
MKY3709	EGFP Abp1-mCherry

	MATa his3Δ200, leu2-3,112, ura3-52, lys2-801, RVS161::URA::RVS161, SLA1-
MKY3711	EGFP::HISMX, ABP1-mCherry::kanMX MATa, his3Δ200, leu2-3,112, ura3-52, lys2-801, Rvs167-
MKY3712	EGFP::his3MX6::hphNT1::Rvs167-EGFP::his3MX6, RVS161::URA::RVS161
MKY3713	MAT α , his3Δ200, leu2-3,112, ura3-52, lys2-801, rvs167-ΔSH3::natN2 MAT α , his3Δ200, leu2-3,112, ura3-52, lys2-801, rvs167-ΔSH3- EGFP::his3MX6::hphNT1::rvs167-ΔSH3-EGFP::his3MX6, ABP1-
MKY3714	mCherry::kanMX MAT α , his3Δ200, leu2-3,112, ura3-52, lys2-801, rvs167-ΔSH3- EGFP::his3MX6::hphNT1::rvs167-ΔSH3-EGFP::his3MX6, ABP1-
MKY3728	mCherry::kanMX, RVS161::URA::RVS161 MATa his3Δ200, leu2-3,112, ura3-52, lys2-801, Rvs167-EGFP::HISMX6 Abp1-
MKY3803	mCherry::KANMX4 MAT α his3Δ200, leu2-3,112, ura3-52, lys2-801, inp52Δ::hphNT1, Abp1-
MKY3804	mCherry::kanMX4 MAT α his3Δ200, leu2-3,112, ura3-52, lys2-801, inp52Δ::hphNT1, Rvs167-
MKY3805	EGFP::HIS3MX6 MATa his3Δ200, leu2-3,112, ura3-52, lys2-801, inp52Δ::hphNT1, Rvs167-
MKY3806	EGFP::HIS3MX6 MAT α , his3Δ200, leu2-3,112, ura3-52, lys2-801, rvs167- ΔSH3::natNT2::hphNT1::rvs167-ΔSH3::natNT2, SLA1-EGFP::HISMX, ABP1-
MKY3826	mCherry::kanMX MAT α , his3Δ200, leu2-3,112, ura3-52, lys2-801, inp52Δ::hphNT1, SLA1-
MKY3827	EGFP::HISMX, ABP1-mCherry::kanMX MATa/ALPHA his3Δ200, leu2-3,112, ura3-52, lys2-801 RVS161::URA::RVS161/RVS161::URA::RVS161, Rvs167- EGFP::his3MX6::hphNT1::Rvs167-EGFP::his3MX6/Rvs167- EGFP::his3MX6::hphNT1::Rvs167-EGFP::his3MX6, ABP1-
MKY3945	mCHerry::KANMX4/Abp1 MATa/ALPHA, his3Δ200, leu2-3,112, ura3-52, lys2-801, Rvs167-
MKY3946	EGFP::HIS3MX6/Rvs167-EGFP::HIS3MX6, ABP1-mCHerry::KANMX4/Abp1 MATa/ α , his3-delta200, leu2-3,112, ura3-52, RVS167- EGFP::HIS3MX6/rvs167delta::cgLEU2, rvs161delta::cgLEU2/RVS161, ABP1-
MKY3947	RFP::HIS3MX6/ABP1
MKY3948	MATa, his3Δ200, leu2-3,112, ura3-52, lys2-801, Inp53-EGFP::HIS3MX6

5.1.2 Buffers and plasmids

BUFFERS

PEG buffer

Lithium acetate	100 mM
Tris-HCl pH 8	10 mM
EDTA pH 8	1 mM
Polyethylene glycol	4 % w/v

SORB buffer

Lithium acetate	100 mM
Tris-HCl pH 8	10 mM
EDTA pH 8	1 mM
Sorbitol	1 M

S buffer

K2HPO4 pH 7.2	10 mM
EDTA	10 mM
β-mercaptoethanol	50 mM
Zymolyase	50 µg/mL

Lysis Buffer

Sodium dodecyl sulphate (SDS)	2.5 % w/v
Tris-HCl pH 7.5	25 mM
EDTA	25 mM

PLASMIDS

Name	Purpose	Selection	Source
pFA6a-EGFP-HIS4MX	EGFP tag	his3MX6	Janke, 2004
pFA6a-mCherry-KanMX4	mCherry tag	kanMX4	Janke, 2004
pFA6a-natNT2	deletion	natNT2	Janke, 2004
pks133	deletion, duplication	hphNT1	Janke, 2004
pFA6a-KiUra	deletion	kiURA	

5.1.3 Media

Yeast extract Peptone Dextrose (YPD)

BactoYeast Extract	1 % w/v
Bacto Peptone	2 % w/v
Glucose	2 % w/v

Synthetic Complete (SC)

DifcoTM Yeast nitrogen base w/o amino acids	0.67 % w/v
Glucose	2 % w/v
Amino acid stock (SC)	10 % v/v

Amino acid stock (SC) –dissolved in 100 mL H₂O

Adenine	0.5 g
Leucine	10 g
Alanine, Arginine, Asparagine, Aspartic acid, Cysteine, Glutamine, Glutamic acid, Glycine, Histidine, Inositol, Isoleucine, Lysine, Methionine, para-Aminobenzoic acid, Phenylalanine, Proline, Serine, Threonine, Tryptophan, Tyrosine, Uracil, Valine. For auxotrophic selection, one amino acid is left out	2 g each

Sporulation plates

Potassium acetate	1 % w/v
Bacto Agar	2 % w/v
Amino acid stock (sporulation plate)	0.25 % v/v

Amino acid stock (sporulation plate) –dissolved in 100 mL

Uracil, Histidine, Methionine	0.2 g
Leucine, Lysine	0.3 g

Antibiotic selection plates

Hygromycin B (Hph) (InvivoGen)	300 mg/L
Geneticin disulphate salt (G418) (Sigma)	200 mg/L
Nourseothricin (clonNAT) (Werner BioAgents)	100 mg/L

5.1.4 Microscopes

Live-cell tracking		
	Name	Supplier
Microscope	IX81	Olympus
Objective	PlanApo 100x/1.45 TIRFM	Olympus
Camera (molecule number quantification)	Orca –ER	Hamamatsu
Fluorescent lamp (molecule number quantification)	X-CITE 120 PC	EXFO
Laser source for GFP excitation	Sapphire 488-100	Coherent
Laser source for RFP excitation	Compass 315M (561 nm)	Coherent
Camera	ImagEM EMCCD	Hamamatsu
Microscope (TIRF)	IX83	Olympus
Camera (TIRF)	Image mX2 EMCCD	Hamamatsu
Objective (TIRF)		
Laser source (TIRF)	VS-LMS	Visitron

Electron microscopy		
Microscope	Tecnai F30 300kV FEG	FEI
Camera	4k Eagle	FEI

5.2 Methods

5.2.1 Homologous recombination with PCR cassette insertion

Tagging or deletion of endogenous genes was done by homologous integration of the product of a Polymerase Chain Reaction using appropriate primers and a plasmid containing a selection cassette and fluorescent tag, or only selection cassette for gene deletions. Primers were designed according to Janke et al, 2004. PCRs used the Velocity Polymerase for fluorescent tagging, and Q5 for gene deletions using the NAT cassette. All fluorescently tagged genes have a C-terminus tag and are expressed endogenously. Gene deletions and fluorescent tags are checked by PCR. Vps1del and gene duplications were confirmed by sequencing.

5.2.2 Live-cell imaging

Sample preparation for live imaging

40 μ L Concanavalin A (ConA) was incubated on a coverslip for 10 minutes. 40 μ L Yeast cells incubated overnight at 25C in imaging medium SC-TRP was added to the coverslip after removing the ConA, and incubated for another 10 minutes. Cells were then removed, adhered cells were washed 3x in SC-TRP, and 40 μ L SC-TRP was finally added to the coverslip to prevent cells from drying.

Sample preparation for live imaging in LatA and sorbitol treated cells

Cells went through the same procedure as above till the last washing step. Instead of SC-TRP, 100x diluted LatA, or Sorbitol at a final concentration of 0.2M in SC-TRP was added to the adhered cells. For LatA experiments, cells were incubated in LatA for 10 minutes before imaging. For sorbitol treatments, cells were imaged within 5 minutes of adding sorbitol.

Epifluorescent imaging for centroid tracking

Live-cell imaging was performed as in Picco et al., 2015. All images

were obtained at room temperature using an Olympus IX81 microscope equipped with a 100 \times /NA 1.45 PlanApo objective , with an additional 1.6x magnification lens and an EMCCD camera. The GFP channel was imaged using a 470/22 nm band-pass excitation filter and a 520/35 nm band-pass emission filter. mCherry epifluorescence imaging was carried out using a 556/20 nm band-pass excitation filter and a 624/40 band-pass emission filter. GFP was excited using a 488 nm solid state laser and mCherry was excited using a 561 nm solid state laser. Hardware was controlled using Metamorph software. For single-channel images, 80-120ms was used as exposure time. All dual-channel images were acquired using 250ms exposure time. Simultaneous dual-color images were obtained using a dichroic mirror, with TetraSpeck beads used to correct for chromatic abberation.

Epifluorescent imaging for molecule number quantification

Images were acquired as in Picco et al., 2015. Z-stacks of cells containing the GFP-tagged protein of interest, incubated along with cells containing Nuf2-GFP, were acquired using 400ms exposure using a mercury vapour lamp, on a CCD camera. Z stacks were spaced at 200nm.

TIRF imaging

TIRF microscopy was performed under similar conditions on an Olympus IX83 microscope. GFP was excited using a 488 nm solid state laser and mCherry was excited using a 561 nm solid state laser. Lasers, and shutters were controlled by Visitron Systems VS-Laser Control. VisiView software controlled the image acquisition and hardware-software feedback. Images were processed using ImageJ, quantification was done on R.

5.2.2.1 Live-cell image analysis

Images were processed for background noise using a rolling ball radius of 90 pixels. Particle detection, and tracking was performed for a particle size of 6 pixels, using scripts that combine background subtraction with Particle Tracker and Detector, that can be found on ImageJ (<http://imagej.nih.gov>). Further analysis for centroid averaging, alignments between dual-color images and single channel images, for

alignment to the reference Abp1 were done using scripts written in Matlab (Mathworks) and R (www.r-project.org), written originally by Andrea Picco, and modified by me. Details of analysis can be found at Picco et al., 2015. All movement and intensity plots from centroid tracking show the average centroid with 95% confidence interval. All molecule number quantifications report either the median or maximum number of molecules with standard error of mean. Maximum number is preferred over median in cases when the rate of change of fluorescent intensity of two populations being compared are not similar, and the lifetime of the protein populations being compared are not similar. The median in this case underreports the differences in protein accumulation.

5.2.2.2 Cytoplasmic background quantification

On a maximum intensity projection of time-lapse images, the average pixel intensity within a circle of set radius in the cytoplasm was measured. This circle is manually arranged so that cortical patches were excluded, and mean intensity was acquired for about 10 cells of each cell type. A fixed area outside the cells was drawn, and mean intensity was calculated to establish "background intensity". This background intensity was then subtracted from the mean intensity to obtain a rough measure of cytoplasmic intensity. There are some caveats with this quantification: the cells were not incubated in the same field of view, cellular autofluorescence is assumed to be equal for the different strains.

5.2.2.3 CLEM

Samples were prepared for CLEM as described in Wanda et al. Briefly, cells expressing Rvs167-GFP and Abp1-mCherry, and BAR-GFP and Abp1-mCherry cells were grown overnight in YPD, at 24C. They were then diluted to an OD₆₀₀ of 0.2, and grown to OD₆₀₀ between 0.8 and 1.2. These cells were then concentrated to a filter paper using a vacuum pump, and high-pressure frozen. Samples were freeze substituted in Lowycryl HM20 using the Kukulski freeze substitution protocol using an automated robot. Samples in resin were sliced to 300nm sections using a diamond knife, and loaded to carbon-coated

copper grids. TetraSpec beads were incubated on the slices and these slices were imaged using epifluorescence microscopy in GFP and RFP channels for GFP and m-Cherry, and Cyan channel for separating the signal from the Tetraspec beads, that would later be used as fiducials to correlate these fluorescent images with electron tomograms. Gold fiducials were incubated on the grids, and lead citrate was added to stain the membrane. Low magnification tilts were acquired at 3 degree increments. High magnification tilts were performed at 1 degree increments from -60 to 60 degrees. Tomograms were reconstructed using IMOD. Invagination lengths were measured at the longest axis of the invagination, using IMOD.

6 | Appendix

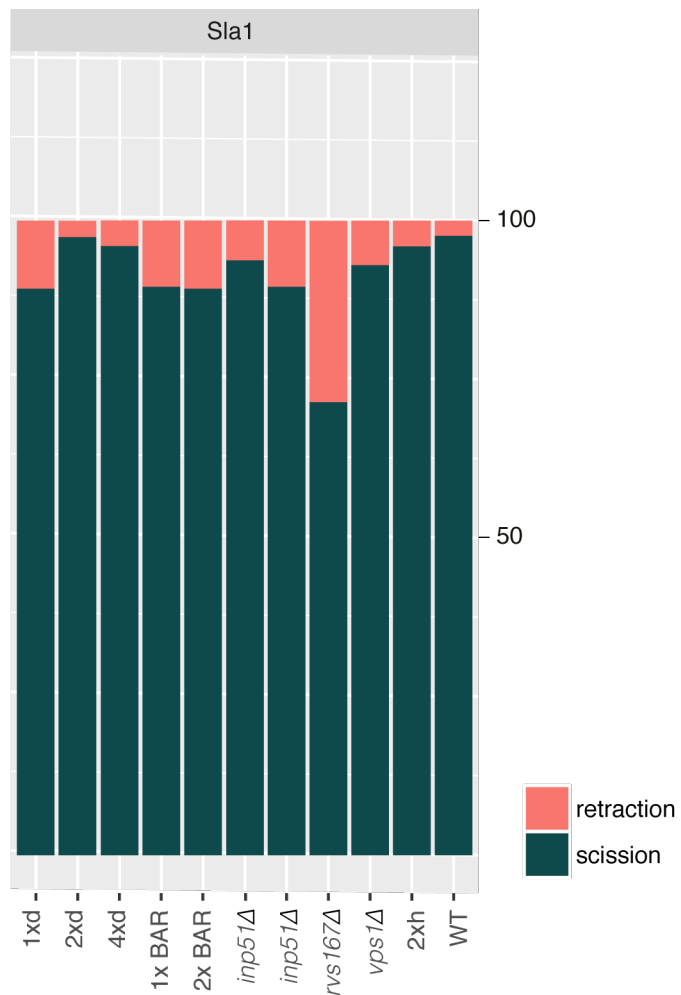


Figure 6.1 – Sla1-GFP retraction rates for various strains

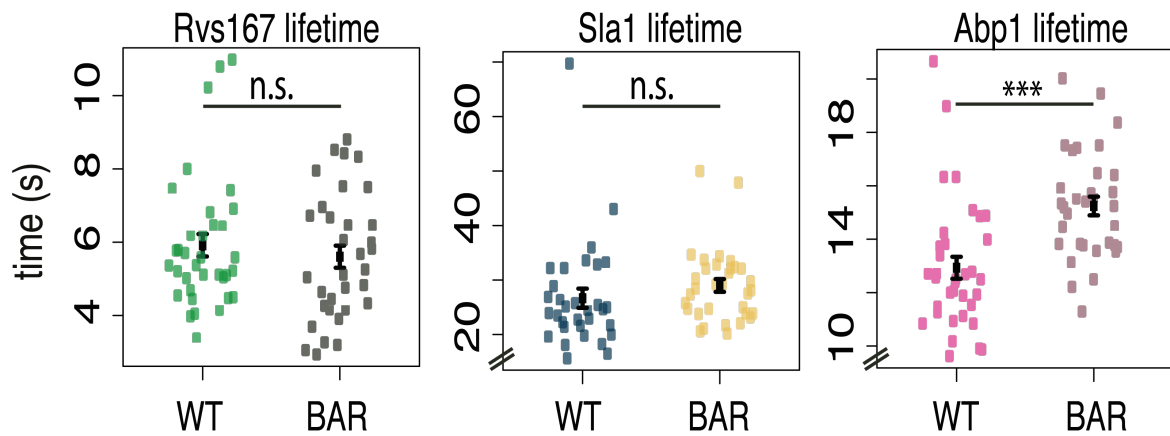


Figure 6.2 – Lifetimes of proteins in WT and BAR cells measured by TIRF microscopy

Bibliography

- Adams, A. E. and Pringle, J. R. (1984) 'Relationship of actin and tubulin distribution to bud growth in wild-type and morphogenetic-mutant *Saccharomyces cerevisiae*.' *The Journal of cell biology*. Rockefeller University Press, 98(3), pp. 934–45. doi: 10.1083/JCB.98.3.934.
- Aghamohammadazadeh, S. and Ayscough, K. R. (2009) 'Under Pressure: the Differential Requirements for Actin during Yeast and Mammalian Endocytosis', *Nature cell biology*, 11(8), pp. 1039–1042. doi: 10.1038/ncb1918.
- Anderson, B. L., Boldogh, I., Evangelista, M., Boone, C., Greene, L. A. and Pon, L. A. (1998) 'The Src homology domain 3 (SH3) of a yeast type I myosin, Myo5p, binds to verprolin and is required for targeting to sites of actin polarization.' *The Journal of cell biology*, 141(6), pp. 1357–70. doi: 10.1083/jcb.141.6.1357.
- Anderson, R. G., Goldstein, J. L. and Brown, M. S. (1976) 'Localization of low density lipoprotein receptors on plasma membrane of normal human fibroblasts and their absence in cells from a familial hypercholesterolemia homozygote.' *Proceedings of the National Academy of Sciences of the United States of America*. National Academy of Sciences, 73(7), pp. 2434–8. Available at: <http://www.ncbi.nlm.nih.gov/pubmed/181751> (Accessed: 8 June 2018).
- Antonny, B., Burd, C., De Camilli, P., Chen, E., Daumke, O., Faelber, K., Ford, M., Frolov, V. A., Frost, A., Hinshaw, J. E., Kirchhausen, T., Kozlov, M. M., Lenz, M., Low, H. H., McMahon, H., Merrifield, C., Pollard, T. D., Robinson, P. J., Roux, A. and

Schmid, S. (2016) 'Membrane fission by dynamin: what we know and what we need to know', *The EMBO Journal*, 35(21), pp. 2270–2284. doi: 10.15252/embj.201694613.

Arkhipov, A., Yin, Y. and Schulten, K. (2009) 'Membrane-Bending Mechanism of Amphiphysin N-BAR Domains', *Biophysical Journal*. Cell Press, 97(10), pp. 2727–2735. doi: 10.1016/j.bpj.2009.08.051.

Basu, R., Munteanu, E. L. and Chang, F. (2014) 'Role of turgor pressure in endocytosis in fission yeast', *Molecular Biology of the Cell*, 25(5), pp. 679–687. doi: 10.1091/mcb.E13-10-0618.

Bauer, F., Urdaci, M., Aigle, M. and Crouzet, M. (1993) 'Alteration of a yeast SH3 protein leads to conditional viability with defects in cytoskeletal and budding patterns.', *Molecular and Cellular Biology*, 13(8), pp. 5070–5084. Available at: <http://www.ncbi.nlm.nih.gov/pmc/articles/PMC360159/> (Accessed: 4 August 2015).

Bazinet, C., Katzen, A. L., Morgan, M., Mahowald, A. P. and Lemmon, S. K. (1993) 'The Drosophila clathrin heavy chain gene: clathrin function is essential in a multicellular organism.', *Genetics*, 134(4), pp. 1119–34. Available at: <http://www.ncbi.nlm.nih.gov/pubmed/8375651> (Accessed: 2 June 2018).

Bensen, E. S., Costaguta, G. and Payne, G. S. (2000) 'Synthetic genetic interactions with temperature-sensitive clathrin in *Saccharomyces cerevisiae*. Roles for synaptojanin-like Inp53p and dynamin-related Vps1p in clathrin-dependent protein sorting at the trans-Golgi network.', *Genetics*, 154(1), pp. 83–97. Available at: <http://www.ncbi.nlm.nih.gov/pubmed/10628971> (Accessed: 9 August 2018).

Bitsikas, V., Corrêa, I. R. and Nichols, B. J. (2014) 'Clathrin-independent pathways do not contribute significantly to endocytic flux', *eLife*. eLife Sciences Publications Limited, 3, p. e03970. doi: 10.7554/eLife.03970.

van der Bliek, A. M. and Meyerowitz, E. M. (1991) 'Dynamin-like protein encoded by the *Drosophila shibire* gene associated with vesicular traffic', *Nature*,

351(6325), pp. 411–414. doi: 10.1038/351411a0.

Boeke, D., Trautmann, S., Meurer, M., Wachsmuth, M., Godlee, C., Knop, M. and Kaksonen, M. (2014a) ‘Quantification of cytosolic interactions identifies Ede1 oligomers as key organizers of endocytosis’, *Molecular Systems Biology*, 10(11), pp. 756–756. doi: 10.15252/msb.20145422.

Boettner, D. R., Chi, R. J. and Lemmon, S. K. (2012) ‘Lessons from yeast for clathrin-mediated endocytosis’, *Nature Cell Biology*, 14(1), pp. 2–10. doi: 10.1038/ncb2403.

Boucrot, E., Pick, A., Çamdere, G., Liska, N., Evergren, E., McMahon, H. T. and Kozlov, M. M. (2012) ‘Membrane Fission Is Promoted by Insertion of Amphipathic Helices and Is Restricted by Crescent BAR Domains’, *Cell*. Cell Press, 149(1), p. 124–136s. doi: 10.1016/J.CELL.2012.01.047.

Brach, T., Godlee, C., Moeller-Hansen, I., Boeke, D. and Kaksonen, M. (2014) ‘The Initiation of Clathrin-Mediated Endocytosis Is Mechanistically Highly Flexible’, *Current Biology*. Cell Press, 24(5), pp. 548–554. doi: 10.1016/J.CUB.2014.01.048.

Brizzio, V., Gammie, A. E. and Rose, M. D. (1998) ‘Rvs161p interacts with Fus2p to promote cell fusion in *Saccharomyces cerevisiae*.’, *The Journal of cell biology*, 141(3), pp. 567–84. doi: 10.1083/jcb.141.3.567.

Bui, H. T., Karren, M. A., Bhar, D. and Shaw, J. M. (2012) ‘A novel motif in the yeast mitochondrial dynamin Dnm1 is essential for adaptor binding and membrane recruitment.’, *The Journal of cell biology*. Rockefeller University Press, 199(4), pp. 613–22. doi: 10.1083/jcb.201207079.

Cerveny, K. L., Tamura, Y., Zhang, Z., Jensen, R. E. and Sesaki, H. (2007) ‘Regulation of mitochondrial fusion and division’, *Trends in Cell Biology*. Elsevier Current Trends, 17(11), pp. 563–569. doi: 10.1016/J.TCB.2007.08.006.

Cestra, G., Castagnoli, L., Dente, L., Minenkova, O., Petrelli, A., Migone, N., Hoffmüller, U., Schneider-Mergener, J. and Cesareni, G. (1999) ‘The SH3 domains

of endophilin and amphiphysin bind to the proline-rich region of synaptojanin 1 at distinct sites that display an unconventional binding specificity.', *The Journal of biological chemistry*. American Society for Biochemistry and Molecular Biology, 274(45), pp. 32001–7. doi: 10.1074/jbc.274.45.32001.

Chen, M. S., Obar, R. A., Schroeder, C. C., Austin, T. W., Poodry, C. A., Wadsworth, S. C. and Vallee, R. B. (1991) 'Multiple forms of dynamin are encoded by shibire, a Drosophila gene involved in endocytosis', *Nature*. Nature Publishing Group, 351(6327), pp. 583–586. doi: 10.1038/351583a0.

Colwill, K., Field, D., Moore, L., Friesen, J. and Andrews, B. (1999) 'In Vivo Analysis of the Domains of Yeast Rvs167p Suggests Rvs167p Function Is Mediated Through Multiple Protein Interactions', *Genetics*, 152(3).

Crouzet, M., Urdaci, M., Dulau, L. and Aigle, M. (1991) 'Yeast mutant affected for viability upon nutrient starvation: characterization and cloning of the RVS161 gene.', *Yeast (Chichester, England)*, 7(7), pp. 727–43. doi: 10.1002/yea.320070708.

David, C., McPherson, P. S., Mundigl, O. and de Camilli, P. (1996) 'A role of amphiphysin in synaptic vesicle endocytosis suggested by its binding to dynamin in nerve terminals.', *Proceedings of the National Academy of Sciences of the United States of America*. National Academy of Sciences, 93(1), pp. 331–5. doi: 10.1073/pnas.93.1.331.

Dmitrieff, S. and Nédélec, F. (2015) 'Membrane Mechanics of Endocytosis in Cells with Turgor', *PLOS Computational Biology*. Edited by H. Ewers. Public Library of Science, 11(10), p. e1004538. doi: 10.1371/journal.pcbi.1004538.

Fan, J. Y., Carpentier, J. L., Gorden, P., Van Obberghen, E., Blackett, N. M., Grunfeld, C. and Orci, L. (1982) 'Receptor-mediated endocytosis of insulin: role of microvilli, coated pits, and coated vesicles.', *Proceedings of the National Academy of Sciences of the United States of America*. National Academy of Sciences, 79(24), pp. 7788–91. Available at: <http://www.ncbi.nlm.nih.gov/pubmed/6818548> (Accessed: 8 June 2018).

Farsad, K., Ringstad, N., Takei, K., Floyd, S. R., Rose, K. and De Camilli, P. (2001) 'Generation of high curvature membranes mediated by direct endophilin bilayer interactions', *The Journal of Cell Biology*, 155(2), pp. 193–200. doi: 10.1083/jcb.200107075.

Ferguson, S. M., Ferguson, S., Raimondi, A., Paradise, S., Shen, H., Mesaki, K., Ferguson, A., Destaing, O., Ko, G., Takasaki, J., Cremona, O., O' Toole, E. and De Camilli, P. (2009) 'Coordinated actions of actin and BAR proteins upstream of dynamin at endocytic clathrin-coated pits', *Developmental Cell*, 17(6), pp. 811–822. doi: 10.1016/j.devcel.2009.11.005.

Friend, D. S. and Farquhar, M. G. (1967) 'Functions of coated vesicles during protein absorption in the rat vas deferens.', *The Journal of cell biology*. Rockefeller University Press, 35(2), pp. 357–76. doi: 10.1083/JCB.35.2.357.

Friesen, H., Humphries, C., Ho, Y., Schub, O., Colwill, K. and Andrews, B. (2006) 'Characterization of the Yeast Amphiphysins Rvs161p and Rvs167p Reveals Roles for the Rvs Heterodimer In Vivo', *Molecular Biology of the Cell*, 17(3), pp. 1306–1321. doi: 10.1091/mbc.E05-06-0476.

Frost, A., Perera, R., Roux, A., Spasov, K., Destaing, O., Egelman, E. H., De Camilli, P. and Unger, V. M. (2008) 'Structural basis of membrane invagination by F-BAR domains', *Cell*, 132(5), pp. 807–817. doi: 10.1016/j.cell.2007.12.041.

Gallop, J. L., Butler, P. J. G. and McMahon, H. T. (2005) 'Endophilin and CtBP/BARS are not acyl transferases in endocytosis or Golgi fission', *Nature*. Nature Publishing Group, 438(7068), pp. 675–678. doi: 10.1038/nature04136.

Geli, M. I., Lombardi, R., Schmelzl, B. and Riezman, H. (2000) 'An intact SH3 domain is required for myosin I-induced actin polymerization', *The EMBO Journal*, 19(16), pp. 4281–4291. doi: 10.1093/emboj/19.16.4281.

Giachino, C., Lantelme, E., Lanzetti, L., Saccone, S., Valle, G. Della and Migone, N. (1997) 'A Novel SH3-Containing Human Gene Family Preferentially Expressed in the Central Nervous System', *Genomics*. Academic Press, 41(3), pp. 427–434. doi:

10.1006/GENO.1997.4645.

Goldstein, J. L. and Brown, M. S. (1973) 'Familial hypercholesterolemia: identification of a defect in the regulation of 3-hydroxy-3-methylglutaryl coenzyme A reductase activity associated with overproduction of cholesterol.', *Proceedings of the National Academy of Sciences of the United States of America*. National Academy of Sciences, 70(10), pp. 2804–8. Available at: <http://www.ncbi.nlm.nih.gov/pubmed/4355366> (Accessed: 8 June 2018).

Goud Gadila, S. K., Williams, M., Saimani, U., Delgado Cruz, M., Makaraci, P., Woodman, S., Short, J. C. W., McDermott, H. and Kim, K. (2017) 'Yeast dynamin Vps1 associates with clathrin to facilitate vesicular trafficking and controls Golgi homeostasis', *European Journal of Cell Biology*. Urban & Fischer, 96(2), pp. 182–197. doi: 10.1016/J.EJCB.2017.02.004.

Grabs, D., Slepnev, V. I., Songyang, Z., David, C., Lynch, M., Cantley, L. C. and De Camilli, P. (1997) 'The SH3 Domain of Amphiphysin Binds the Proline-rich Domain of Dynamin at a Single Site That Defines a New SH3 Binding Consensus Sequence', *Journal of Biological Chemistry*, 272(20), pp. 13419–13425. doi: 10.1074/jbc.272.20.13419.

Grant, B. and Hirsh, D. (1999) 'Receptor-mediated endocytosis in the *Caenorhabditis elegans* oocyte.', *Molecular biology of the cell*, 10(12), pp. 4311–26. Available at: <http://www.ncbi.nlm.nih.gov/pubmed/10588660> (Accessed: 2 June 2018).

Greer, C. and Schekman, R. (1982) 'Actin from *Saccharomyces cerevisiae*', *Molecular and cellular biology*. American Society for Microbiology (ASM), 2(10), pp. 1270–8. Available at: <http://www.ncbi.nlm.nih.gov/pubmed/6217414> (Accessed: 12 August 2018).

Grigliatti, T. A., Hall, L., Rosenbluth, R. and Suzuki, D. T. (1973) 'Temperature-Sensitive Mutations in *Drosophila melanogaster* XIV. A Selection of Immobile Adults *', *Molec. gen. Genet.*, 120, pp. 107–114. Available at:

<https://link.springer.com/content/pdf/10.1007%2FBF00267238.pdf> (Accessed: 6 June 2018).

Gurunathan, S., David, D. and Gerst, J. E. (2002) 'Dynamin and clathrin are required for the biogenesis of a distinct class of secretory vesicles in yeast.', *The EMBO journal*. European Molecular Biology Organization, 21(4), pp. 602–14. doi: 10.1093/EMBOJ/21.4.602.

Hemmaplardh, D. and Morgan, E. H. (1976) 'Transferrin uptake and release by reticulocytes treated with proteolytic enzymes and neuraminidase', *Biochimica et Biophysica Acta (BBA) - Biomembranes*. Elsevier, 426(3), pp. 385–398. doi: 10.1016/0005-2736(76)90384-9.

Henne, W. M., Boucrot, E., Meinecke, M., Evergren, E., Vallis, Y., Mittal, R. and McMahon, H. T. (2010) 'FCHo Proteins Are Nucleators of Clathrin-Mediated Endocytosis', *Science*, 328(5983), pp. 1281–1284. doi: 10.1126/science.1188462.

Heuser, J. E. and Reese, T. S. (1973) 'Evidence for recycling of synaptic vesicle membrane during transmitter release at the frog neuromuscular junction.', *The Journal of cell biology*, 57(2), pp. 315–44. Available at: <http://www.ncbi.nlm.nih.gov/pubmed/4348786> (Accessed: 2 June 2018).

Hoepfner, D., van den Berg, M., Philippse, P., Tabak, H. F. and Hettema, E. H. (2001) 'A role for Vps1p, actin, and the Myo2p motor in peroxisome abundance and inheritance in *Saccharomyces cerevisiae*', *The Journal of Cell Biology*, 155(6), pp. 979–990. doi: 10.1083/jcb.200107028.

Hohendahl, A., Talledge, N., Galli, V., Shen, P. S., Humbert, F., De Camilli, P., Frost, A. and Roux, A. (2017) 'Structural inhibition of dynamin-mediated membrane fission by endophilin', *eLife*. eLife Sciences Publications Limited, 6, p. e26856. doi: 10.7554/eLife.26856.

Huang, F., Khvorova, A., Marshall, W. and Sorkin, A. (2004) 'Analysis of Clathrin-mediated Endocytosis of Epidermal Growth Factor Receptor by RNA Interference', *Journal of Biological Chemistry*, 279(16), pp. 16657–16661. doi:

10.1074/jbc.C400046200.

Huber, F., Meurer, M., Bunina, D., Kats, I., Maeder, C. I., Štefl, M., Mongis, C. and Knop, M. (2014) ‘PCR Duplication: A One-Step Cloning-Free Method to Generate Duplicated Chromosomal Loci and Interference-Free Expression Reporters in Yeast’, *PLOS ONE*, 9(12), p. e114590. doi: 10.1371/journal.pone.0114590.

Huttner, W. B. and Schmidt, A. (2000) ‘Lipids, lipid modification and lipid–protein interaction in membrane budding and fission — insights from the roles of endophilin A1 and synaptophysin in synaptic vesicle endocytosis’, *Current Opinion in Neurobiology*. Elsevier Current Trends, 10(5), pp. 543–551. doi: 10.1016/S0959-4388(00)00126-4.

Jennifer L Gallop, C. C. J. (2006) ‘Mechanism of endophilin N-BAR domain-mediated membrane curvature.’, *The EMBO journal*, 25(12), pp. 2898–910. doi: 10.1038/sj.emboj.7601174.

Kaksonen, M., Sun, Y. and Drubin, D. G. (2003) ‘A pathway for association of receptors, adaptors, and actin during endocytic internalization’, *Cell*, 115(4), pp. 475–487. Available at: <http://www.ncbi.nlm.nih.gov/pubmed/14622601>.

Kaksonen, M., Toret, C. P. and Drubin, D. G. (2005) ‘A Modular Design for the Clathrin- and Actin-Mediated Endocytosis Machinery’, *Cell*, 123(2), pp. 305–320. doi: 10.1016/j.cell.2005.09.024.

Kanaseki, T. and Kadota, K. (1969) ‘The “vesicle in a basket”. A morphological study of the coated vesicle isolated from the nerve endings of the guinea pig brain, with special reference to the mechanism of membrane movements.’, *The Journal of cell biology*. Rockefeller University Press, 42(1), pp. 202–20. doi: 10.1083/JCB.42.1.202.

Karin, M. and Mintz, B. (1981) ‘Receptor-mediated endocytosis of transferrin in developmentally totipotent mouse teratocarcinoma stem cells.’, *The Journal of biological chemistry*, 256(7), pp. 3245–52. Available at: <http://www.ncbi.nlm.nih.gov/pubmed/6259157> (Accessed: 3 June 2018).

Kearns, B. G., McGee, T. P., Mayinger, P., Gedvilaite, A., Phillips, S. E., Kagiwada, S. and Bankaitis, V. A. (1997) 'Essential role for diacylglycerol in protein transport from the yeast Golgi complex', *Nature*, 387(6628), pp. 101–105. doi: 10.1038/387101a0.

Kishimoto, T., Sun, Y., Buser, C., Liu, J., Michelot, A. and Drubin, D. G. (2011) 'Determinants of endocytic membrane geometry, stability, and scission', *Proceedings of the National Academy of Sciences*, 108(44), pp. E979–E988. doi: 10.1073/pnas.1113413108.

Kishimoto, T., Sun, Y., Buser, C., Liu, J., Michelot, A. and Drubin, D. G. (2011) 'Determinants of endocytic membrane geometry, stability, and scission', *Proceedings of the National Academy of Sciences of the United States of America*, 108(44), pp. E979–E988. doi: 10.1073/pnas.1113413108.

Koteliansky, V. E., Glukhova, M. A., Bejanian, M. V., Surguchov, A. P. and Smirnov, V. N. (1979) 'Isolation and characterization of actin-like protein from yeast *Saccharomyces Cerevisiae*', *FEBS Letters*. No longer published by Elsevier, 102(1), pp. 55–58. doi: 10.1016/0014-5793(79)80927-8.

Kozlovsky, Y. and Kozlov, M. M. (2003) 'Membrane fission: model for intermediate structures.', *Biophysical journal*. Elsevier, 85(1), pp. 85–96. doi: 10.1016/S0006-3495(03)74457-9.

Kübler, E. and Riezman, H. (1993) 'Actin and fimbrin are required for the internalization step of endocytosis in yeast.', *The EMBO Journal*, 12(7), pp. 2855–2862. Available at:

Kukulski, W., Picco, A., Specht, T., Briggs, J. A. and Kaksonen, M. (2016) 'Clathrin modulates vesicle scission, but not invagination shape, in yeast endocytosis', *eLife*, 5. doi: 10.7554/eLife.16036.

Kukulski, W., Schorb, M., Kaksonen, M. and Briggs, J. A. G. (2012) 'Plasma Membrane Reshaping during Endocytosis Is Revealed by Time-Resolved Electron Tomography', *Cell*, 150(3), pp. 508–520. doi: 10.1016/j.cell.2012.05.046.

Lee, E., Marcucci, M., Daniell, L., Pypaert, M., Weisz, O. A., Ochoa, G.-C., Farsad, K., Wenk, M. R. and De Camilli, P. (2002) 'Amphiphysin 2 (Bin1) and T-tubule biogenesis in muscle.', *Science (New York, N.Y.)*. American Association for the Advancement of Science, 297(5584), pp. 1193–6. doi: 10.1126/science.1071362.

Lila, T. and Drubin, D. G. (1997) 'Evidence for physical and functional interactions among two *Saccharomyces cerevisiae* SH3 domain proteins, an adenylyl cyclase-associated protein and the actin cytoskeleton.', *Molecular Biology of the Cell*, 8(2), pp. 367–385. doi: 10.1091/mbc.8.2.367.

Liu, J., Kaksonen, M., Drubin, D. G. and Oster, G. (2006a) 'Endocytic vesicle scission by lipid phase boundary forces.', *Proceedings of the National Academy of Sciences of the United States of America*. National Academy of Sciences, 103(27), pp. 10277–82. doi: 10.1073/pnas.0601045103.

Liu, J., Sun, Y., Drubin, D. G. and Oster, G. F. (2009) 'The Mechanochemistry of Endocytosis', *PLoS Biology*. Edited by F. Hughson. Public Library of Science, 7(9), p. e1000204. doi: 10.1371/journal.pbio.1000204.

Lombardi, R. and Riezman, H. (2001) 'Rvs161p and Rvs167p, the Two Yeast Amphiphysin Homologs, Function Together in Vivo', *Journal of Biological Chemistry*, 276(8), pp. 6016–6022. doi: 10.1074/jbc.M008735200.

Madania, A., Dumoulin, P., Grava, S., Kitamoto, H., Schärer-Brodbeck, C., Soulard, A., Moreau, V. and Winsor, B. (1999) 'The *Saccharomyces cerevisiae* homologue of human Wiskott-Aldrich syndrome protein Las17p interacts with the Arp2/3 complex.', *Molecular biology of the cell*. American Society for Cell Biology, 10(10), pp. 3521–38. doi: 10.1091/MBC.10.10.3521.

Masuda, M., Takeda, S., Sone, M., Ohki, T., Mori, H., Kamioka, Y. and Mochizuki, N. (2006) 'Endophilin BAR domain drives membrane curvature by two newly identified structure-based mechanisms.', *The EMBO journal*. European Molecular Biology Organization, 25(12), pp. 2889–97. doi: 10.1038/sj.emboj.7601176.

Maxfield, F. R. (2014) 'Role of Endosomes and Lysosomes in Human Disease', *Cold*

Spring Harbor Perspectives in Biology, 6(5), pp. a016931–a016931. doi: 10.1101/cshperspect.a016931.

Mayer, B. J. (2001) 'SH3 domains: complexity in moderation.', *Journal of cell science*, 114(Pt 7), pp. 1253–63. Available at: <http://www.ncbi.nlm.nih.gov/pubmed/11256992> (Accessed: 10 July 2018).

McMahon, H. T. and Mills, I. G. (2004) 'COP and clathrin-coated vesicle budding: different pathways, common approaches', *Current Opinion in Cell Biology*. Elsevier Current Trends, 16(4), pp. 379–391. doi: 10.1016/J.CEB.2004.06.009.

McPherson, P. S., Garcia, E. P., Slepnev, V. I., David, C., Zhang, X., Grabs, D., Sossini, W. S., Bauerfeind, R., Nemoto, Y. and De Camilli, P. (1996) 'A presynaptic inositol-5-phosphatase', *Nature*, 379(6563), pp. 353–357. doi: 10.1038/379353a0.

Meinecke, M., Boucrot, E., Camdere, G., Hon, W.-C., Mittal, R. and McMahon, H. T. (2013) 'Cooperative recruitment of dynamin and BIN/amphiphysin/Rvs (BAR) domain-containing proteins leads to GTP-dependent membrane scission.', *The Journal of biological chemistry*. American Society for Biochemistry and Molecular Biology, 288(9), pp. 6651–61. doi: 10.1074/jbc.M112.444869.

Mercer, J., Schelhaas, M. and Helenius, A. (2010) 'Virus Entry by Endocytosis', *Annual Review of Biochemistry*. Annual Reviews , 79(1), pp. 803–833. doi: 10.1146/annurev-biochem-060208-104626.

Micheva, K. D., Ramjaun%, A. R., Kay, B. K. and Mcpherson, P. S. (1997) 'SH3 domain-dependent interactions of endophilin with amphiphysin', *FEBS Letters*, 414, pp. 308–312. Available at: https://ac.els-cdn.com/S0014579397010168/1-s2.0-S0014579397010168-main.pdf?_tid=77135c79-45d8-4ad1-86d6-a495348096e2&acdnat=1528392307_2ab4cf61926e58ed1534623723714913 (Accessed: 7 June 2018).

Mim, C., Cui, H., Gawronski-Salerno, J. A., Frost, A., Lyman, E., Voth, G. A. and Unger, V. M. (2012a) 'Structural basis of membrane bending by the N-BAR protein endophilin.', *Cell. NIH Public Access*, 149(1), pp. 137–45. doi:

10.1016/j.cell.2012.01.048.

Mim, C. and Unger, V. M. (2012) 'Membrane curvature and its generation by BAR proteins', *Trends in biochemical sciences*, 37(12), pp. 526–533. doi: 10.1016/j.tibs.2012.09.001.

Mosesson, Y., Mills, G. B. and Yarden, Y. (2008) 'Derailed endocytosis: an emerging feature of cancer', *Nature Reviews Cancer*. Nature Publishing Group, 8(11), pp. 835–850. doi: 10.1038/nrc2521.

Moustaq, L., Smaczynska-de Rooij, I. I., Palmer, S. E., Marklew, C. J. and Ayscough, K. R. (2016) 'Insights into dynamin-associated disorders through analysis of equivalent mutations in the yeast dynamin Vps1', *Microbial Cell*, 3(4), pp. 147–158. doi: 10.15698/mic2016.04.490.

Mund, M., Beek, J. A. van der, Deschamps, J., Dmitrieff, S., Monster, J. L., Picco, A., Nedelec, F., Kaksonen, M. and Ries, J. (2017) 'Systematic analysis of the molecular architecture of endocytosis reveals a nanoscale actin nucleation template that drives efficient vesicle formation', *bioRxiv*. Cold Spring Harbor Laboratory, p. 217836. doi: 10.1101/217836.

Myers, M. D., Ryazantsev, S., Hicke, L. and Payne, G. S. (2016) 'Calmodulin Promotes N-BAR Domain-Mediated Membrane Constriction and Endocytosis', *Developmental Cell*, 37(2), pp. 162–173. doi: 10.1016/j.devcel.2016.03.012.

Nannapaneni, S., Wang, D., Jain, S., Schroeder, B., Highfill, C., Reustle, L., Pittsley, D., Maysent, A., Moulder, S., McDowell, R. and Kim, K. (2010a) 'The yeast dynamin-like protein Vps1:vps1 mutations perturb the internalization and the motility of endocytic vesicles and endosomes via disorganization of the actin cytoskeleton', *European Journal of Cell Biology*, 89(7), pp. 499–508. doi: 10.1016/j.ejcb.2010.02.002.

Neumann, S. and Schmid, S. L. (2013) 'Dual role of BAR domain-containing proteins in regulating vesicle release catalyzed by the GTPase, dynamin-2.', *The Journal of biological chemistry*. American Society for Biochemistry and Molecular

Biology, 288(35), pp. 25119–28. doi: 10.1074/jbc.M113.490474.

Otsuki, M., Itoh, T. and Takenawa, T. (2003) ‘Neural Wiskott-Aldrich Syndrome Protein Is Recruited to Rafts and Associates with Endophilin A in Response to Epidermal Growth Factor’, *Journal of Biological Chemistry*, 278(8), pp. 6461–6469. doi: 10.1074/jbc.M207433200.

Payne, G. (2013) ‘Clathrin, adaptors and disease: Insights from the yeast *Saccharomyces cerevisiae*’, *Frontiers in Bioscience*, 18(3), p. 862. doi: 10.2741/4149.

Payne, G. S. and Schekman, R. (1985) ‘A test of clathrin function in protein secretion and cell growth.’, *Science (New York, N.Y.)*, 230(4729), pp. 1009–14. Available at: <http://www.ncbi.nlm.nih.gov/pubmed/2865811> (Accessed: 2 June 2018).

Pearse, B. M. (1976) ‘Clathrin: a unique protein associated with intracellular transfer of membrane by coated vesicles.’, *Proceedings of the National Academy of Sciences*, 73(4), pp. 1255–1259. doi: 10.1073/pnas.73.4.1255.

Peter, B. J., Kent, H. M., Mills, I. G., Vallis, Y., Butler, P. J. G., Evans, P. R. and McMahon, H. T. (2004) ‘BAR Domains as Sensors of Membrane Curvature: The Amphiphysin BAR Structure’, *Science*, 303(5657), pp. 495–499. doi: 10.1126/science.1092586.

Peters, C., Baars, T. L., Bühler, S. and Mayer, A. (2004) ‘Mutual control of membrane fission and fusion proteins.’, *Cell*. Elsevier, 119(5), pp. 667–78. doi: 10.1016/j.cell.2004.11.023.

Picco, A., Kukulski, W., Manenschijn, H. E., Specht, T., Briggs, J. A. G. and Kaksonen, M. (2018) ‘The contributions of the actin machinery to endocytic membrane bending and vesicle formation’, *Molecular Biology of the Cell*, 29(11), pp. 1346–1358. doi: 10.1091/mbc.E17-11-0688.

Picco, A., Mund, M., Ries, J., Nédélec, F. and Kaksonen, M. (2015) ‘Visualizing the

functional architecture of the endocytic machinery', *eLife*, p. e04535. doi: 10.7554/eLife.04535.

Poodry, C. A. and Edgar, L. (1979) 'Reversible alteration in the neuromuscular junctions of *Drosophila melanogaster* bearing a temperature-sensitive mutation, shibire.', *The Journal of cell biology*. Rockefeller University Press, 81(3), pp. 520–7. doi: 10.1083/JCB.81.3.520.

Pykäläinen, A., Boczkowska, M., Zhao, H., Saarikangas, J., Rebowski, G., Jansen, M., Hakanen, J., Koskela, E. V., Peränen, J., Vihinen, H., Jokitalo, E., Salminen, M., Ikonen, E., Dominguez, R. and Lappalainen, P. (2011) 'Pinkbar is an epithelial-specific BAR domain protein that generates planar membrane structures.', *Nature structural & molecular biology*. NIH Public Access, 18(8), pp. 902–7. doi: 10.1038/nsmb.2079.

Qualmann, B., Koch, D. and Kessels, M. M. (2011) 'Let's go bananas: revisiting the endocytic BAR code', *The EMBO Journal*, 30(17), pp. 3501–3515. doi: 10.1038/emboj.2011.266.

Razzaq, A., Robinson, I. M., McMahon, H. T., Skepper, J. N., Su, Y., Zelhof, A. C., Jackson, A. P., Gay, N. J. and O'Kane, C. J. (2001) 'Amphiphysin is necessary for organization of the excitation-contraction coupling machinery of muscles, but not for synaptic vesicle endocytosis in *Drosophila*', *Genes & development*. Cold Spring Harbor Laboratory Press, 15(22), pp. 2967–79. doi: 10.1101/gad.207801.

Ren, G., Vajjhala, P., Lee, J. S., Winsor, B. and Munn, A. L. (2006) 'The BAR domain proteins: molding membranes in fission, fusion, and phagy.', *Microbiology and molecular biology reviews : MMBR*. American Society for Microbiology (ASM), 70(1), pp. 37–120. doi: 10.1128/MMBR.70.1.37-120.2006.

Riezman, H. (1985) 'Endocytosis in Yeast: Several of the Yeast Secretory Mutants Are Defective in Endocytosis', *Cell*, 40(0), pp. 1001–1009. Available at: [https://www.cell.com/cell/pdf/0092-8674\(85\)90360-5.pdf](https://www.cell.com/cell/pdf/0092-8674(85)90360-5.pdf) (Accessed: 3 June 2018).

Ringstad, N., Nemoto, Y. and De Camilli, P. (1997) 'The SH3p4/Sh3p8/SIH3p13 protein family: binding partners for synaptosomal-associated protein 25 kDa and dynamin via a Grb2-like Src homology 3 domain.', *Proceedings of the National Academy of Sciences of the United States of America*. National Academy of Sciences, 94(16), pp. 8569–74. doi: 10.1073/PNAS.94.16.8569.

Rooij, I. I. S. -d., Allwood, E. G., Aghamohammadzadeh, S., Hettema, E. H., Goldberg, M. W. and Ayscough, K. R. (2010) 'A role for the dynamin-like protein Vps1 during endocytosis in yeast', *Journal of Cell Science*, 123(20), pp. 3496–3506. doi: 10.1242/jcs.070508.

ROTH, T. F. and PORTER, K. R. (1964) 'YOLK PROTEIN UPTAKE IN THE OOCYTE OF THE MOSQUITO AEDES AEGYPTI. I.', *The Journal of cell biology*, 20, pp. 313–32. Available at: <http://www.ncbi.nlm.nih.gov/pubmed/14126875> (Accessed: 28 December 2017).

Rothman, J. H., Raymond, C. K., Gilbert, T., O'Hara, P. J. and Stevens, T. H. (1990) 'A putative GTP binding protein homologous to interferon-inducible Mx proteins performs an essential function in yeast protein sorting.', *Cell*. Elsevier, 61(6), pp. 1063–74. doi: 10.1016/0092-8674(90)90070-U.

Saarikangas, J., Zhao, H., Pykäläinen, A., Laurinmäki, P., Mattila, P. K., Kinnunen, P. K. J., Butcher, S. J. and Lappalainen, P. (2009) 'Molecular Mechanisms of Membrane Deformation by I-BAR Domain Proteins', *Current Biology*, 19(2), pp. 95–107. doi: 10.1016/j.cub.2008.12.029.

Sakamuro, D., Elliott, K. J., Wechsler-Reya, R. and Prendergast, G. C. (1996) 'BIN1 is a novel MYC-interacting protein with features of a tumour suppressor.', *Nature genetics*, 14(1), pp. 69–77. doi: 10.1038/ng0996-69.

Shimada, A., Niwa, H., Tsujita, K., Suetsugu, S., Nitta, K., Hanawa-Suetsugu, K., Akasaka, R., Nishino, Y., Toyama, M., Chen, L., Liu, Z.-J., Wang, B.-C., Yamamoto, M., Terada, T., Miyazawa, A., Tanaka, A., Sugano, S., Shirouzu, M., Nagayama, K., Takenawa, T. and Yokoyama, S. (2007) 'Curved EFC/F-BAR-domain dimers are

joined end to end into a filament for membrane invagination in endocytosis', *Cell*, 129(4), pp. 761–772. doi: 10.1016/j.cell.2007.03.040.

Shpetner, H. S. and Vallee, R. B. (1989) 'Identification of dynamin, a novel mechanochemical enzyme that mediates interactions between microtubules.', *Cell*. Elsevier, 59(3), pp. 421–32. doi: 10.1016/0092-8674(89)90027-5.

Shupliakov, O., Löw, P., Grabs, D., Gad, H., Chen, H., David, C., Takei, K., De Camilli, P. and Brodin, L. (1997) 'Synaptic vesicle endocytosis impaired by disruption of dynamin-SH3 domain interactions.', *Science (New York, N.Y.)*, 276(5310), pp. 259–63. Available at: <http://www.ncbi.nlm.nih.gov/pubmed/9092476> (Accessed: 27 May 2018).

Simunovic, M., Manneville, J.-B., Renard, H.-F. O., Johannes, L., Bassereau, P., Callan, A., Correspondence, -Jones, Evergren, E., Raghunathan, K., Bhatia, D., Kenworthy, A. K., Voth, G. A., Prost, J., Mcmahon, H. T. and Callan-Jones, A. (2017a) 'Friction Mediates Scission of Tubular Membranes Scaffolded by BAR Proteins', *Cell*. Elsevier Inc, 170, pp. 1–13. doi: 10.1016/j.cell.2017.05.047.

Singer-Krüger, B., Nemoto, Y., Daniell, L., Ferro-Novick, S. and De Camilli, P. (1998) 'Synaptojanin family members are implicated in endocytic membrane traffic in yeast.', *Journal of cell science*, 111 (Pt 2, pp. 3347–3356. Available at: <http://jcs.biologists.org/content/joces/111/22/3347.full.pdf> (Accessed: 24 October 2017).

Sivadon, P., Bauer, F., Aigle, M. and Crouzet, M. (1995) 'Actin cytoskeleton and budding pattern are altered in the yeast rvs161 mutant: the Rvs161 protein shares common domains with the brain protein amphiphysin.', *Molecular & general genetics : MGG*, 246(4), pp. 485–95. doi: 10.1007/bf00290452.

Sivadon, P., Crouzet, M. and Aigle, M. (1997a) 'Functional assessment of the yeast Rvs161 and Rvs167 protein domains.', *FEBS letters*, 417(1), pp. 21–7. doi: 10.1016/s0014-5793(97)01248-9.

Skruzny, M., Brach, T., Ciuffa, R., Rybina, S., Wachsmuth, M. and Kaksonen, M.

(2012) 'Molecular basis for coupling the plasma membrane to the actin cytoskeleton during clathrin-mediated endocytosis.', *Proceedings of the National Academy of Sciences of the United States of America*. National Academy of Sciences, 109(38), pp. E2533-42. doi: 10.1073/pnas.1207011109.

Snead, W., Zeno, W., Kago, G., Perkins, R., Richter, J. B., Lafer, E. and Stachowiak, J. (2018) 'BAR scaffolds drive membrane fission by crowding disordered domains', *bioRxiv*. Cold Spring Harbor Laboratory, p. 276147. doi: 10.1101/276147.

Sorre, B., Callan-Jones, A., Manzi, J., Goud, B., Prost, J., Bassereau, P. and Roux, A. (2012) 'Nature of curvature coupling of amphiphysin with membranes depends on its bound density', *Proceedings of the National Academy of Sciences*, 109(1), pp. 173–178. doi: 10.1073/pnas.1103594108.

Srinivasan, S., Seaman, M., Nemoto, Y., Daniell, L., Suchy, S. F., Emr, S., De Camilli, P. and Nussbaum, R. (1997) 'Disruption of three phosphatidylinositol-polyphosphate 5-phosphatase genes from *Saccharomyces cerevisiae* results in pleiotropic abnormalities of vacuole morphology, cell shape, and osmohomeostasis.', *European journal of cell biology*, 74(4), pp. 350–60. Available at: <http://www.ncbi.nlm.nih.gov/pubmed/9438131> (Accessed: 25 October 2017).

Stachowiak, J. C., Brodsky, F. M. and Miller, E. A. (2013) 'A cost-benefit analysis of the physical mechanisms of membrane curvature', *Nature Cell Biology*, 15(9), pp. 1019–1027. doi: 10.1038/ncb2832.

Stefan, C. J., Audhya, A. and Emr, S. D. (2002) 'The Yeast Synaptojanin-like Proteins Control the Cellular Distribution of Phosphatidylinositol (4,5)-Bisphosphate', *Molecular Biology of the Cell*, 13(2), pp. 542–557. doi: 10.1091/mbc.01-10-0476.

Stoltz, L. E., Huynh, C. V., Thorner, J. and York, J. D. (1998) 'Identification and Characterization of an Essential Family of Inositol Polyphosphate 5-Phosphatases (INP51, INP52 and INP53 Gene Products) in the Yeast *Saccharomyces cerevisiae*'. Available at:

<https://www.ncbi.nlm.nih.gov/pmc/articles/PMC1460112/pdf/9560389.pdf>

(Accessed: 5 April 2017).

Sun, Y., Carroll, S., Kaksonen, M., Toshima, J. Y. and Drubin, D. G. (2007) 'PtdIns(4,5)P₂ turnover is required for multiple stages during clathrin- and actin-dependent endocytic internalization', *The Journal of cell biology*, 177(2), pp. 355–367. doi: 10.1083/jcb.200611011.

Sun, Y., Leong, N. T., Wong, T. and Drubin, D. G. (2015) 'A Pan1/End3/Sla1 complex links Arp2/3-mediated actin assembly to sites of clathrin-mediated endocytosis', *Molecular Biology of the Cell*, 26(21), pp. 3841–3856. doi: 10.1091/mcb.E15-04-0252.

Sweitzer, S. M. and Hinshaw, J. E. (1998) 'Dynamin Undergoes a GTP-Dependent Conformational Change Causing Vesiculation', *Cell*. Cell Press, 93(6), pp. 1021–1029. doi: 10.1016/S0092-8674(00)81207-6.

Takei, K., McPherson, P. S., Schmid, S. L. and Camilli, P. De (1995) 'Tubular membrane invaginations coated by dynamin rings are induced by GTP-γS in nerve terminals', *Nature*. Nature Publishing Group, 374(6518), pp. 186–190. doi: 10.1038/374186a0.

Takei, K., Slepnev, V. I., Haucke, V. and De Camilli, P. (1999) 'Functional partnership between amphiphysin and dynamin in clathrin-mediated endocytosis', *Nature Cell Biology*, 1(1), pp. 33–39. doi: 10.1038/9004.

Taylor, M. J., Perrais, D. and Merrifield, C. J. (2011) 'A high precision survey of the molecular dynamics of mammalian clathrin-mediated endocytosis', *PLoS biology*, 9(3), p. e1000604. doi: 10.1371/journal.pbio.1000604.

Toshima, J. Y., Furuya, E., Nagano, M., Kanno, C., Sakamoto, Y., Ebihara, M., Siekhaus, D. E. and Toshima, J. (2016) 'Yeast Eps15-like endocytic protein Pan1p regulates the interaction between endocytic vesicles, endosomes and the actin cytoskeleton.', *eLife*. eLife Sciences Publications, Ltd, 5. doi: 10.7554/eLife.10276.

Toume, M. and Tani, M. (2016) 'Yeast lacking the amphiphysin family protein

Rvs167 is sensitive to disruptions in sphingolipid levels', *The FEBS Journal*, 283(15), pp. 2911–2928. doi: 10.1111/febs.13783.

Traub, L. M. (2005) 'Common principles in clathrin-mediated sorting at the Golgi and the plasma membrane', *Biochimica et Biophysica Acta (BBA) - Molecular Cell Research*, 1744(3), pp. 415–437. doi: 10.1016/j.bbamcr.2005.04.005.

Ungewickell, E. and Branton, D. (1981) 'Assembly units of clathrin coats', *Nature*. Nature Publishing Group, 289(5796), pp. 420–422. doi: 10.1038/289420a0.

Varkey, J., Isas, J. M., Mizuno, N., Jensen, M. B., Bhatia, V. K., Jao, C. C., Petrlova, J., Voss, J. C., Stamou, D. G., Steven, A. C. and Langen, R. (2010) 'Membrane curvature induction and tubulation are common features of synucleins and apolipoproteins.', *The Journal of biological chemistry*. American Society for Biochemistry and Molecular Biology, 285(42), pp. 32486–93. doi: 10.1074/jbc.M110.139576.

Verschueren, E., Spiess, M., Gkourtsa, A., Avula, T., Landgraf, C., Mancilla, V. T., Huber, A., Volkmer, R., Winsor, B., Serrano, L., Hochstenbach, F. and Distel, B. (2015) 'Evolution of the SH3 Domain Specificity Landscape in Yeasts', *PLoS ONE*, 10(6). doi: 10.1371/journal.pone.0129229.

Weinberg, J. and Drubin, D. G. (2012) 'Clathrin-mediated endocytosis in budding yeast.', *Trends in cell biology*. NIH Public Access, 22(1), pp. 1–13. doi: 10.1016/j.tcb.2011.09.001.

Weissenhorn, W. (2005) 'Crystal Structure of the Endophilin-A1 BAR Domain', *Journal of Molecular Biology*. Academic Press, 351(3), pp. 653–661. doi: 10.1016/J.JMB.2005.06.013.

Wendland, B. and Emr, S. D. (1998) 'Pan1p, yeast eps15, functions as a multivalent adaptor that coordinates protein-protein interactions essential for endocytosis.', *The Journal of cell biology*. Rockefeller University Press, 141(1), pp. 71–84. doi: 10.1083/JCB.141.1.71.

Wong, M. H., Meng, L., Rajmohan, R., Yu, S. and Thanabalu, T. (2010) 'Vrp1p-Las17p interaction is critical for actin patch polarization but is not essential for growth or fluid phase endocytosis in *S. cerevisiae*', *Biochimica et biophysica acta*, 1803(12), pp. 1332–1346. doi: 10.1016/j.bbamcr.2010.08.013.

Yidi Sun, A. C. M. (2006) 'Endocytic internalization in budding yeast requires coordinated actin nucleation and myosin motor activity.', *Developmental cell*, 11(1), pp. 33–46. doi: 10.1016/j.devcel.2006.05.008.

Youn, J.-Y., Friesen, H., Kishimoto, T., Henne, W. M., Kurat, C. F., Ye, W., Ceccarelli, D. F., Sicheri, F., Kohlwein, S. D., McMahon, H. T. and Andrews, B. J. (2010) 'Dissecting BAR Domain Function in the Yeast Amphiphysins Rvs161 and Rvs167 during Endocytosis', *Molecular Biology of the Cell*, 21(17), pp. 3054–3069. doi: 10.1091/mbc.E10-03-0181.

Yu, X. (2004) 'The yeast dynamin-related GTPase Vps1p functions in the organization of the actin cytoskeleton via interaction with Sla1p', *Journal of Cell Science*, 117(17), pp. 3839–3853. doi: 10.1242/jcs.01239.

Zhang, P. and Hinshaw, J. E. (2001) 'Three-dimensional reconstruction of dynamin in the constricted state', *Nature Cell Biology*. Nature Publishing Group, 3(10), pp. 922–926. doi: 10.1038/ncb1001-922.

Zhao, W.-D., Hamid, E., Shin, W., Wen, P. J., Krystofiak, E. S., Villarreal, S. A., Chiang, H.-C., Kachar, B. and Wu, L.-G. (2016) 'Hemi-fused structure mediates and controls fusion and fission in live cells.', *Nature*. NIH Public Access, 534(7608), pp. 548–52. doi: 10.1038/nature18598.